

RDU1703266

DEVELOPING OF HEC/PVA FIBERS WITH CELLULOSE NANOCRYSTAL AS A BONE
TISSUE ENGINEERING SCAFFOLD.

FARAH HANANI ZULKIFLI

RESEARCH VOTE NO:

RDU1703266

Faculty of Industrial Sciences and Technology
Universiti Malaysia Pahang

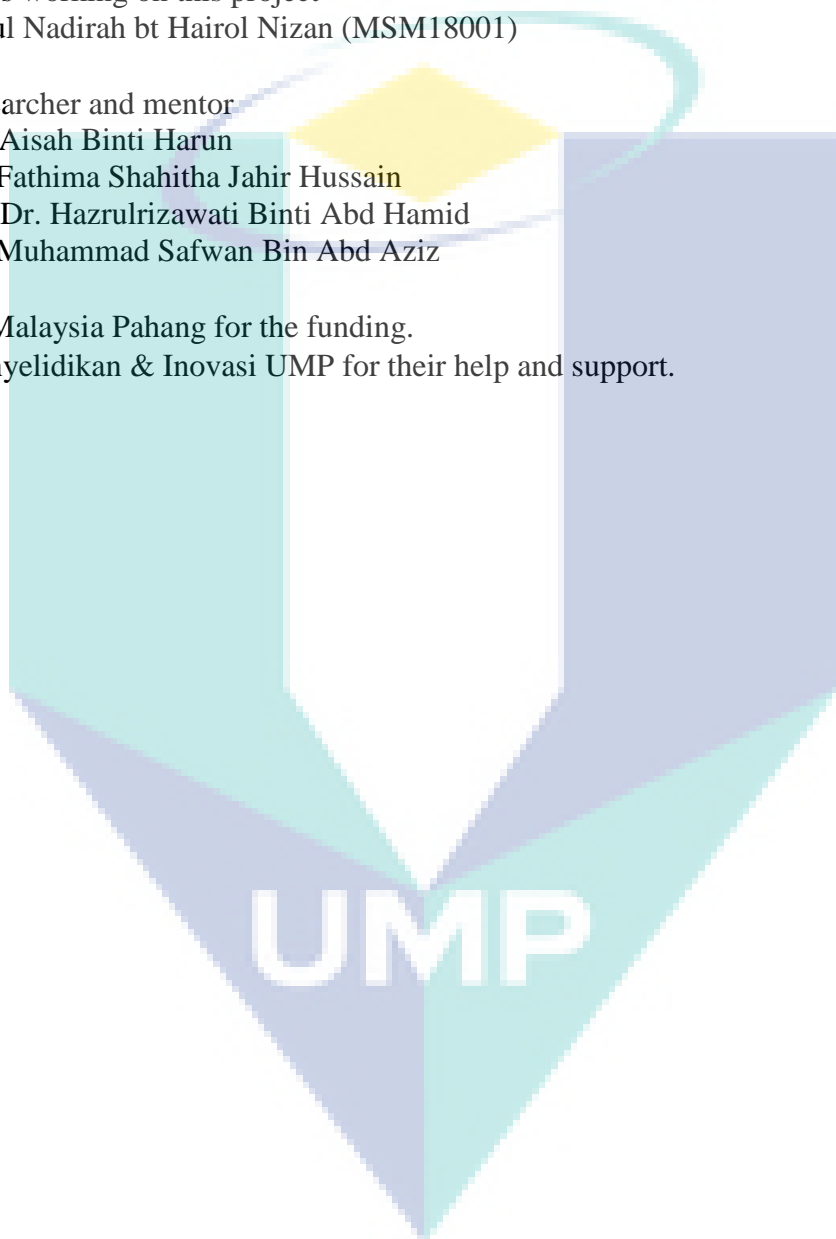
2020

UMP

ACKNOWLEDGEMENT

I would like to thank the following people and organisations;

- The students working on this project
Nor Sarahtul Nadirah bt Hairol Nizan (MSM18001)
- The co-researcher and mentor
 - Siti Aisah Binti Harun
 - Dr. Fathima Shahitha Jahir Hussain
 - PM Dr. Hazrulrizawati Binti Abd Hamid
 - Dr. Muhammad Safwan Bin Abd Aziz
- Universiti Malaysia Pahang for the funding.
- Jabatan Penyelidikan & Inovasi UMP for their help and support.



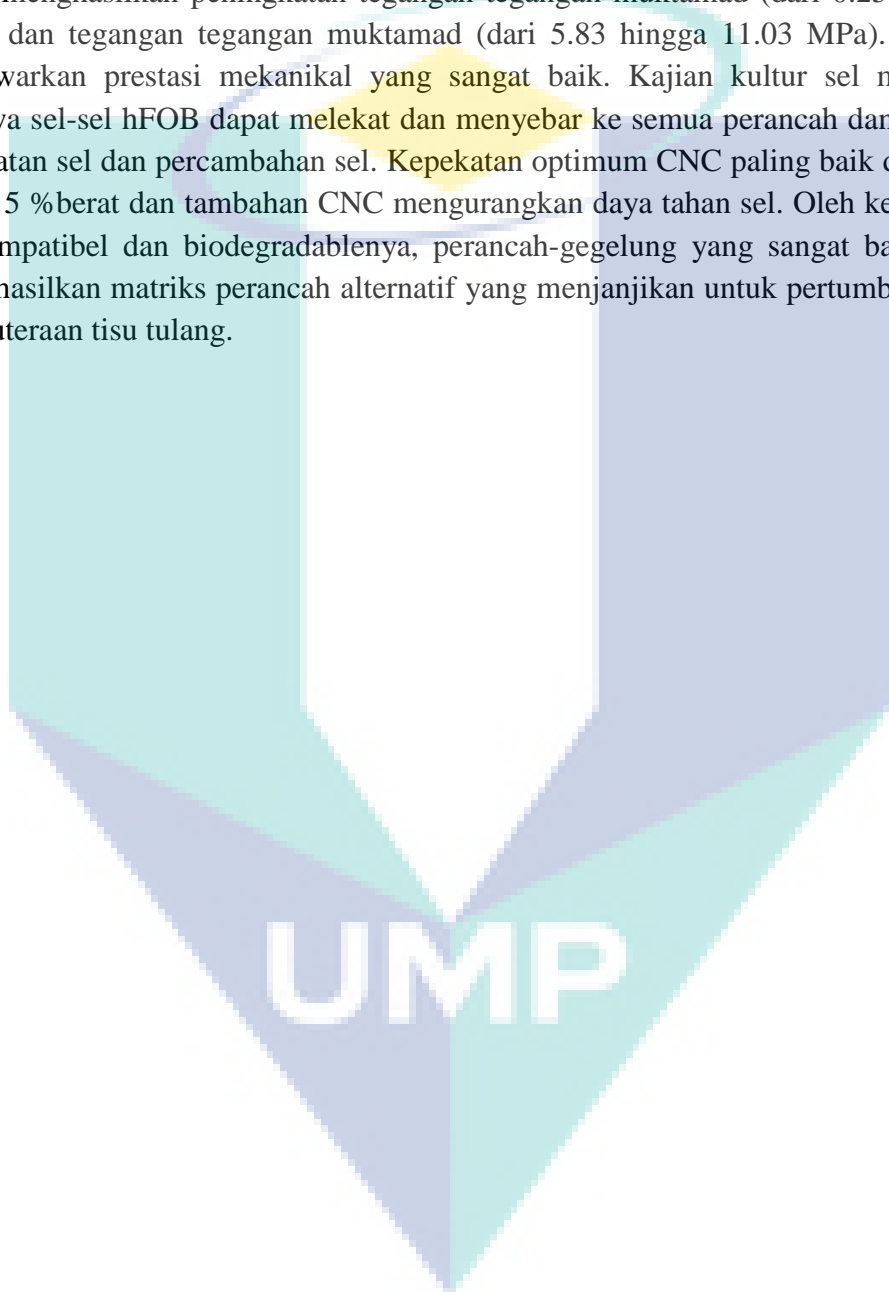
Abstrak

DEVELOPING OF HEC/PVA FIBERS WITH CELLULOSE NANOCRYSTAL AS A BONE TISSUE ENGINEERING SCAFFOLD.

(Keywords: hydroxypropyl methylcellulose, cellulose nanocrystals, bone tissue engineering)

Biomaterial adalah istilah perubatan yang digunakan untuk menggambarkan semua sumber semulajadi atau sintetik seperti polimer yang berguna dalam pengenalan tisu hidup sebagai sebahagian daripada peranti perubatan atau implan tanpa menyebabkan sebarang tindak balas imun. Selulosa telah diterokai secara meluas sejak beberapa dekad sebagai salah satu daripada biomaterial yang digunakan dalam aplikasi kejuruteraan tisu kerana sifatnya yang unik yang kos rendah, biokompatibilitas yang baik dan sifat mekanikal yang baik. Penyediaan nanocrystal selulosa (CNC) dari pulpa selulosa adalah cara alternatif untuk memenuhi permintaan CNC. Dalam kejuruteraan tisu, penggantian atau regenerasi tulang yang rosak adalah satu cabaran utama dalam pembedahan ortopedik. Oleh itu, reka bentuk kejuruteraan tisu tulang berasaskan perancah untuk mengatasi kecacatan tulang ini. Laporan ini terdiri daripada dua bahagian. Bahagian pertama adalah mengenai fabrikasi dan pencirian CNC manakala bahagian kedua adalah fabrikasi dan pencirian scaffolds termasuk degradasi in vitro dan kajian hidup sel. Dalam kerja-kerja ini, CNC yang dihasilkan daripada tandan buah kosong (EFB) berjaya dihasilkan oleh hidrolisis asid. Pulpa selulosa dipanaskan pada suhu 85 °C dalam 65 % asid sulfurik. Pengantungan selulosa telah dicairkan, disenyapkan, sonication, dan kemudian mengalami pengeringan beku untuk mendapatkan CNC. CNC bertindak sebagai nanofiller dalam perancah akan secara fizikal, kimia dan termal dicirikan dengan menggunakan mikroskop elektron pengimbasan pelepasan medan (FESEM), keseluruhan reflektansi dilemahkan-Fourier mengubah spektroskopi inframerah (ATR-FTIR) dan calorimetry scanning differential (DSC). Keputusan FESEM menunjukkan bahawa CNC muncul dalam bentuk sfera dengan dimensi zarah dalam jarak antara diameter 5 hingga 30 nm. Spektrum penyerapan CNC muncul dalam kumpulan tertentu yang berada pada 1045, 1346, 1637, 2903, dan 3391 cm^{-1} . Termometer DSC menunjukkan bahawa suhu lebur, T_m berlaku pada 197.1 °C, manakala suhu peralihan kaca, T_g ialah 65.2 °C. Seterusnya, perancah tiga dimensi (3D) porous HEC / PVA dan HEC / PVA / CNC telah berjaya direka oleh teknik pengeringan beku. HEC (5 %berat) dan PVA (15 %berat) telah dibubarkan dan dicampur pada nisbah 50:50 dan digabungkan dengan pelbagai kepekatan CNC (1, 3, 5 dan 7 %berat). Ciri-ciri morfologi, mekanikal dan terma perancah dicirikan oleh SEM, ATR-FTIR, DSC, thermogravimetric (TGA), dan mesin tegangan sejangat (UTM). Tingkah laku perancah scaffolds dicirikan oleh satu siri analisis termasuk nisbah pembengkakan, penurunan berat badan dan perubahan pH. Sementara itu, kajian sitotoksikiti pada kedua-dua biomaterial scaffold porous dilakukan

dengan menggunakan sel osteoblast janin manusia (hFOB) menggunakan ujian MTT dan kajian morfologi perancah sel. Gabungan HEC/PVA dengan CNC dipamerkan kefungsiannya yang lebih baik yang mengakibatkan penurunan ukuran liang rata-rata dan terdapat sedikit perubahan dalam struktur kimia seperti yang ditentukan oleh spektrum FTIR. Kajian termal menunjukkan bahawa suhu lebur perancah HEC/PVA/CNC sedikit beralih kepada nilai yang lebih tinggi. Selain itu, dapat dilihat bahawa penambahan CNC menghasilkan peningkatan tegangan muktamad (dari 0.25 hingga 0.92 MPa) dan tegangan muktamad (dari 5.83 hingga 11.03 MPa). Oleh itu, ia menawarkan prestasi mekanikal yang sangat baik. Kajian kultur sel mendedahkan bahawa sel-sel hFOB dapat melekat dan menyebar ke semua perancah dan menyokong perekatan sel dan percambahan sel. Kepekatan optimum CNC paling baik didapati pada 3 dan 5 % berat dan tambahan CNC mengurangkan daya tahan sel. Oleh kerana ciri-ciri biokompatibel dan biodegradabelnya, perancah-gegelung yang sangat baru ini boleh menghasilkan matriks perancah alternatif yang menjanjikan untuk pertumbuhan semula kejuruteraan tisu tulang.



E-mail : farahhanani@ump.edu.my
Tel. No. : +60162054397

Vote No. : **RDU1703266**

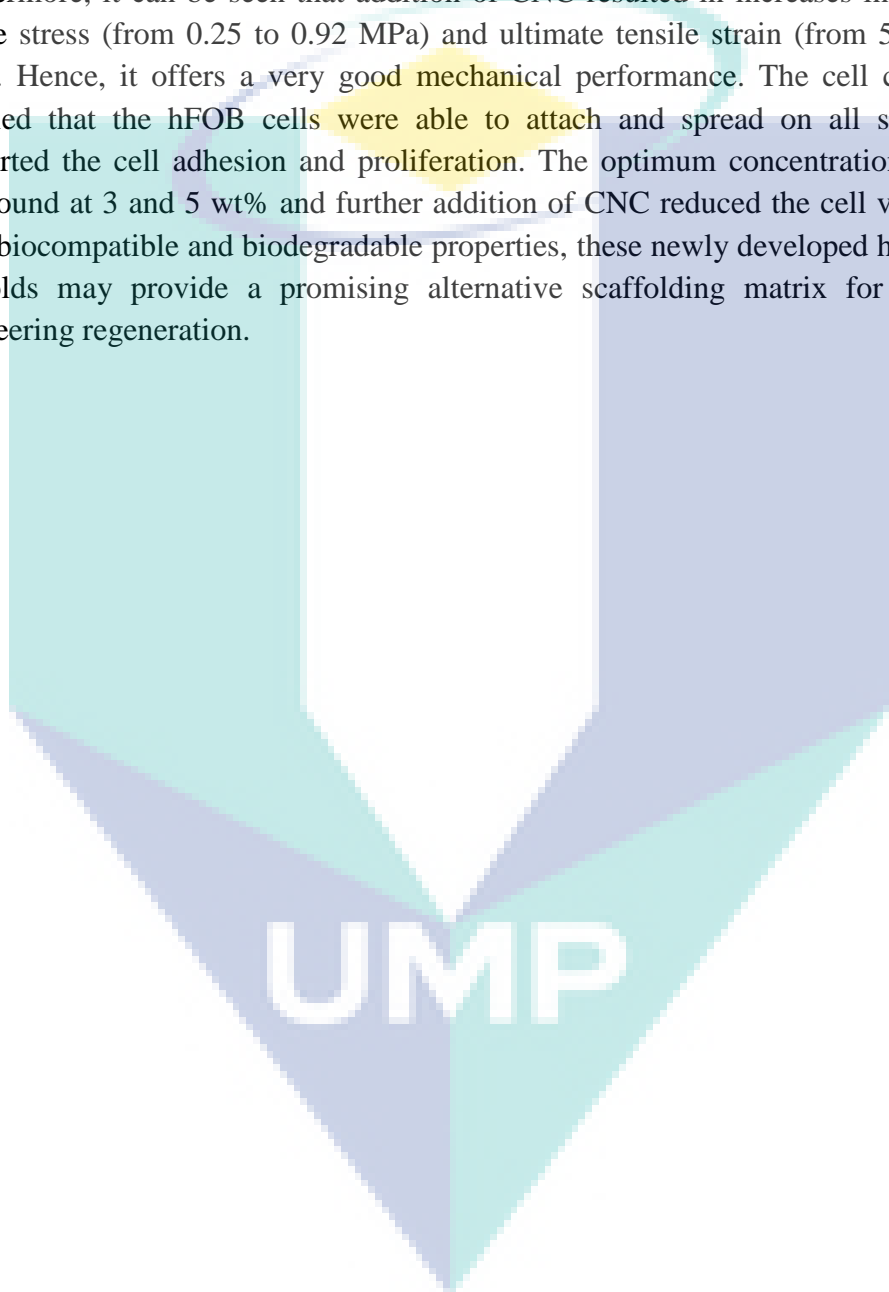
ABSTRACT

CELLULOSE NANOCRYSTALS INCORPORATED WITH HYDROXYPROPYL METHYLCELLULOSE AS BIOCOMPOSITE SCAFFOLDS FOR BONE TISSUE ENGINEERING

(Keywords: hydroxypropyl methylcellulose, cellulose nanocrystals, bone tissue engineering)

Biomaterial is a medical terminology that used to describe all natural or synthetic resources such as polymer that are useful in the introduction of living tissue as part of medical device or implant without causing any adverse of immune rejection reaction. Cellulose has been extensively explored over decades as one of the biomaterials used in tissue engineering application due to their unique properties which are low cost, good biocompatibility and good mechanical properties. Preparation of cellulose nanocrystal (CNC) from cellulose pulp is an alternative way to fulfil the CNC demand. In tissue engineering, replacement or regeneration of damaged bone is a major challenge in orthopedic surgery. Hence, scaffold-based bone tissue engineering designs to overcome these bone defects. This report comprised of two parts. The first part is about the fabrication and characterization of CNC while the second part is the fabrication and characterization of scaffolds including in vitro degradation and cell culture studies. In this present work, CNC produced from empty fruit bunch (EFB) were successfully fabricated by acid hydrolysis. Cellulose pulps were heated at 85 °C in 65 % of sulphuric acid. The cellulose suspension was diluted, centrifuged, sonication, and then undergoes freeze-drying to obtain CNC. CNC acts as nanofillers in scaffolds will be physically, chemically and thermally characterized by using field emission scanning electron microscope (FESEM), attenuated total reflectance-Fourier transform infrared spectroscopy (ATR-FTIR) and differential scanning calorimetry (DSC). FESEM results showed that CNC appeared in spherical shape with particle dimension in the range between 5 to 30 nm in diameter. The absorption spectra of CNC appeared in specific bands which are at 1045, 1346, 1637, 2903, and 3391 cm^{-1} . DSC thermograms shows that melting temperature, T_m is occur at 197.1 °C, while the glass transition temperature, T_g is 65.2 °C. Next, a porous three-dimensional (3D) scaffold of HEC/PVA and HEC/PVA/CNC were successfully fabricated by freeze-drying technique. HEC (5 wt%) and PVA (15 wt%) were dissolved and blended at a ratio of 50:50 and incorporated with various concentration of CNC (1, 3, 5 and 7 wt%). The morphology, mechanical and thermal properties of scaffolds were characterized by SEM, ATR-FTIR, DSC, thermogravimetric (TGA), and universal tensile machine (UTM). The degradation behaviors of scaffolds were characterized by a series of analysis including swelling ratio, weight loss and pH changes. Meanwhile, cytotoxicity

studies on both porous scaffold biomaterials were carried out by utilizing human fetal osteoblast (hFOB) cells using MTT assays and cell-scaffold morphological study. Incorporated HEC/PVA with CNC were exhibited superior functionality which resulted in decreasing average pore size and there were some slightly changes in the chemical structure as determined by FTIR spectra. Thermal studies revealed that the melting temperatures of HEC/PVA/CNC scaffold were slightly shifted to a higher value. Furthermore, it can be seen that addition of CNC resulted in increases in the ultimate tensile stress (from 0.25 to 0.92 MPa) and ultimate tensile strain (from 5.83 to 11.03 MPa). Hence, it offers a very good mechanical performance. The cell culture study revealed that the hFOB cells were able to attach and spread on all scaffolds and supported the cell adhesion and proliferation. The optimum concentration of CNC is best found at 3 and 5 wt% and further addition of CNC reduced the cell viability. Due to its biocompatible and biodegradable properties, these newly developed highly porous scaffolds may provide a promising alternative scaffolding matrix for bone tissue engineering regeneration.



E-mail : *farahhanani@ump.edu.my*
Tel. No. : +60162054397
Vote No. : RDU1703266

TABLE OF CONTENT

ABSTRAK		iii
ABSTRACT		v
TABLE OF CONTENT		vii
LIST OF TABLES		x
LIST OF FIGURES		xi
LIST OF SYMBOLS		xii
LIST OF ABBREVIATIONS		xv
CHAPTER 1 INTRODUCTION		
1.1	Background	1
1.2	Problem statement	3
1.3	Significance of studies	4
1.4	Research objective	5
1.5	Research scope	5
1.6	Thesis outline	6
CHAPTER 2 LITERATURE REVIEW		
2.1	General function of bone	7
2.1.1	Structural and mechanical properties of bone	8
2.2	Bone tissue engineering	10
2.3	Biomaterials in tissue engineering	11
2.3.1	Evolution of biomaterials	12
2.3.2	Characteristics of biomaterials scaffold	12
2.3.3	Hydroxyethyl cellulose (HEC)	13
2.3.4	Poly (vinyl) Alcohol (PVA)	14
2.3.5	Cellulose nanocrystal (CNC)	15
2.4	Fabrication of scaffolds	16

2.4.1	Freeze-drying technique	17
2.5	Summary	20
CHAPTER 3 METHODOLOGY		
3.1	Research methodology	22
3.2	Raw materials	24
3.3	Synthesis of CNC	24
3.4	Preparation of polymeric solution	26
3.5	Fabrication of HEC/PVA/CNC scaffolds using freeze-drying method	26
3.6	Samples crosslinking	28
3.7	Characterization of CNC nanoparticle and HEC/PVA/CNCs scaffolds	28
3.7.1	Field emission scanning electron microscope (FESEM)	28
3.7.2	Scanning electron microscope (SEM)	29
3.7.3	Porosity study	30
3.7.4	Attenuated total reflectance-Fourier transform infrared spectroscopy (ATR- FTIR)	31
3.7.5	Thermogravimetric (TGA) analysis	32
3.7.6	Differential scanning calorimetry (DSC)	33
3.7.7	Mechanical testing	35
3.8	In vitro degradation study	36
3.8.1	Swelling ratio study	36
3.8.2	pH value measurements	36
3.8.3	Weight loss study	37
3.9	Cell culture study	38
3.9.1	In vitro cell culture study of HEC/PVA/CNC scaffolds	38
3.9.2	hFOB cells expansion and seeding	39
3.9.3	hFOB cells proliferation study	41
3.9.4	hFOB cells morphology studies	43
CHAPTER 4 RESULTS AND DISCUSSION		
4.1	Characterization of CNC	44
4.1.1	Morphology of CNC	44
4.1.2	Chemical properties of CNC	47
4.1.3	Thermal study of CNC	48

4.2	Characterization of HEC/PVA and HEC/PVA/CNCs scaffolds	49
4.2.1	Morphology of scaffolds	51
4.2.2	Porosity	57
4.2.3	ATR-FTIR study	59
4.2.4	TGA measurements	61
4.2.5	DSC study	65
4.2.6	Mechanical properties	68
4.3	In vitro degradation study of HEC/PVA and HEC/PVA/CNCs scaffolds	70
4.3.1	Weight loss, swelling ratio and pH value analysis	70
4.4	Cell culture studies on HEC/PVA and HEC/PVA/CNCs for bone tissue engineering applications	73
4.4.1	hFOB cells proliferation on scaffolds	74
4.4.2	hFOB cells morphology studies on scaffolds	78
CHAPTER 5 CONCLUSION		
5.1	Summary	82
5.2	Recommendations for future studies	83
REFERENCES		84
APPENDIX A SAMPLE APPENDIX 1		



UMP

LIST OF TABLES

Table No.	Title	Page
2.1	Characteristics of scaffolds for tissue engineering application	12
2.2	Past research projects used freeze-drying method	17
3.1	Composition of CNCs in HEC/PVA blended polymer	26
4.1	ATR-FTIR spectral peak assignments for CNC nanoparticle	48
4.2	Porosity of all samples	58
4.3	TGA and DTG for all scaffolds	64
4.4	DSC data for all scaffolds	67
4.5	Mechanical data observed for all scaffolds	69

The logo for UIMP (Universiti Malaysia Perlis) is a large, downward-pointing arrow shape. It is composed of four triangular sections meeting at a central point. The top-left and bottom-right sections are light blue, while the top-right and bottom-left sections are a slightly darker shade of blue. The letters 'UIMP' are printed in a large, white, sans-serif font across the center of the arrow.

UIMP

LIST OF FIGURES

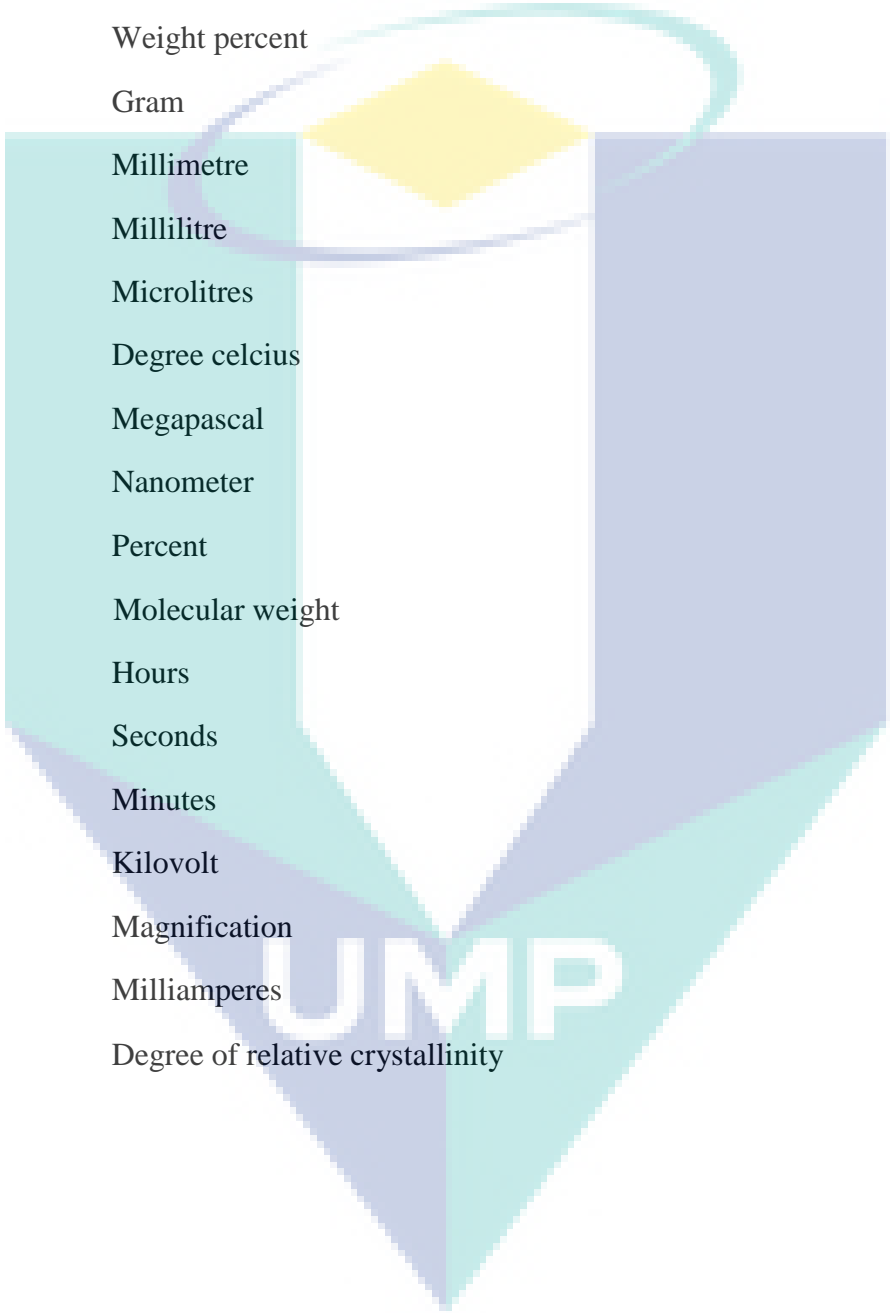
Figure No.	Title	Page
2.1	Bone anatomy cortex: (i) Cancellous bone and (ii) Cortical bone	8
2.2	Cellular components of bone	10
2.3	Molecular structure of HEC	14
2.4	Molecular structure of PVA	14
2.5	Molecular structure of CNC	16
3.1	Flowchart of research methodology implemented in this research	23
3.2	CNC in (a) powder form and suspension	25
3.3	Photograph of freeze-dryer machine, Labconco	27
3.4	Photograph of FESEM, JSM-7800F Extreme-resolution Analytical	29
3.5	Photograph of SEM, FEI QUANTA 450	30
3.6	Photograph of ATR-FTIR, Perkin-Elmer.	31
3.7	Photograph of TGA, Q500.	33
3.8	Photographs of DSC, NETZSCH	33
3.9	DSC thermograms	34
3.10	Photograph of universal testing machine, Shimadzu	35
3.11	Photograph of Horiba LAQUA Handheld Water Quality Analysis Meters	37
3.12	Summarize of cell culture study	38
3.13	hFOB cell in cell culture flask	39

3.14	Cell culture studies of scaffolds at different weight ratios	40
3.15	Photograph of NanoQuant micro plate reader (Infinite M200PRO)	42
3.16	Photograph of EVOS inverted microscope	43
4.1	FESEM micrographs of CNC nanoparticle at (a) low magnification (50,000×) and (b) high magnification (130,000×)	
4.2	ATR-FTIR analysis of CNC nanoparticle	
4.3	DSC thermograms of CNC nanoparticle	
4.4	HEC/PVA and HEC/PVA/CNC (1, 3, 5, 7 wt%) polymeric solutions	
4.5	HEC/PVA and HEC/PVA/CNC (1,3,5,7 wt%) scaffolds	
4.6	SEM micrographs of HEC/PVA at (a) 230×, (b) 1000× and (c) 2000×	
4.7	SEM micrographs of HEC/PVA/CNC (1wt%) at (a) 250×, (b) 1000× and (c) 2000×	
4.8	SEM micrographs of HEC/PVA/CNC (3wt%) at (a) 500×, (b) 1000× and (c) 2000×	
4.9	SEM micrographs of HEC/PVA/CNC (5wt%) at (a) 250×, (b) 1000× and (c) 2000×	
4.10	SEM micrographs of HEC/PVA/CNC (7wt%) at (a) 250×, (b) 1000× and (c) 2000×	
4.11	Porosity of CNC, HEC and PVA alone and HEC/PVA scaffolds with different CNC concentration at (1,3,5 and 7 wt%)	
4.12	ATR-FTIR spectra of CNC, HEC and PVA alone and HEC/PVA scaffolds with different CNC concentration at (1,3,5 and 7 wt%)	
4.13	TGA and DTG curves for (a) HEC/PVA, HEC/PVA/CNC (b) 1wt%, (c) 3wt%, (d) 5wt% and (e) 7wt%	


- 4.14 DSC thermograms of CNC, HEC and PVA alone and HEC/PVA scaffolds with different CNC concentration at (1,3,5 and 7 wt%)
- 4.15 Stress-strain curves for (a) HEC/PVA, HEC/PVA/CNC (b) 1wt%, (c) 3wt%, (d) 5wt% and (e) 7wt%
- 4.16 Weight loss for HEC/PVA scaffolds with different CNC concentration at (1,3,5 and 7 wt%)
- 4.17 Swelling ratio of
- 4.18 pH value analysis of HEC/PVA and HEC/PVA/CNC (1, 3, 5, 7 wt%) porous scaffolds
- 4.19 Graph showing human osteoblast viability after 1, 3, 5 and 7 days of incubation (1×10^5 cells/well in complete DMEM) at different weight ratios of scaffolds
- 4.20 Trypan blue osteoblast cells grown in all scaffolds at (a) 3 days and (b) 7 days under light microscope
- 4.21 SEM micrograph images of hFOB cells attached on after (a) day 3 and (b) day 7 cell culture (black arrow indicates the growth cells)



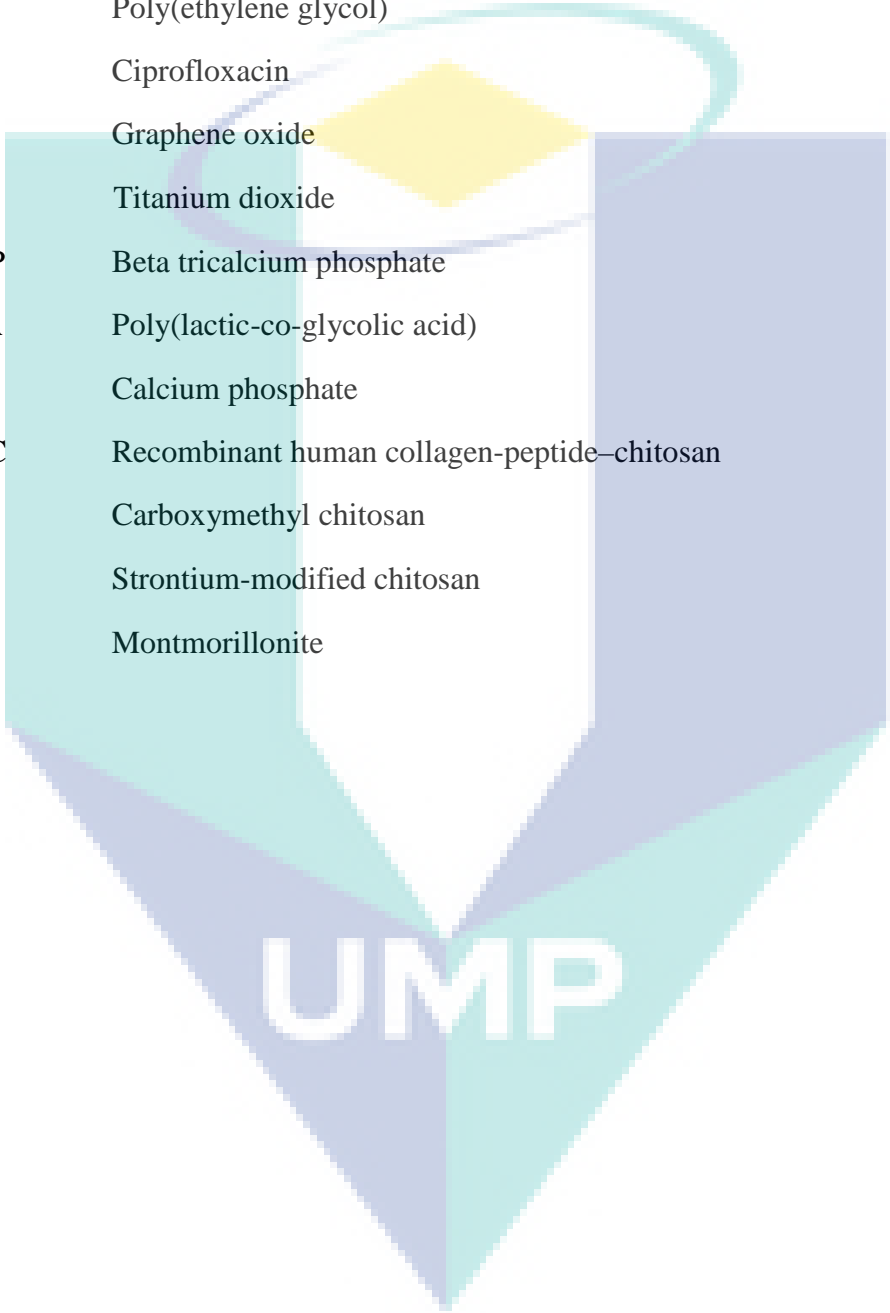
UMP

LIST OF SYMBOLS/UNITS

cm	Centimetres
wt	Weight percent
g	Gram
mm	Millimetre
mL	Millilitre
μL	Microlitres
$^{\circ}\text{C}$	Degree celcius
MPa	Megapascal
nm	Nanometer
%	Percent
M_w	Molecular weight
h	Hours
s	Seconds
min	Minutes
kV	Kilovolt
x	Magnification
mA	Milliamperes
χ_c	Degree of relative crystallinity

LIST OF ABBREVIATIONS

HEC	Hydroxethyl cellulose
PVA	Poly (vinyl alcohol)
CNC	Cellulose nanocrystal
ATR	Attenuated Total Reflectance
FTIR	Fourier Transform Infrared Spectroscopy
FESEM	Field Emission Scanning Electron Microscopy
FTIR	Fourier Transform Infrared
DSC	Differential scanning calorimetry
SEM	Scanning Electron Microscopy
TGA	Thermogravimetric
UTM	Universal Tensile Machine
DTA	Differential thermal analysis
3D	Three-dimensional
ECM	Extracellular matrix
GAG	Glycosaminoglycan
hFOB	human fetal osteoblast cells
PBS	Phosphate buffer saline
DMEM	Dulbecco's Modified Eagle Medium
GA	Glutaraldehyde
DAPI	4,6-diamidino-2-phenylindole
CO ₂	Carbon dioxide
CS	Chitosan
MC	Methylcellulose
ZN	Zein



HAp	Hydroxyapatite
nHAp	Nanohydroxyapatite
SDACNFs	Surface-deacetylated chitin nanofibers
SBE- β -CD	Sulfobutyl ether β -cyclodextrin gel
PEG	Poly(ethylene glycol)
Cip	Ciprofloxacin
GO	Graphene oxide
TiO ₂	Titanium dioxide
β -TCP	Beta tricalcium phosphate
PLGA	Poly(lactic-co-glycolic acid)
CaP	Calcium phosphate
RHCC	Recombinant human collagen-peptide-chitosan
CMC	Carboxymethyl chitosan
Sr-C	Strontium-modified chitosan
MMT	Montmorillonite

CHAPTER 1

INTRODUCTION

1.1 Background

The emergence field of tissue engineering has substantially revolutionized the functionalization of biomaterials, thus overcome the limitation of traditional tissue transplantation (Bhat & Kumar, 2013). Generally, tissue and organ transplantations represent accepted therapies, but they are dramatically limited by donor shortages (Caló & Khutoryanskiy, 2015). Tissue engineering or regenerative medicine promises to solve problems in organ transplantation by utilized the application of chemical, biological and engineering principles to replace or repair the damaged or effected living tissues like bone, cartilage and skin using biomaterials, cells, and growth factors, alone or in combination. The strategies are categorized into three groups which are direct injection of cells into the tissue of interest, implantation of cell-scaffold constructs (3D tissue structure), and scaffold-based delivery of drugs and/or signaling molecules such as growth factors to stimulate cell growth, migration, and differentiation (Kumar et al., 2016).

Next, the most critical factor to be considered in tissue engineering is the interaction of cells with ideal scaffolds, which serve to be the template in order to promote growth of the tissue. Scaffold can be described as a temporary substrate to support the neovascularization and propagation of cells at the defects area of living tissue. In bone tissue engineering, scaffold plays an important role in manipulating the functions of osteoblasts and acts as central role to guide new bone formation into desired shapes (Saber-Samandari, Saber-Samandari, Kiyazar, Aghazadeh, & Sadeghi,

2016). Scaffolds that are being placed and introduced at the defective site should mimic the artificial extracellular matrix (ECM) of human body (Hirano & Mooney, 2004). ECM consists of fibrous collagen and proteoglycans. Proteoglycans are made of proteins and polysaccharide chains known as glycosaminoglycan (GAG). The interaction between the cells and the ECM is very important in biological systems. An ideal scaffold should biodegrade as the native tissue integrates and actively promote desirable physiological responses. Besides, an excellent scaffold should possess porous architecture, produce non-toxic degradation product and should be capable of sterilization without loss of bioactivity and should deliver bioactive molecules in a controlled fashion to accelerate healing. Hence, a suitable material scaffold is very important in all the strategies to engineer tissues.

Biomaterial is known to be a biological or synthetic substance which can be introduced into body tissue to replace or repair damaged tissue. Many natural and synthetic polymers were used as scaffolds due to its biocompatibility and biodegradability. Although there is wide range of biomaterials being fabricated and used as scaffolds, there is only few biopolymers that closely mimic to ECM by having polysaccharide chains in them. The most commonly biopolymer with chemical structure similar to GAGs in ECM is chitosan, which is a biocompatible and widely used in wound healing application (Kousaku Ohkawa, 2004). Other than that, cellulose which can be derived from natural resources such as plant, animal, or mineral plants has the potential to be used in various applications like sensor, biomedical and pharmaceutical and in packaging industries (Edwards, Prevost, Sethumadhavan, Ullah, & Condon, 2013).

Hydroxethyl cellulose (HEC) is a non-ionic with β (1 \rightarrow 4) glycosidic linkage held together with H-bonds. It is a biocompatible water soluble polysaccharide material with protective colloidal action. It is less expensive and commonly used in various pharmaceutical compositions, wound dressing and wound healing applications (Zhang, Nie, Li, White, & Zhu, 2009). In this study, HEC will be mixed with poly (vinyl alcohol) (PVA), a polyhydroxy water soluble polymer. It is biocompatible and biodegradable and widely used in biomedical applications which include drug delivery reservoirs, resorbable surgical sponges and many more. Combination of HEC with

other hydrogel like PVA improves the mechanical properties such as elasticity and elongation (Zulkifli, Hussain, Rasad, & Mohd Yusoff, 2014).

Cellulose nanocrystals (CNCs) have lots of advantages over other nanoparticles such as high surface area, high, non-toxicity, biodegradability and other optical properties. In general studies, CNCs are used to improve various mechanical and barrier properties of various biopolymers (Borkotoky, Dhar, & Katiyar, 2018).

The aim of this research is to elucidate the properties of HEC/PVA scaffolds which incorporated with various concentrations of CNCs produced by freeze-drying technique and its potential as a substrate in bone tissue engineering. According to literature review, HEC/PVA/CNC porous scaffolds have gained less attention as no reliable evidence about the development, which gave us the motivation to carry out this study. Herein, the physical and chemical interactions, and mechanical and thermal properties of scaffolds were characterized by SEM, ATR-FTIR, TGA, DSC and mechanical testing. Besides that, in vitro degradation and cell culture studies were carried out to investigate the biocompatibility of cell-scaffolds as this research was focusing on the bone tissue engineering application.

1.2 Problem statement

The aging population and the increasing numbers of patients suffering from bone defects due to accidents or trauma leads to tremendous demand for bone substitute. The traditional methods that had been introduced since many years ago which are autografts and allografts being used to treat burns or other full thickness skin defects. Autografts have a higher success rate but are limited in supply and may cause donor site morbidity where allografts have always given risk for disease transmission and immunological rejection. Nowadays, scientists and researchers were constantly and continually developing method to overcome the problem arises in traditional methods.

Thus, tissue engineering has emerged as a promising alternative to treat injuries involves scaffolds, cells and biological cues alone or in combination (MacNeil, 2007). In tissue engineering, scaffolds, on which tissue was grown is one of the fundamental structures to be optimized for desired bone implant. Although bone tissue engineering has been the issue of considerable research in the era of regenerative medicine over the

past two decades, many skeletal problems stay undertreated. These might be due to the current high cost of scaffolding technique, incompatible with native tissues, toxicity, and unmatched biodegradable healing periods. For that reason, the requirement for reliable, humane, and ecofriendly scaffold must be given attention in order to investigate a biomimetic scaffold that not only possess biocompatible, biodegradable, non-toxic and neovascularization properties, but also cost-effective and shelf presented. Besides, although intensive studies have been done to find an alternative bone implants, the commercialization of this product is yet to be reached. Due to that motivation, a depth study to develop a new combination of biopolymeric materials is crucial yet favorable, so that the gap between the demand and the lack of supply of orthopedic products could be filled.

1.3 Significance of studies

In this work, HEC/PVA/CNCs polymeric solutions were prepared using deionized water as the only solvent, fabricated using freeze-drying technique and cross linked via heat treatment. This research aims to develop non-toxic, biocompatible, and biodegradable scaffolds since the demands on economical, safe and rapid-healing process of implant tissues or organs are intensely increased by year. It is worth to mention that CNC have garnered a tremendous level of attention in material community due to its unique features. The outcomes of this study may contribute to the medical community especially those who work in bone tissue engineering as well as low and middle-class patients who suffered from bone injuries or defects that prerequisite cost-effective scaffolds with rapid healing response. To the best of our knowledge, this is the first study on the effect of concentration of CNCs in HEC/PVA porous scaffolds, characterized, and applied in the bone tissue engineering application. This research may give contribution to the development of tissue engineering products in healthcare industry.

1.4 Research objective

The objectives of this research are:

1. To produce CNC from cellulose pulp and characterize the physical, chemical and thermal properties of CNC.
2. To fabricate HEC/PVA porous scaffolds incorporated with CNCs as nanofillers using freeze-drying technique.
3. To study the effect of various concentrations of CNCs in HEC/PVA scaffold based on the physical and chemical interaction, thermal and mechanical properties.
4. To investigate the biocompatibility of HEC/PVA/CNC scaffolds as a potential substrate for bone tissue engineering application.

1.5 Research scope

The following research scopes are essential to achieve the first objective:

- i. To prepare CNC from cellulose pulp using acid hydrolysis.
- ii. To observe the image of CNC using FESEM and measure its dimensions by using ImageJ software.
- iii. To identify the functional groups of CNC using ATR-FTIR spectra.
- iv. To study the thermal stability of CNC using DSC.

The following research scopes are necessary to achieve the second and third objectives:

- i. To observe the surface morphology of all scaffolds via SEM images and measure the pore size by ImageJ software.
- ii. To identify the functional groups of all scaffolds using ATR-FTIR spectra.
- iii. To study the thermal stability and decomposition behavior of scaffolds using TGA and DSC.
- iv. To study the mechanical strength of scaffolds by analyzing the stress-strain curves using UTM.

- v. To investigate the degradation behavior of porous scaffolds in PBS at different time points. The analysis will involve pH changes of the solution, weight loss and swelling ratio.

Finally, the following research scopes are necessary to achieve the fourth objective:

- i. To investigate the cellular biocompatibility by carrying out in vitro cell culture studies using human fetal osteoblast (hFOB) cell.
- ii. To determine the adherence, differentiation and proliferation of hFOB cells on the scaffolds using MTT assays by measuring the absorbance value and observe the surface morphology changes by SEM.
- iii. To identify the optimum concentration of CNCs in HEC/PVA scaffolds that display better responsive towards hFOB cells.

1.6 Thesis outline

The following is a brief outline regarding the contents of this thesis. Chapter 2 provides a comprehensive overview on related topics to this study including recent research on bone tissue engineering and details of polymeric materials involved in this project. In Chapter 3, the research methodology will be stated including the materials used and experimental method applied in this research. The working principle of each instruments used for characterization will be also mentioned. Next, Chapter 4 will be discussed the synthesis and characterization of CNC and all scaffolds including the cell culture studies for bone tissue engineering application. Finally, in Chapter 5, the summary of this research and the recommendations for future reference will be discussed.

CHAPTER 2

LITERATURE REVIEW

2.1 General function of bone

Bone is a special form of connective tissue. There are four categories of bones which are long bones (e.g. ulnae, fibulae), short bones (e.g. carpal, tarsal), flat bones (e.g. skull, rib), and irregular bones (e.g. vertebrae, sacrum). (Clarke, 2008). Generally, bone is known as a multifunctional tissue that is important for mechanical support and protection. Our bone provides structural support for the body and protects the internal organs including lungs, heart, brain and spinal cord. Besides that, it supports hematopoiesis in bone marrow. The hematopoiesis is defined as the lifelong process of continuous formation and turnover of blood cells to meet everyday demands as well as respond to increased demand, for example, injury or infection (Hoggatt & Pelus, 2013). As vascularized tissues, bone acts as the basis of posture and locomotion by allowing the attachments of muscles, ligaments, and tendons. Finally, the bone serves as a mineral reservoir and in particular helps regulate calcium homeostasis.

Bone matrix acts as a reservoir for a number of minerals important to the functioning of the body, especially calcium, and potassium. These minerals, incorporated into bone tissue, can be released back into the bloodstream to maintain levels needed to support physiological processes. Calcium ions, for example, are essential for muscle contractions and controlling the flow of other ions involved in the transmission of nerve impulses.

2.1.1 Structural and mechanical properties of bone

The adult human skeleton has a total of 213 bones, excluding the sesamoid bones. The appendicular skeleton has 126 bones, axial skeleton 74 bones, and auditory ossicles 6 bones. Each bone constantly undergoes modeling during life to help it adapt to changing biomechanical forces, as well as remodeling to remove old, microdamaged bone and replace it with new, mechanically stronger bone to help preserve bone strength (Clarke, 2008).

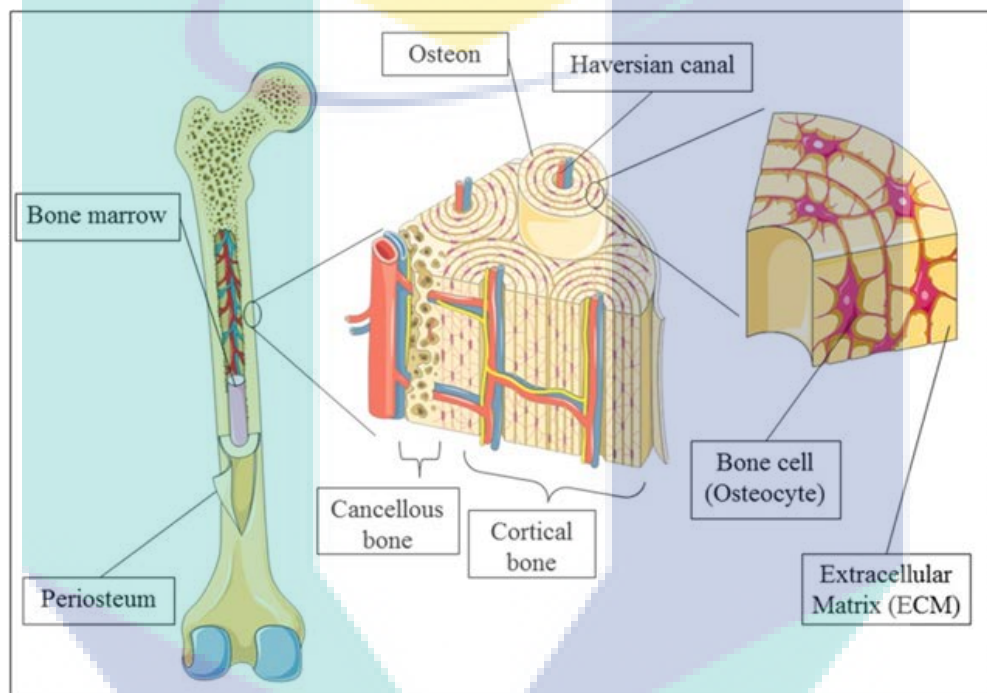


Figure 2.1 Bone anatomy cortex: (i) Cancellous bone and (ii) Cortical bone
(Source: <https://www.pinterest.com>)

Figure 2.1 shows the bone anatomy cortex. Bones contain compact (cortical) and spongy (cancellous) tissue, but their distribution and concentration vary based on the bone's overall function. Compact bone is denser and can be found under the periosteum and in the diaphysis of long bones, where it provides support and protection by withstand compressive forces, while spongy bone has open spaces and supports shifts in weight distribution. The compressive strength of (i) cancellous bone is $\sim 7\text{--}10$ MPa and for the (ii) cortical bone is $\sim 170\text{--}193$ MPa, respectively (Kumar et al., 2016).

Therefore, to ensure the stability of implant, it is crucial to have a biomaterial with mechanical properties that is more or less similar to the bone.

There are four types of cells in bones which are osteocytes, osteoclasts, osteoblasts and osteoprogenitor cells. However, in different locations in bones, these cell types have different functions. Osteoblast, which is found in the growing portions of bone, including endosteum and periosteum, is responsible for forming new bone. These cells do not divide, synthesize and secrete the collagen matrix and calcium salts. With the secreted matrix surrounding the osteoblast calcifies, osteoblast becomes trapped within it. And then, its structure changes, becoming an osteocyte, which is the primary cell of mature bone and the most common type of bone cell. With the help of secretion of enzymes, osteocytes can maintain the mineral concentration of the matrix.

The most important cell is osteogenic cell, which is undifferentiated with high mitotic activity, is the only bone cells that are capable of dividing. It plays very crucial role when the function of mitosis of osteoblasts and osteocytes disappeared. As for the osteoclasts, they continually break down old bone when osteoblast cells are forming new bone. This function is really necessary in maintenance, repair and remodeling of bones of the vertebral skeleton.

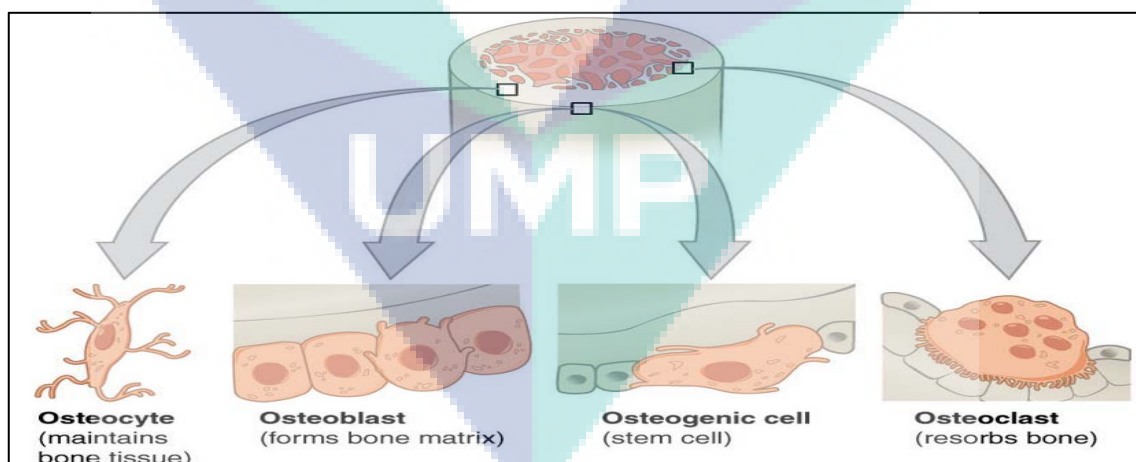


Figure 2.2 Cellular components of bone (Source: <https://teachmeanatomy.info/the-basics/ultrastructure/bone>)

2.2 Bone tissue engineering

Bone tissue engineering involves the improvement or replacement of specific tissues or organs by engineered the bio-based materials to restore, remain or/and improve the function of the injured/affected tissues (Caló & Khutoryanskiy, 2015). This scaffold served as a template for tissue formation by allowing cells to migrate, adhere, and produce tissue. Unlike many other tissues in the body, bones possess the property of regeneration and remodeling in response to injury. Bone remodeling is influenced by the calcium levels in the blood and the pull of muscles on bone (Preethi Soundarya, Sanjay, Haritha Menon, Dhivya, & Selvamurugan, 2018). Primary bone is defined as new bone formed in a space where previously no bone existed, or formed on an existing surface of bone or mineralized cartilage. Thus, primary bone requires only bone formation, whereas secondary bone is defined as bone which is produced by the resorption of previously deposited bone followed by the formation of new bone in its place, a process called remodelling.

From the literature review, it is reported that there are millions of patients suffering from the loss or failure of an organ or a tissue caused by an accident or a disease every year. Over 8 million surgeries are conducted to treat these patients in the United State, U.S. each year, and the overall cost of these issues to the U.S. economy is estimated to be around \$400 billion per year. With increasing numbers of bone injuries cases reported, tissue engineers face one of the biggest challenges in order to come out with a new and advance invention with low cost consuming. Solutions to these problems will significantly advance tissue engineering and regenerative medicine.

2.3 Biomaterials in tissue engineering

Biomaterial can be classified into two categories; (i) natural and (ii) synthetic polymers. Natural polymers such as collagen, fibrin, chitosan and starch exhibit good biocompatibility and some osteoconductive properties but suffer from some disadvantages. Due to that, synthetic polymers are preferred over natural polymers (Gavasane, 2014). The use of natural polymer is limited due to their low stability in aqueous environment, difficulty to be electrospun and very low mechanical stability (Schieker, Seitz, Drosse, Seitz, & Mutschler, 2006).

The synthetic polymers are categorized into biodegradable and non-biodegradable polymers. The selection of a polymer is a challenging task because of the inherent diversity of structures and thus it requires a thorough understanding of the surface and bulk properties of the polymer that can give the desired chemical, interfacial, mechanical and biological functions. Biodegradable polymers are currently being investigated as drug delivery systems or as scaffolds for tissue engineering. Polymers possess a unique strength in tissue engineering which enables the new advancement in human bone system which improves the therapy and treatment. Biodegradable polymers have proven their potential for the development of new, advanced and efficient in this field (Gavasane, 2014).

In addition, the use of biodegradable polymers as scaffolds on which layers of cells are grown is an alternate tissue-engineering approach for the development of a functional bone tissue. The scaffold degrades and is replaced and remodeled by the ECM secreted by the cells. An alternative strategy to synthetic and degradable scaffold is the manipulation of proteins that constitute the architecture of native ECM. Ultimately, the success of this approach is dependent on appropriate cell migration, adhesion and proliferation, as well as ECM production, on the biomimetic surfaces.

2.3.1 Evolution of biomaterials

Previously, osteoporosis caused by either trauma or diseases which are categorized as the bone fractures and skeletal disorders are traditionally treated by reconstructed the bone using permanent or/and temporary implant which involve the usage of titanium, alloys and stainless steel. The mechanical properties and materials of implants must be suitable for long term performance under physiological condition. Nowadays, composite materials such as ceramics and polymers become the better choices as bone tissue engineering scaffolds, since natural bone matrix is an organic/inorganic composite material. Composite materials often show an excellent balance between strength and toughness, and usually have characteristics that are improvements on those of their individual components. Besides having enough mechanical strength to provide structural support, the scaffold's material must be biocompatible and osteoconductive. Materials that have been documented and used most often in scaffold fabrication include sodium alginate (Sultan & Mathew, 2018),

chitosan (Kavitha Sankar, Rajmohan, & Rosemary, 2017), cellulose (Butylina, Geng, & Oksman, 2016), and hydroxyapatite (Saber-Samandari et al., 2016).

2.3.2 Characteristics of biomaterials scaffold

An excellent scaffold should possess some important characteristics to meet the criteria. All characteristics are presented in Table 2.1 as follows.

Table 2.1 Characteristics of scaffolds for tissue engineering application.

Characteristic	Explanations
Biocompatibility	Scaffold must elicit a negligible immune reaction in order to prevent it causing such a severe inflammatory response that it might reduce healing or cause rejection by the body.
Biodegradability	Scaffolds and constructs, are not intended as permanent implants. The scaffold must therefore be biodegradable so as to allow cells to produce their own extracellular matrix. The by-products of this degradation should also be non-toxic and able to exit the body without interference with other organs.
Scaffold architecture	Scaffolds should have an interconnected pore structure and high porosity to ensure cellular penetration and adequate diffusion of nutrients to cells within the construct and to the extra-cellular matrix formed by these cells. Furthermore, a porous interconnected structure is required to allow diffusion of waste products out of the scaffold, and the products of scaffold degradation should be able to exit the body without interference with other organs and surrounding tissues.
Mechanical properties	The implanted scaffold must have sufficient mechanical integrity to allow surgical handling during implantation and to function from the time of implantation to the completion of the remodeling process.

Manufacturing technology	In order for a particular scaffold or tissue engineered construct to become clinically and commercially viable, it should be cost effective and it should be possible to scale-up from making one at a time in a research laboratory to small batch production.
--------------------------	---

2.3.3 Hydroxyethyl cellulose (HEC)

HEC is a white or light yellow fibrous or powdery solid, tasteless and nontoxic, prepared from the alkaline cellulose and ethylene oxide (or chlorine ethanol) by etherification, and belongs to non-ionic soluble cellulose ethers. HEC is a non-ionic hydrophilic polysaccharides biopolymers with $\beta(1\rightarrow4)$ glycosidic linkage. HEC groups attach to the OH groups of the polysaccharide structure by ether linkages as shown in Figure 2.3. This hydrogel functions as a stabilizing and protective colloid. HEC is widely used in cosmetic, pharmaceutical and wound healing applications. It is well known that these types of hydrogels with large amount of water diffused in three dimensional polymeric networks are highly needed in biomedical and health applications. Cross-linking these hydrogels by various chemical bonds and physical interactions can significantly improve their mechanical, thermal and chemical properties.

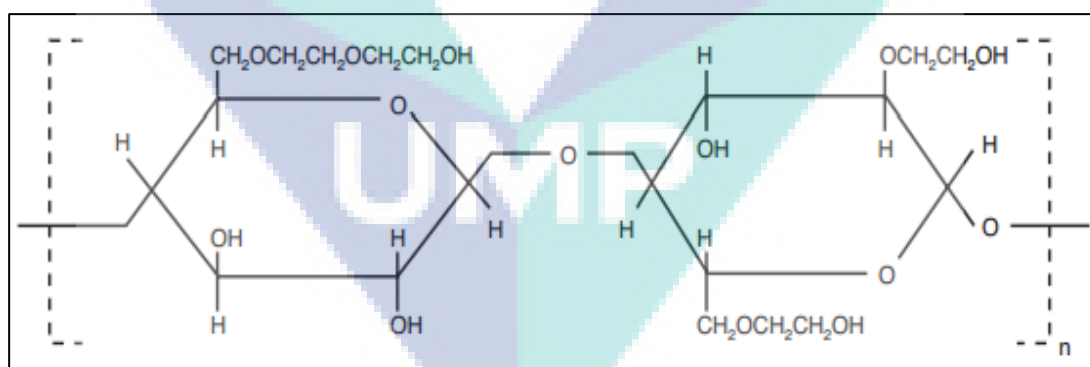


Figure 2.3 Molecular structure of HEC

2.3.4 Poly (vinyl alcohol) (PVA)

Poly (vinyl alcohol) (PVA) has excellent film- and fiber-forming, emulsifying, surfactant and adhesive properties. It is also utilized to fabricate unique porous

scaffolds composition matrix polymers. PVA is odorless and nontoxic, and has high tensile strength and flexibility, as well as high oxygen and aroma barrier properties. All of these properties ultimately depend on the humidity of PVA (with higher humidity more water is absorbed). The water, which acts as a plasticizer, will reduce tensile strength, but increase the material's elongation and tear strength. PVA has a melting point of 230 °C and 180 and 190 °C for the fully hydrolyzed and partially hydrolyzed grades, respectively. PVA decomposes rapidly above 200 °C as it can undergo pyrolysis at high temperatures (Gokmen et al., 2015). In previous research, the development of 3D structure with well-interconnected porous architecture was successfully fabricated by mechanical stirring of PVA solution followed by freeze-drying (Ye, Mohanty, & Ghosh, 2014).

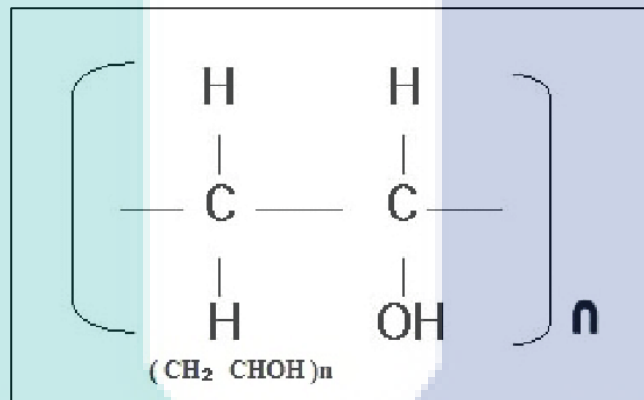


Figure 2.4 Molecular structure of PVA

2.3.5 Cellulose nanocrystal (CNC)

Cellulose is the world's most abundant renewable polymer resource and has been used as an engineering material for thousands of years. By extracting cellulose at the nanoscale, the majority of the defects associated with its hierarchical structure can be removed, and a new generation of material–cellulose nanoparticles can be obtained, which is an ideal material to base the new biopolymer nanocomposite industry. The preparation of reinforced polymer materials with cellulose nanoparticles has seen rapid advances and considerable interest in the last decade owing to its renewable nature, high mechanical properties, and low density, as well as its availability and the diversity of its sources.

Cellulose nanocrystals (CNCs) is produced when cellulose is subjected to acid hydrolysis from wide variety of natural sources such as wood, grass stalks, bacteria and alga. When cellulose is subjected to pure acid hydrolysis treatment, the amorphous regions of cellulose microfibrils are selectively hydrolysed under certain conditions, as they are more susceptible to being attacked by acids in contrast to the crystalline domains. Consequently, these microfibrils break down into shorter crystalline parts with a high degree of crystallinity (Youssef Habibi, 2009).

CNCs have attracted great attention due to their high aspect ratio (3 to 5 nm wide, 50 to 500 nm in length) and high crystallinity (54 to 88 %) (C. Zhang et al., 2015). In addition, CNCs are highly hydrophilic with a multitude of hydroxyl groups available, which can offer binding sites for bone cells and make it superior to other materials such as collagen and silk fibroin. Although CNCs are not capable of being degraded in the human body, it is highly biocompatible which will not cause any inflammatory response after implanting (Huang et al., 2019). Due to that, CNCs has become promising raw material for new bio based composites and potential for some applications including reinforcing filler for polymers. Apart from their use as reinforcing filler for polymers, it have been used to fabricate a wide range of other functional materials such as transparent barrier films, optical and electronic devices, drug carriers and many more (Sofla, Brown, Tsuzuki, & Rainey, 2016).

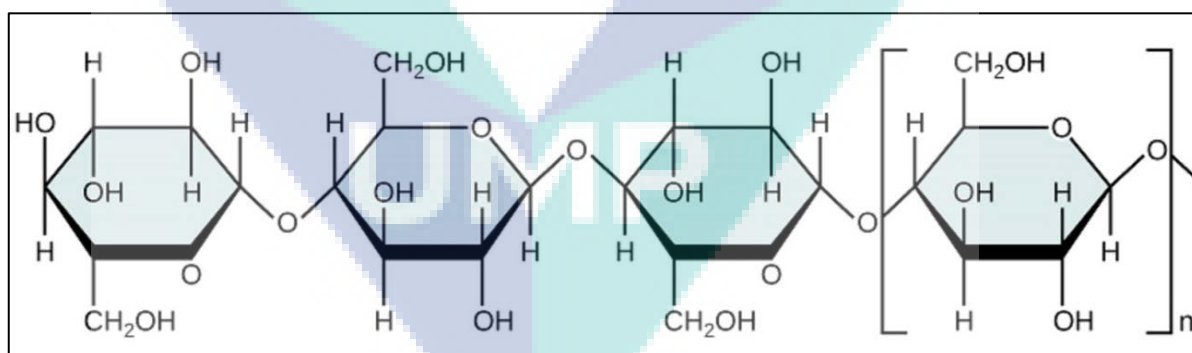


Figure 2.5 Chemical structure of cellulose

In order to enhance certain properties or create new functionalities, a wide variety of materials may be used to fabricate scaffolds. For instance, one of the common problems with hydrogel biomaterials is their poor mechanical properties. Thus, by incorporating nanobiomaterials into the polymer blend, the mechanical properties of

materials could be enhanced (Jia An, 2013). As shown by Kai et al (2012), incorporation of poly(ϵ -caprolactone) nanofibers into gelatin hydrogel resulted in the increase of the Young's modulus of the composite hydrogels from 3.29 to 20.3 kPa (Kai et al., 2012). Other than that, previous research is done by Zulkifli et al. (2014) where HEC/PVA nanofibers were successfully fabricated using electrospinning method revealed that the scaffolds could be potential substrates for skin tissue engineering (Zulkifli et al., 2014). In this research, incorporation with CNC into HEC/PVA polymer blended is expected to enhance the properties of scaffolds and could promote cell growth for bone tissue application.

2.4 Fabrication of scaffolds

From year to year, researchers from all over the world kept find a way to produce scaffolds made of biomaterials that mimic those found in the natural environment, with multi-functional properties, such as improving cell adhesion, proliferation, and differentiation. Researchers are focusing on developing and improving new materials to imitate the native biological neighborhood as authentically as possible. The most promising is a combination of cells and matrices (scaffolds) that can be fabricated from different kinds of materials (Chocholata, Kulda, & Babuska, 2019).

The fabrication of porous scaffolds from various polymers that could mimic the natural ECM structure have been extensively explored for decades. Some of the techniques include gas-forming foam, three-dimensional printing, solvent casting/particulate leaching, thermal-induced phase separation, freeze-drying and electrospinning (Saber-Samandari et al., 2016). In this research, freeze-drying technique is used in order to obtain highly porous scaffold that is highly favorable and suitable for cell adhesion, proliferation and differentiation for regenerative medicine applications.

2.4.1 Freeze-drying technique

Freeze drying can be describe as the technique used to improve the physical and chemical stability of colloidal nanoparticles by removal of water from the aqueous dispersionsto obtain them in a dried form (Ali & Lamprecht, 2017). As this method has proven a time- and energy-consuming method, a lot of research is invested into

shortening and optimizing freeze-drying processes. The lyophilization or freeze drying is frequently based in empirical principles, without considering the physical-chemical properties of formulations and the engineering principles of lyophilization. Therefore, the optimization of formulations and the lyophilization cycle is crucial to obtain a good lyophilizate, and guarantee the preservation of nanoparticles (Fonte, Reis, & Sarmiento, 2016). Table 2.2 summarized some of the research that has been done using freeze-drying method to get scaffold.

Table 2.2 Past research projects used freeze-drying method

Biomaterials	Application	Authors	Year
CS/PVA/MC	Tissue engineering	(Kanimozhi, Khaleel Basha, & Sugantha Kumari, 2016)	2016
PVA/CNF	Nanocomposite	(Salehpour, Rafieian, Jonoobi, & Oksman, 2018)	2018
ZN/CS/nHAp	Bone tissue engineering	(Shahbazarab, Teimouri, Chermahini, & Azadi, 2018)	2018
SDACNFs/SBE- β -CD	Wound dressing applications	(Tabuchi et al., 2016)	2016
PVA/PEG/Cip	Drug control release	(Zhou et al., 2016)	2016
GO/CS/HAp	Bone tissue engineering	(Yılmaz, öztürk Er, Bakırdere, ülgen, & özbek, 2019)	2019
TiO ₂ /CS/HAp	Bone tissue	(Abd-Khorsand, Saber-Samandari, &	2017

	engineering	Saber-Samandari, 2017)	
Gelatin/CS	Skin tissue engineering	(Alizadeh, Abbasi, Khoshfetrat, & Ghaleh, 2013)	2013
Silk fibroin protein	Soft tissue engineering	(Bhardwaj, Chakraborty, & Kundu, 2011)	2011
PCL/ZN	Drug delivery	(Fereshteh, Fathi, Bagri, & Boccaccini, 2016)	2016
β -TCP/chitin/gelatin	Tissue engineering	(Geetha, Premkumar, Pradeep, & Krishnakumar, 2019)	2019
CNF/PVA	Skin tissue engineering	(Ghafari, Jonoobi, Amirabad, Oksman, & Taheri, 2019)	2019
PLGA/gelatin	Artificial peripheral nerve	(Ghorbani, Zamanian, & Nojehdehian, 2017)	2017
Calcium silicate scaffold loaded by celecoxib drug	Bone tissue engineering	(Kordjamshidi, Saber-Samandari, Ghadiri Nejad, & Khandan, 2019)	2019
CS and multiphasic CaP	Bone tissue engineering	(Mohammadi, Mesgar, & Rasouli-	2016

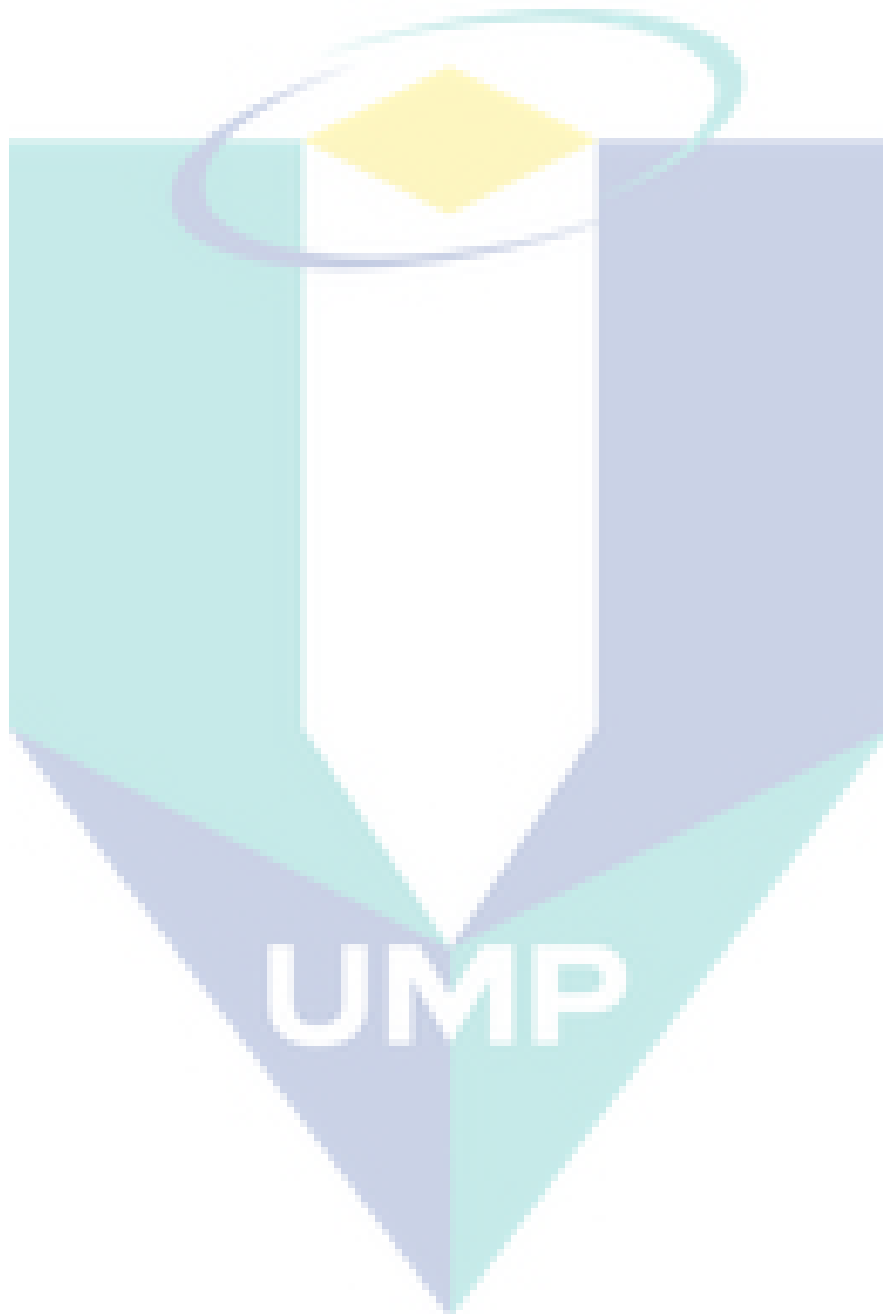
		Disfani, 2016)	
CS	Cartilage tissue engineering	(Reys et al., 2017)	2017
diopside/HAp	Tissue engineering	(Sayed, Mahmoud, Bondioli, & Naga, 2019)	2019
CaP	Tissue engineering	(Shazni, Mariatti, Nurazreena, & Razak, 2016)	2016
RHCC	Tissue engineering	(J. Zhang et al., 2015)	2015
PLGA/carbonated apatite	Bone tissue engineering	(ScharDOSim et al., 2017)	2017
Gellan and guar gum with HAp	Bone tissue engineering	(Anandan, Madhumathi, Nambiraj, & Jaiswal, 2019)	2019
Gelatin/CMC/nHAp	Bone tissue engineering	(Maji, Agarwal, Das, & Maiti, 2018)	2018
HAp-gelatin with dexamethasone loaded PLGA microspheres	Hard tissue engineering applications	(Ghorbani, Nojehdehian, & Zamanian, 2016)	2016

HEC/PVA	Skin tissue engineering	(Zulkifli, Hussain, Harun, & Yusoff, 2019)	2019
Titanium	Bone tissue engineering	(Yan et al., 2017)	2017
CS/HAp	Tissue engineering	(Qasim et al., 2017)	2017
Silk fibroin/hyaluronic acid/sodium alginate	Wound dressing for skin repair	(Yang et al., 2019)	2019
Sr-C/MMT	Bone tissue engineering	(Koc Demir, Elcin, & Elcin, 2018)	2018

2.5 Summary

To summarize, an amount of research has been undertaken to find the ideal scaffolds for bone tissue engineering applications. Although many products are commercially available in the market, there are still limitations in several criteria such as high costs, history of unsuccessful treatments, weak tensile properties, toxicity and instability during storage. In addition, most biomaterial polymers are found to dissolve the polymers. Regular or high exposures to organic solvents may induce environmental contamination as well as toxicity and general hazards to the workers. This research aims to fabricate HEC/PVA/CNC using deionized water as the only solvent and then investigate their potential as scaffolds in bone tissue engineering applications. By using extremely simple methods which is freeze drying, scaffolds produced *via* a 'green' environmentally friendly approach are easy and capable of processing in a large scale. To the best of our knowledge, this is the first report where CNC is synthesized and then followed by fabrication of HEC/PVA/CNCs scaffolds via freeze-drying methods. All the characterization will be studied based on the application in bone tissue regeneration. In this study, CNC nanoparticle is chosen as additive polymers due to their biocompatibility, biodegradability and non-toxicity properties that offer better cell

adherence, differentiation and proliferation on the scaffold's surfaces. All scaffolds will undergo an in vitro cell culture study by using human fetal osteoblast cells.



CHAPTER 3

METHODOLOGY

3.1 Research methodology

This chapter discussed clearly about the whole process of the research. All materials and methods that have been applied in this research were explained in details starting with research methodology including the flow chart of this research, until the fabrication and characterizations of porous scaffolds and the procedures involved in the cell-culture experiment.

Figure 3.1 shows the details of flow chart about this research. Freeze-drying method was conducted in order to obtain a highly porous scaffold. Firstly, CNCs were extracted from cellulose by acid hydrolysis and the aqueous polymeric solutions of HEC, PVA with various concentrations of CNCs were prepared by dissolving all the solutions in deionized water until obtained a homogenous solution. Then, the porous freeze-dried scaffolds were characterized based on their physical, chemical, thermal and mechanical properties. Finally, cell culture studies were carried out to observe the cell compatibility

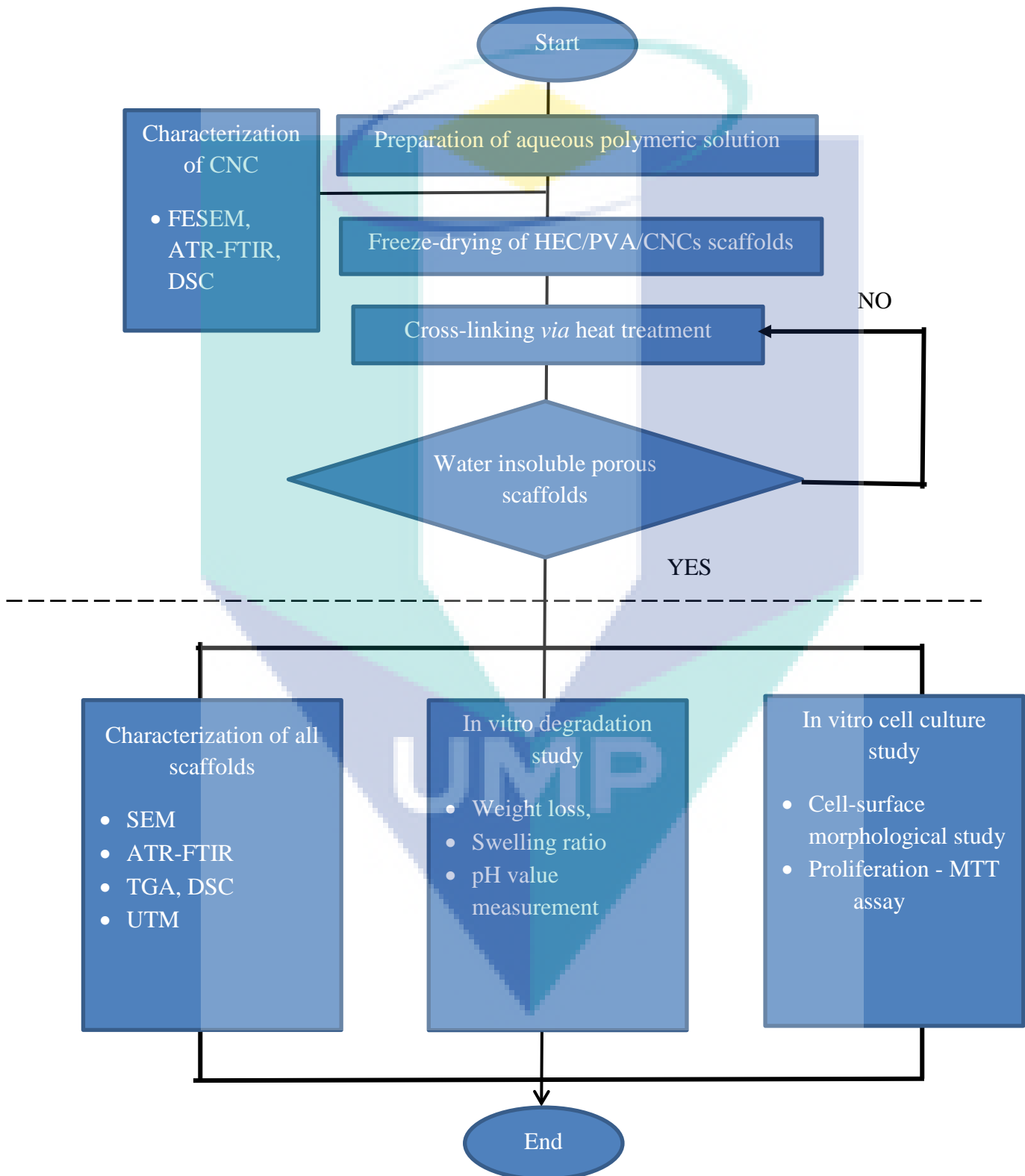


Figure 3.1 Flowchart of research methodology implemented in this research

3.2 Raw materials

PVA ($M_w = 95,000$) was purchased from ACROS, New Jersey, USA. HEC ($M_w = 250,000$) and glutaraldehyde (GA) solution (25 %) were purchased from Merck-Schuchardt, Germany. Phosphate buffer saline (PBS) was purchased from Gibco Life Technologies, USA and Dulbecco's Modified Eagle Medium (DMEM) was purchased from Life Technologies, USA. Human fetal osteoblast (hFOB) 1.19 (ATCC® CRL-11372™), SV4D large T-antigen transfected was supplied from American Type Culture Collection (ATCC), USA for cell culture studies part. All chemicals were characterized by analytical purity and applied without further treatment. All the solutions were prepared using Millipore water.

3.3 Synthesis of CNC

Firstly, 65% concentrated sulphuric acid solution were prepared. Equation 3.1 shows on how to calculate the correct amount of solution needs.

$$C_1V_1 = C_2V_2 \quad (3.1)$$

For 65% of sulphuric acid;

$$C_1V_1 = C_2V_2$$

$$95(V_1) = 65(1 \text{ l})$$

$$V_1 = 0.684 \text{ ml (amount of sulphuric acid in 1 l of deionized water)}$$

Next, a 100 mL of 65 % sulphuric acid was heated at 85 °C for 30 minutes with 10 g of EFB to make 10 mL/g cellulose suspension. After heating, the suspension was directly put into ice to stop the reaction and diluted them with 6 folds of deionized water. Then, the diluted suspension was stored in the 2 mL Schott bottle. The cellulose suspension was divided into 45 mL of centrifuge tube and then undergoes centrifuged in order to increase the pH value in the solution. This step was repeated until the solution reached pH 5 or greater than that, respectively. Next, the suspension was sonicated for 30 minutes to get the homogenous solution with constant pH value. Finally, the suspension is kept in the freezer at ~ -80 °C for 48 hours. The frozen samples were lyophilized in a freeze-dryer where water was removed from the sample by primary drying (sublimation process). In secondary drying, the sample was dried under the atmospheric pressure by desorption process.

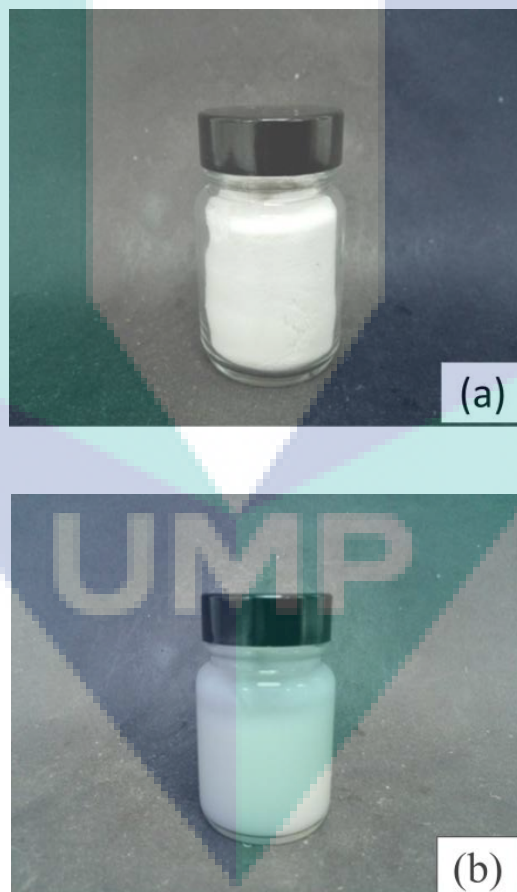


Figure 3.2 CNC in (a) powder form and (b) suspension

3.4 Preparation of polymeric solution

Firstly, HEC (5 wt%) solution was prepared by dissolving 5 g of HEC powder in 100 ml of Millipore water and stirred for 14 h at room temperature until the solution became clear and thickened as the viscosity were slightly increased. In the meantime, 15 g of PVA granules were dissolved in 100 ml of Millipore water and stirred for about 2 h at 80 °C for fasten the time taken to dissolve the granules completely. PVA (15 wt%) solution were kept cool at room temperature and stirred continuously for another 12 h to ensure complete mixing. Then, HEC and PVA solution were mixed together with ratios 50:50 and then stirred overnight to get a homogeneous mixture. Finally, cellulose suspension as shown in Figure 3.2 was added into HEC/PVA blended polymer with different concentration for ternary blend system and stirred continuously for 24 h to get homogenous blend solution. The compositions of HEC/PVA modified with CNCs are presented in Table 3.1.

Table 3.1 Composition of CNCs in HEC/PVA blended polymer

HEC (ml)	PVA (ml)	CNC (ml)	CNC (wt%)
		0	0
		1.5	1
75	75	4.5	3
		7.5	5
		10.5	7

3.5 Fabrication of HEC/PVA/CNC porous material using freeze-drying method

Freeze-drying or lyophilization is the process of drying materials in the frozen state. This fabrication method is widely used especially in the laboratory and in industrial processes for the concentration, storage, and distribution of biological materials. Samples to be lyophilized should be aqueous solutions and there is a variety of containers are suitable for lyophilization. A proper container should withstand the

outside pressure during lyophilization under high vacuum, and should be made of a material that allows a reasonable transfer of heat from outside to inside. The most commonly used containers in the laboratory are glass ampules and round-bottom flasks.

Freeze-drying were basically involved in three main steps which are freezing, primary drying and secondary drying. At freezing step, the polymeric solutions were frozen at a low temperature in the freezer. Then, at the primary drying step, the temperature was raised under vacuum where the water is removed by direct sublimation from the frozen samples in freeze-drying machine. In order to have a good freeze-drying practice and to avoid samples from collapse, it is better to keep the product temperature below the glass transition temperature, T_g or slightly higher collapse temperature, T_c of the product during primary drying (Kasper, Winter, & Friess, 2013). At the final step, which is secondary drying step, the elimination of the adsorbed water from the sample were occurred, which did not sublime upon primary drying because was not previously separated as ice during freezing (Fonte et al., 2016).

In this recent research, the scaffolds were fabricated by pouring the aqueous polymeric solutions into the falcon tube and kept in a deep freezer at $-80\text{ }^{\circ}\text{C}$ for 24 h. Then, the samples were lyophilized at $-50\text{ }^{\circ}\text{C}$ for 72 h in a freeze-dryer (FreeZone 6 Liter Benchtop Freeze Dry System, Labconco) as shown in Figure 3.3.



Figure 3.3 Photograph of freeze-dryer machine, Labconco

3.6 Samples crosslinking

All samples were under went heat treatment at 80 °C for 30 minutes in a vacuum oven. Water resistance of the scaffolds was evaluated in which the scaffolds were taken off from the falcon tube and then immersed them in distilled water. After proving that the scaffolds were not soluble or degrade in a short period of time, all the samples were dried in a vacuum oven and then kept in the dry box for further use.

3.7 Characterization of CNC nanoparticle and HEC/PVA/CNCs scaffolds

For CNC characterization, FESEM is used to observe its morphology. The chemical structural of CNC is carried out using ATR-FTIR, and then DSC is used to observe the thermal properties of CNC. Next, the morphology of HEC/PVA and HEC/PVA/CNC (1, 3, 5 and 7 wt%) scaffolds were studied by using SEM. Meanwhile, ATR-FTIR is performed to chemically confirm the presence of CNCs inside the matrices of all blended scaffolds. The thermal and mechanical properties were measured by DSC, TGA and UTM to evaluate the effect of CNC in HEC/PVA.

3.7.1 Field emission scanning electron microscope (FESEM)

FESEM is a powerful instrument for analyzing topographic at nano-scale levels. It uses windows XP-based computerized operating system with high-resolution digital processing capacity. In this present study, the dimensions of CNCs nanoparticles were observed by using FESEM. Figure 3.4 shows the JSM-7800F Extreme-resolution Analytical FESEM that has been used in this research. This equipment provides images at very high magnification and resolution (1.3 nm @ 30 kV). For this study, the range of magnification used is between 10 000 × to 150 000 ×.



Figure 3.4 Photograph of FESEM, JSM-7800F Extreme-resolution analytical

3.7.2 Scanning electron microscope (SEM)

The observation on the morphology and porosity of the lyophilized scaffolds can be easily carried out by SEM. In bone tissue engineering, study on the surface of scaffolds is important to observe the actual morphology, pore structure and adherence of cells, as initial indications of potential tissue scaffolds.

The FEI ESEM Quanta 450 FEG is a versatile scanning electron microscope with three imaging modes which are high vacuum (HV), low vacuum (LV) and environmental SEM (ESEM) mode. HV mode is a conventional SEM mode with the need of conventional specimen preparation, while in the LV mode electrically non-conductive samples can be imaged without the need of a conductive layer such as carbon and gold. Whereas, in the ESEM mode, wet samples can be investigated in their natural state. The thermally assisted field emission gun (FEG) delivers high brightness of the electron beam and high imaging resolution.

In this present study, the surface morphology of all scaffolds was observed using FEI QUANTA 450 as shown in Figure 3.5 at an accelerating voltage of 15 kV. To

have a better SEM images without giving bad effect to the images produced especially on scaffold's pore size, the scaffolds need to be cut right after applying liquid nitrogen all over the materials. Then, the samples were sputter coated with a thin layer of platinum in double 30 s consecutive cycles at 45 mA to reduce charging and produce conductive surfaces. Based on the SEM images produced, the pore sizes were analyzed using image visualization software, ImageJ.



Figure 3.5 Photograph of SEM, FEI QUANTA 450

3.7.3 Porosity study

The porosity of scaffolds was measured by using liquid displacement method. All samples were cut $1\text{ cm} \times 1\text{ cm} \times 1\text{ cm}$, weighed and then immersed in deionized water as the displacement liquid for 30 min in a falcon tube. This method is based on the known volume before immersed of sample (V_1) in a falcon tube, the unknown volume after 30 min immersed sample (V_2) and the volume after removing of impregnated sample (V_3). The porosity of the sample can be calculated by the Equation 3.2.

$$\text{Porosity (100\%)} = \frac{V_1 - V_3}{V_2 - V_3} \times 100\% \quad (3.2)$$

3.7.4 Attenuated total reflectance-Fourier Transform Infrared Spectroscopy (ATR-FTIR)

Fourier Transform Infrared Spectroscopy (FTIR) is based on electromagnetic-wave absorption due to molecule vibrations. Characteristic IR-spectra of solid and liquid samples provide qualitative and semi-quantitative analyses. Two techniques are used for solid analyses which are Attenuated Total Reflection (ATR) and Potassium Bromide Disk method. In this study, ATR-FTIR spectroscopic analysis of scaffolds was performed on Spectrum One (Perkin-Elmer, USA) spectrophotometer, as shown in Figure 3.6, over a range of 700 to 4000 cm^{-1} at a resolution of 2 cm^{-1} with 100 scans per sample. This characterization was important to ensure the functional group of individual and the effect of blended HEC, PVA, and CNCs on their intensities and peaks in the ATR-FTIR spectrum.



Figure 3.6 Photograph of ATR-FTIR, Perkin-Elmer.

3.7.5 Thermogravimetric (TGA) analysis

TGA is used basically to investigate the thermal stability or better known as the strength of the material at a given temperature, oxidative stabilities where the oxygen absorption rate on the material, and the compositional properties such as fillers, polymer resin, solvents of the samples. In modern TGA, it performs to determine the quantity and the frequency of the weight variation of the samples against temperature and time in a controlled atmosphere.

Typically, a TGA instrument offers a temperature range from 1000 to 1600 °C and the heating rate can be set from a range of a few decimal places to hundreds of °C/min. However, typical heating rate is between 1 and 20 °C/min, with very fast (>20 °C/min) or very slow (<1 °C/min) rates used only for some special reactions. The resolution of the thermogram can be controlled by the programmed heat rate, and usually the slower the heating rate the higher the resolution of the curves (Ng et al., 2018).

Differential thermal analysis (DTA) is usually incorporated with TGA to measure the temperature difference between a sample and a reference material as a function of temperature as they are heated or cooled or kept at a constant temperature. This differential temperature is then plotted against time or temperature. Changes in the sample, either exothermic or endothermic, can be detected relative to the inert reference. Consequently, the DTG curve may provide data on the transformations that have occurred such as glass transitions, crystallization, melting and sublimation.

In this present research, thermal analysis of scaffolds was performed using Q500 (TA instruments, New Castle, USA). Each sample was heat treated from 30 to 750 °C at a heating rate of 10 °C/min with nitrogen as purge gas.

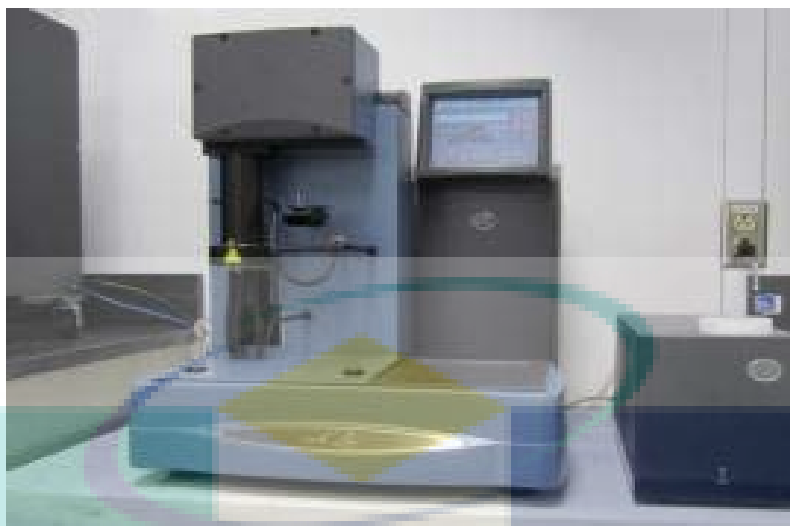


Figure 3.7 Photograph of TGA, Q500.

3.7.6 Differential scanning calorimetry (DSC)

Due to its versatility and the high significance of its analytical output, differential scanning calorimetry (DSC) is the most often employed method for thermal analysis. DSC can be used to obtain thermal critical points like the temperatures of melting point (T_m), crystallization (T_c), or glass transition (T_g), of the sample. The DSC 214 Polyma instrument from NETZSCH as shown in Figure 3.8 can be used to test on different types of samples such as powdered or compact solid, films and fibers at a broad temperature range from $-180\text{ }^{\circ}\text{C}$ to $1750\text{ }^{\circ}\text{C}$.



Figure 3.8 Photographs of DSC, NETZSCH

Glass transitions may occur as the temperature of an amorphous solid is increased. These transitions appear as a step in the baseline of the recorded DSC signal. This is due to the sample undergoing a change in heat capacity; no formal phase change occurs. As the temperature increases, an amorphous solid will become less viscous. At some point the molecules may obtain enough freedom of motion to spontaneously arrange themselves into a crystalline form. This is known as the cold crystallization temperature. This transition from amorphous solid to crystalline solid is an exothermic process and results in a peak in the DSC signal. As the temperature increases the sample eventually reaches its melting temperature. The melting process results in an endothermic peak in the DSC curve. The ability to determine transition temperatures and enthalpies makes DSC a valuable tool in producing phase diagrams for various chemical systems. The output data displays a thermogram of heat flow (dQ/dt) against temperature as shown in Figure 3.9; ΔH is the estimated area of the DSC peak.

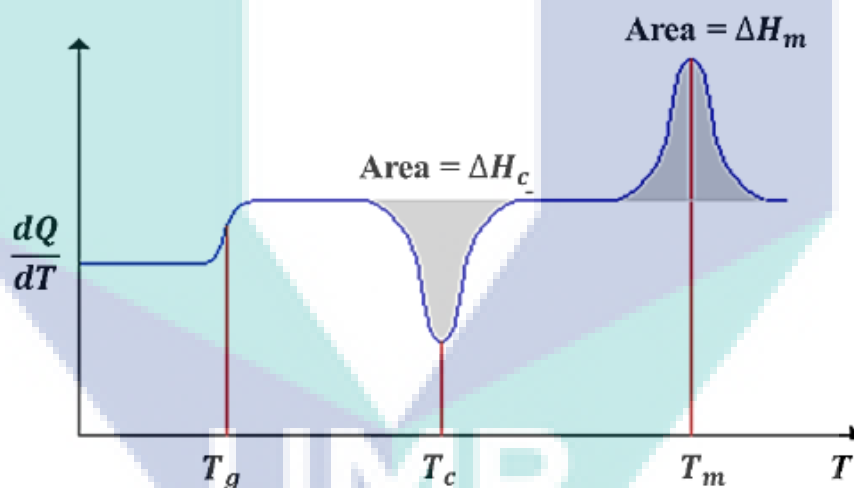


Figure 3.9 DSC thermograms

In this work, about 5 mg of sample was heat-treated from 50 to 250 °C at a heating rate of 10 °C/min, under atmospheric conditions. The degree of relative crystallinity, χ_c can be expected from the endothermic area by the following equation:

$$\chi_c = \Delta H_f / \Delta H_f^\circ \quad (3.3)$$

where, ΔH_f = measured enthalpy of fusion from DSC thermograms and ΔH_f° = enthalpy of fusion for 100 % crystalline polymer, which in this case is PVA=138.6 J/g (Merrill, 1976)

3.7.7 Mechanical properties

Mechanical testing such as hardness, tensile strength and compressive strength is important in bone tissue engineering application. Basically, this testing involved by applying a certain tensile force to a sample with known dimension, clamping at the end of the sample and the sample will be stretching after the system is running. The system stops automatically when the materials achieve break point. In this recent research, the mechanical properties of the scaffolds were measured using a universal testing machine (UTM) (Autograph AGS-X series, Shimadzu) as shown in Figure 3.10. The samples were cut in rectangular shape with same dimensions for all scaffolds. The room conditions were controlled at 25 °C and 34% humidity. The speed rate used is 10 mm/min. The AGS-X comes standard with industry-leading TRAPEZIUM X data processing software. The tensile stress and strain at break were calculated based on the obtained tensile stress-strain curve.



UMP

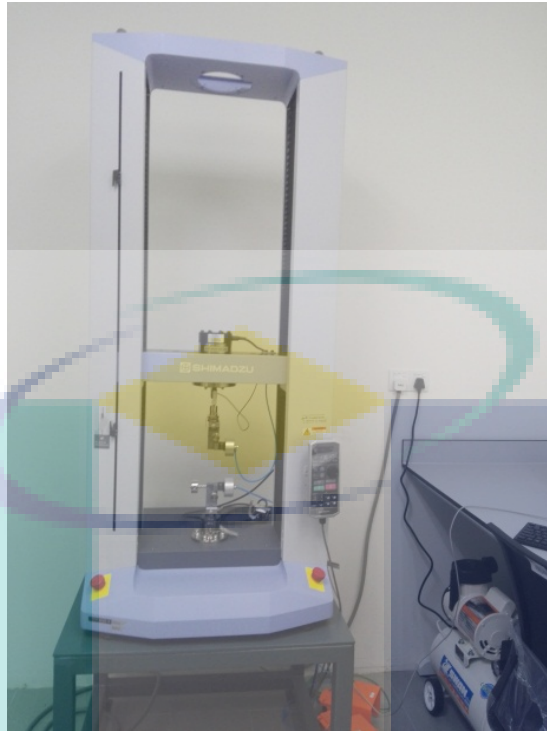


Figure 3.10 Photograph of universal testing machine, Shimadzu

3.8 In vitro degradation study

This study was focused on the degradation behavior of HEC/PVA/CNCs porous scaffolds, as potential substrates for bone tissue engineering in a biologically related media which is phosphate buffered solution (PBS). The scaffolds were characterized at different degradation times by a series of analysis including swelling ratio, weight loss and pH changes.

3.8.1 Swelling ratio study

All scaffolds were cut into $1\text{ cm} \times 1\text{ cm} \times 1\text{ cm}$ and placed in falcon tube. The scaffolds were weighed (W_d) before submerged in PBS. The solution needs to be maintained at $37\text{ }^\circ\text{C}$ throughout the analysis. The wet weight of the samples (W_t) was determined after 1, 3 and 7 days by gently blotting them on filter paper. The water uptake or swelling analysis was conducted in triplicates for all types of scaffolds. Swelling ratio was calculated according to Equation 3.4.

$$\text{Swelling ratio (\%)} = \frac{W_t - W_d}{W_d} \times 100 \% \quad (3.4)$$

3.8.2 pH value measurements

The pH value measurement was done for all scaffolds after the degradations at each time point were obtained by using a pH meter (Horiba LAQUA Handheld Water Quality Analysis Meters) as shown in Figure 3.11. Note that, pH value for PBS is 7.4.



Figure 3.11 Photograph of Horiba LAQUA Handheld Water Quality Analysis Meters

3.8.3 Weight loss study

Weight loss percentages were determined after drying the samples in vacuum by comparing the dry weight, W_d at a certain time point with the initial weight, W_0 according to Equation 3.5.

$$\text{Weight loss (\%)} = \frac{W_0 - W_d}{W_0} \times 100 \% \quad (3.5)$$

The lyophilized scaffolds were cut into 1 cm × 1 cm × 1 cm and placed in Falcon tube containing 3 ml of PBS and incubated at 37 °C. The samples were then taken out at

different periods of time which is at 1, 3 and 7 days. After testing, the scaffolds were washed with distilled water and kept dry in a desiccator for further use.

3.9 Cell culture study

The cell culture studies were carried out to examine the interaction of cell with the prepared scaffolds. Figure 3.12 shows the basic step for cell culture where the primary cells were expanded in tissue culture flask at first, then underwent subculture and finally, seeded on the scaffolds.

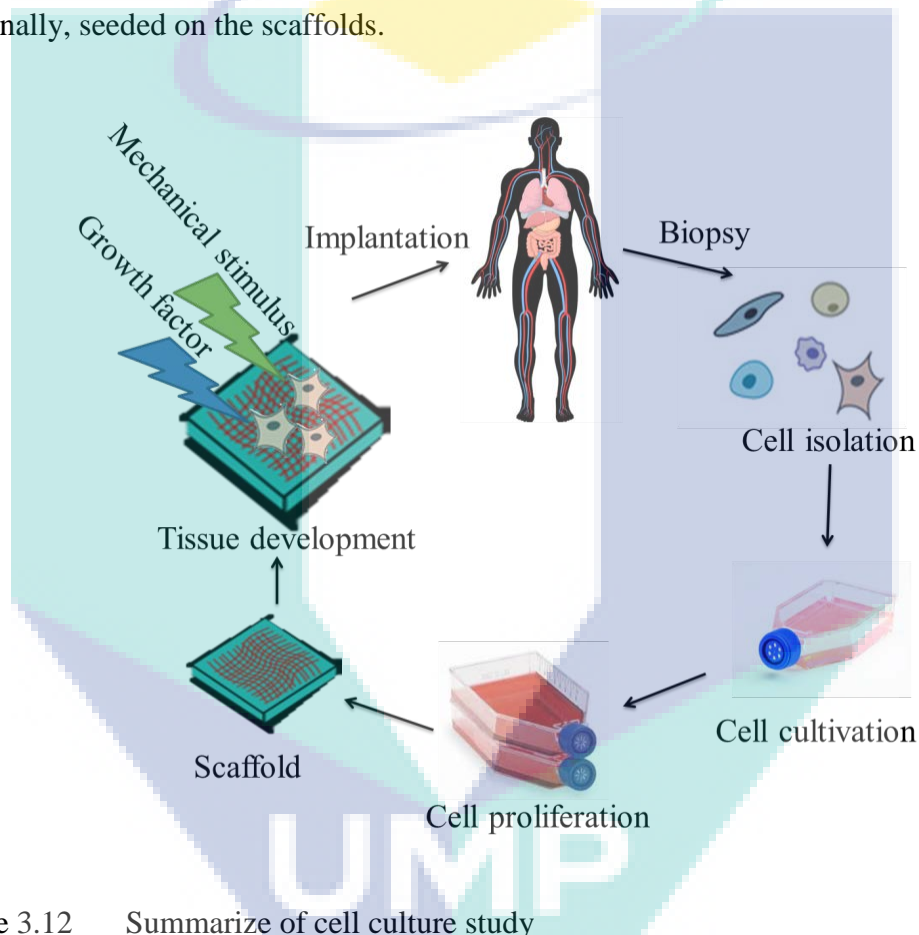


Figure 3.12 Summarize of cell culture study

3.9.1 In vitro cell culture study of HEC/PVA/CNC scaffolds

Human fetal osteoblast (hFOB) cells is cultured, expanded and seeded on HEC/PVA/CNC scaffolds. The cells-scaffolds were incubated to facilitate cells growth and observe after 1, 3, 5 and 7 days. The cell proliferation is measured by MTT assay and images taken from Trypan blue staining under light microscope, while the morphology of hFOB cells on scaffolds were observed under SEM images.

3.9.2 hFOb cells expansion and seeding

Firstly, the scaffolds; HEC/PVA, HEC/PVA/CNC (1,3,5,7 wt%) were cut into small disks with 10 mm diameter, soaked in 100 % ethanol for 24 h, and then sterilized under UV light for 3 h and subsequently immersed in cell culture medium, Dulbecco's modified Eagle's medium (DMEM) solution. Then, the scaffolds were kept in incubator at 37 °C in 5 % carbon dioxide (CO₂) humidified atmosphere for five days. All changes were observed including the pH of media before and after five days in the incubator. Finally, the scaffolds were washed thrice with sterile PBS and transferred into a 24-well tissue culture plate.

hFOB cell lines were propagated in Dulbecco's modified Eagle's medium (DMEM) in a cell culture flask, all supplemented with 10 % fetal bovine serum and 5 % penicillin/ streptomycin and maintained at 37 °C in 5 % carbon dioxide (CO₂) humidified atmosphere.



Figure 3.13 hFOB cell in cell culture flask

It is crucial to maintain and feeding the hFOB cell regularly and routinely. The cell morphology, color, and turbidity were checked by microscope to ensure there is no presence of contaminants. DMEM solution was changed once for each two days to avoid the cells from depleting, depriving of specific nutrients, or becoming acidic. For media changing, the spent media was removed and equal volume of fresh media (5 ml)

was added to the cell culture flasks. The flasks were stored and maintained in 5 % carbon dioxide (CO₂) humidified atmosphere at 37 °C in the incubator.

In order to perform subculture of cell, hFOB cells were passaged when they have reached 80-90 % confluence of the surface area of a flask to maintain healthy growth. DMEM solution were removed and discarded. Then, TrypLE solution was added to cell culture flask to detach the cells and swirled across the adhered cells to ensure it reaches all cells. The detachments of the cells were checked by using microscope after the flasks being incubated for about 5 minutes. Once the cells were detached from the flask, the cell suspensions were transferred into 15mL tube and centrifuged at 800 rpm for 5 minutes. Finally, TrypLE solution was removed and fresh DMEM solution containing serum was then added to inactivate the TrypLE solution in the cell suspension.

The aliquot of cell suspensions was placed into a new flask containing 5 mL of DMEM solution, then stored in the incubator. After 24 hours, the cultures were checked to ensure that cells were reattached. The medium was changed as necessary until the next subculture. The cell-scaffolds were incubated in 24-well plate at different time points as shown in Figure 3.14. Note that the control is the cell with the media only.



Figure 3.14 Cell culture studies of scaffolds at different weight ratios

3.9.3 hFOb cells proliferation study

In order to perform the proliferation assay for hFOB cell, at least 5,000 or 5×10^3 cells per well are recommended. In this study, the cells were distributed in 24-well cell culture plates at a concentration of approximately 10×10^3 cells prior adding the scaffolds in each different well with DMEM solution. The proliferation test was observed using MTT assay test by measuring the reduction of the yellow tetrazolium salt to purple formazan crystals by dehydrogenase enzymes secreted from the mitochondria of metabolically active cells. The amount of the purple formazan crystals formed is proportional to the number of viable cells. For this study, 150 μ L of Dimethyl sulfoxide (DMSO) solvent was added into each of the cell-scaffolds to dissolve the MTT formazon crystal. The well plate was placed in a NanoQuant micro plate reader (Infinite M200PRO) to detect biological, chemical or physical events of samples by using emitting light. The absorbance was recorded at 570 nm with background 630 nm representing the number of viable cells was measured. For data analysis, the cell proliferation is calculated using the following formula:

$$\text{Cell viability (\%)} = \frac{(A_{\text{sample}} - A_{\text{blank}}) - (A_{\text{control}} - A_{\text{blank}})}{(A_{\text{control}} - A_{\text{blank}})} \times 100\% \quad (3.6)$$

where A_{sample} = absorbance at 570 nm of the sample, A_{control} = absorbance at 570 nm of the positive control which is cells in complete medium incubated in the absence of the scaffolds and A_{blank} = background absorbance of the blank wells. An average of triplicate reading was calculated for each sample.



Figure 3.15 Photograph of NanoQuant micro plate reader (Infinite M200PRO)

Trypan blue assay was one of the most common and earliest methods used for cell viability measurement. It is impermeable for the normal cell membrane and therefore only enters the cell with compromised membrane. After entering the cell, it binds into the intracellular proteins and renders them bluish color. It also helps in the identification and counting of live or dead cells in the given cell population. The viable cells are shown small, rounded, and refractive, whereas dead cells are shown swollen, large, and dark blue.

For this research, the cell-scaffolds were cultured on glass coverslips in 24-well cell culture plates according to the standard protocol. Trypan blue has a strong affinity for serum proteins, which affects staining if serum is present. Hence, each of the samples were washed about 3 min with PBS solution to eliminate any residual serum. Then, 0.2 % Trypan blue solution is added for 1 min. After that, the Trypan Blue solution were removed and immediately fix the samples with 4% paraformaldehyde (PFA), pH 7.5, for 10 min at 22 °C, or 20 min at 0 °C. After fixation, rinse the samples with PBS for 3 to 4 times with gentle shaking until the PBS is clear of any residual blue color. The coverslips were lifted gently to free Trypan blue from underneath. The coverslips were dehydrated through sequential ethanol washes. Finally, the coverslips were mounted onto glass slides with a compatible permanent mounting solution such as REFRACT Mounting Medium (Anatech) and visualise using light microscope.



Figure 3.16 Photograph of light microscope, EVOS XL

3.9.4 hFOb cells morphology studies

After the cell is cultured, hFOB cells grown on scaffolds were rinsed twice with PBS and fixed in 3 % GA for 30 min. Thereafter, the scaffolds were dehydrated with increasing concentrations of alcohol (20, 40, 60, 80 and 100 %). The samples were air dried by keeping the samples in a fume hood. Lastly, the scaffolds were observed using SEM at an accelerating voltage of 10 kV.

CHAPTER 4

RESULTS AND DISCUSSION

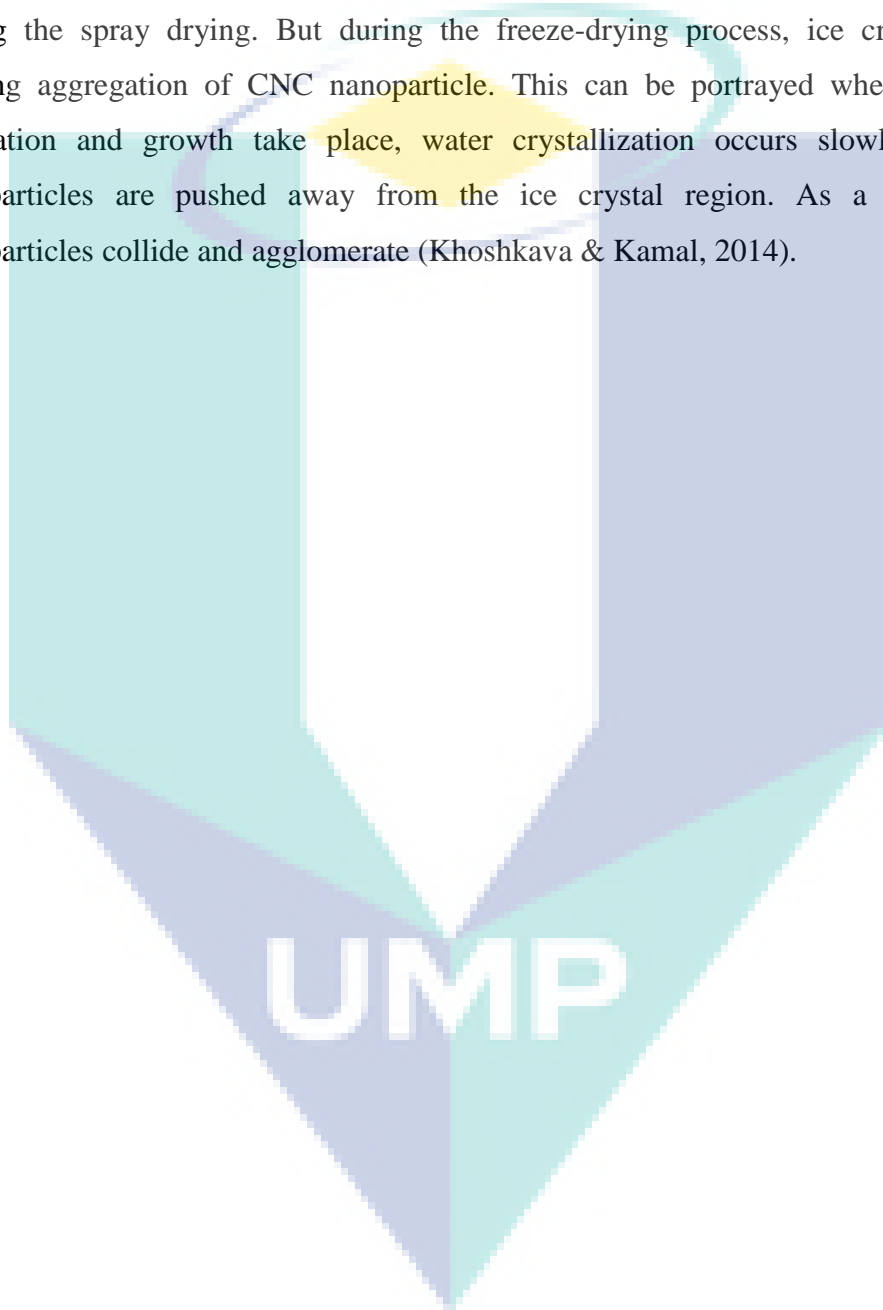
4.1 Characterization of CNC

Firstly, the characterization of nanoparticle to be used in this research will be discussed in this section. These include the study of morphology, chemical and thermal properties of CNCs. CNCs produced from acid hydrolysis will be used as nanofillers in producing scaffold materials. Acid hydrolysis has been used to extract the crystalline particles from a variety of cellulose sources. Basically, the process preferentially removes (hydrolyze) the amorphous regions within the cellulose microfibrils. In general, the 'purified' starting material is mixed into deionized water with a given concentration of acid. Sulphuric acid is most typically used as it produces a negative surface charge on the particles, leading to more stable suspensions.

4.1.1 Morphology of CNC

The morphology of CNCs including its dimension and shape were successfully examined by FESEM. These properties are important as it depends on the cellulose source and the fabrication of CNCs. For this study, CNC is successfully obtained from cellulose pulp of empty fruit bunch (EFB) by using acid hydrolysis technique. The cellulose was heated at 85 °C in 65 % of sulphuric acid. Previous report suggested that CNCs are commonly in a rod-shaped with remarkable uniform width and a wide distribution of lengths.

Figure 4.1 displays the FESEM image of CNC nanoparticle. It can be observed that a broad range of CNC particle dimension in the range between 5 to 30 nm in diameter were measured using ImageJ software. On the other side, the shape of CNC nanoparticles is mostly appeared in spherical shape and they were loosely packed. Previous research reported that CNC particles are not around sphere due to shrinkage during the spray drying. But during the freeze-drying process, ice crystal growth causing aggregation of CNC nanoparticle. This can be portrayed when ice crystal nucleation and growth take place, water crystallization occurs slowly and CNC nanoparticles are pushed away from the ice crystal region. As a result, CNC nanoparticles collide and agglomerate (Khoshkava & Kamal, 2014).



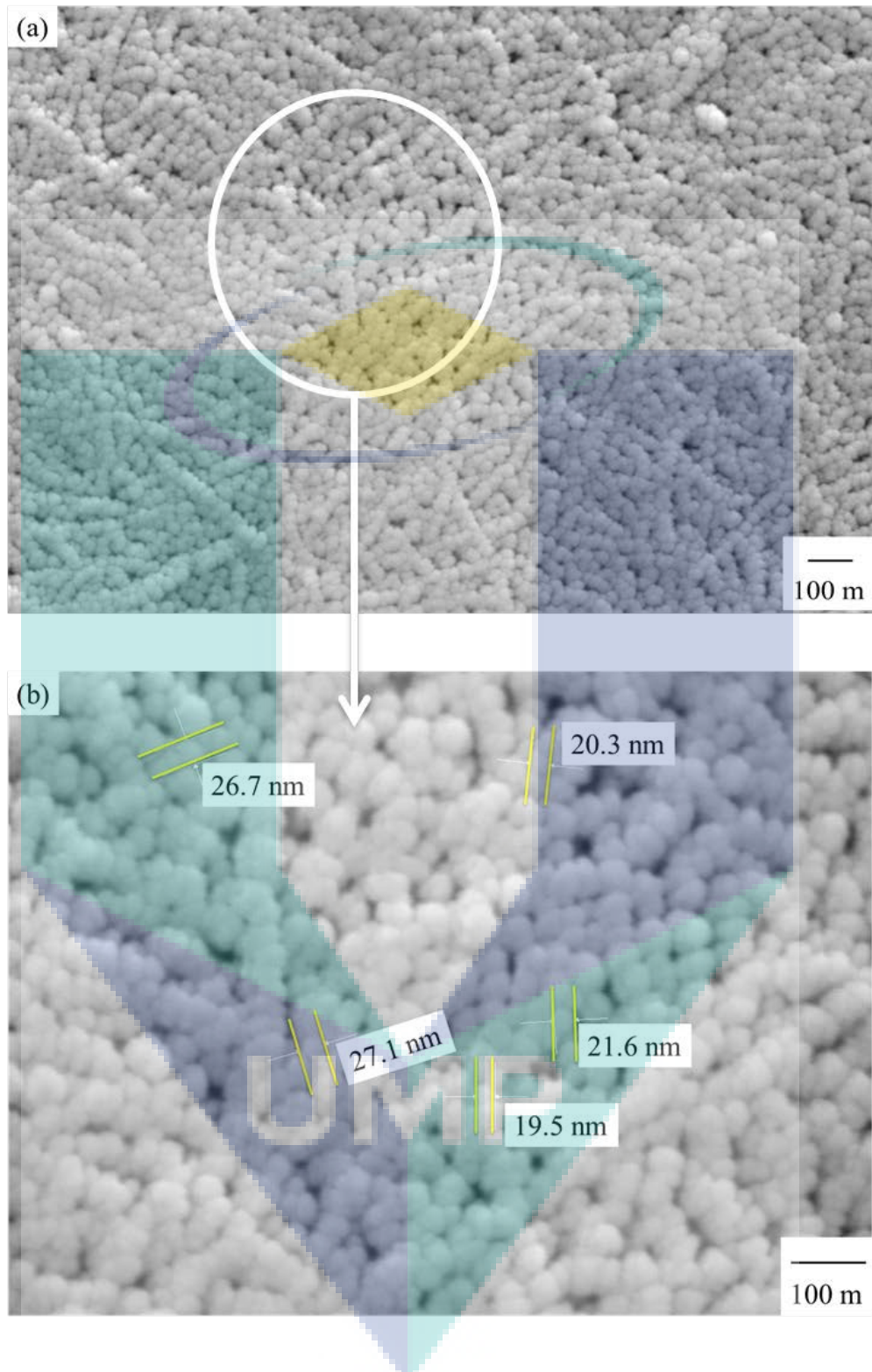


Figure 4.1 FESEM micrographs of CNC nanoparticle at (a) low magnification (50,000 \times) and (b) high magnification (130,000 \times)

4.1.2 Chemical properties of CNC

The chemical properties of CNC were observed using ATR-FTIR analysis. The FTIR spectra of CNC are shown in Figure 4.2. Accordingly, CNC nanoparticles presented in two main absorbance regions in the range of 1000–1800 cm^{-1} and 2000–3500 cm^{-1} . When CNC are desired to be obtained from biomass, including wood and agricultural residues, not only cellulose is present but also different extractives, hemicelluloses, lignin, or inorganic particles. The FTIR spectra of these nanoparticles has shown a strong and wide band in the region between 3000 and 3500 cm^{-1} that indicates the O-H stretching vibration of OH groups in cellulose (Li et al., 2014). The absorption peak at 2903 cm^{-1} refers to the aliphatic saturated C-H stretching, associated with methylene groups in cellulose. The absorption band at 1346 cm^{-1} in CNC is attributed to the presence of C-H asymmetric stretching while O-H bending occurs at 1637 cm^{-1} indicates the absorption of water and some of the carboxylate groups (Lamaming et al., 2015). C-O stretching of alcohol species at 1045 cm^{-1} . Based on the results, it can be concluded that CNC obtained from acid hydrolysis contains small amounts of lignin, hemicellulose and other impurities.

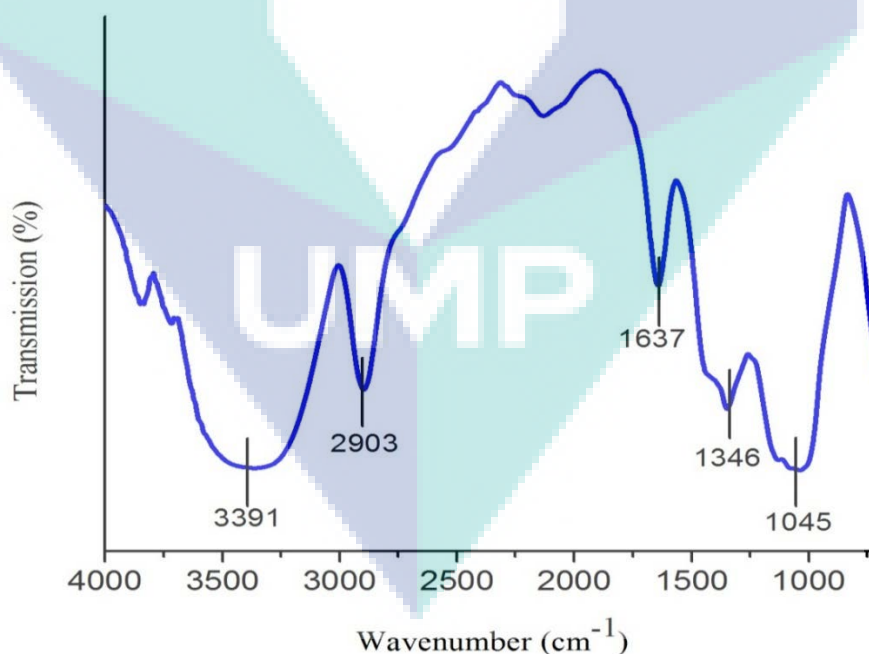


Figure 4.2 ATR-FTIR analysis of CNC nanoparticle

Table 4.1 ATR-FTIR spectral peak assignments for CNC nanoparticle

Bond	Possible arrangement	Wavenumber(cm^{-1})
C-O stretching	Stretching of alcohol	1045
C-H asymmetric stretching	Hemicellulose	1346
O-H bending	Presence of water in hemicellulose	1637
C-H stretching	Methylene groups in cellulose	2903
O-H stretching	Cellulose, hemicelluloses and lignin	3391

4.1.3 Thermal study of CNC

The most important properties that gives significant effect to the performance of scaffold materials is the thermal properties of nanoparticle used in the materials. It is very crucial to determine the optimum thermal properties of nanoparticle used based on the application. According to recent research, CNC will not only improve the thermal stability but they can also increase the degradation stability of produced scaffolds in different kind of fluids type. From Figure 4.3, DSC thermograms shows that melting temperature, T_m is occur at 336.4 °C, while the glass transition temperature, T_g is 43.5 °C. It is likely to mention that thermal stability of CNC was better due to the introduced of sulphate groups into CNC by hydrolysis with sulphuric acid. During acid hydrolysis process, the sulphate groups of the cellulose's outer layer caused dehydration of cellulose thus reduce the thermal stability. Previous research from N. J. Cao et al had been carried out the acid hydrolysis process of cellulose using zinc chloride. It is reported that zinc chloride not only catalyzes the hydrolysis, but also drastically reduces the glucose degradation in the heating process by the forming of zinc-carbohydrate

complex (N. J. Cao, 1995). Overall, acid treatments helped to increase the degree of crystallinity and inner hydrogen bonding of the CNCs.

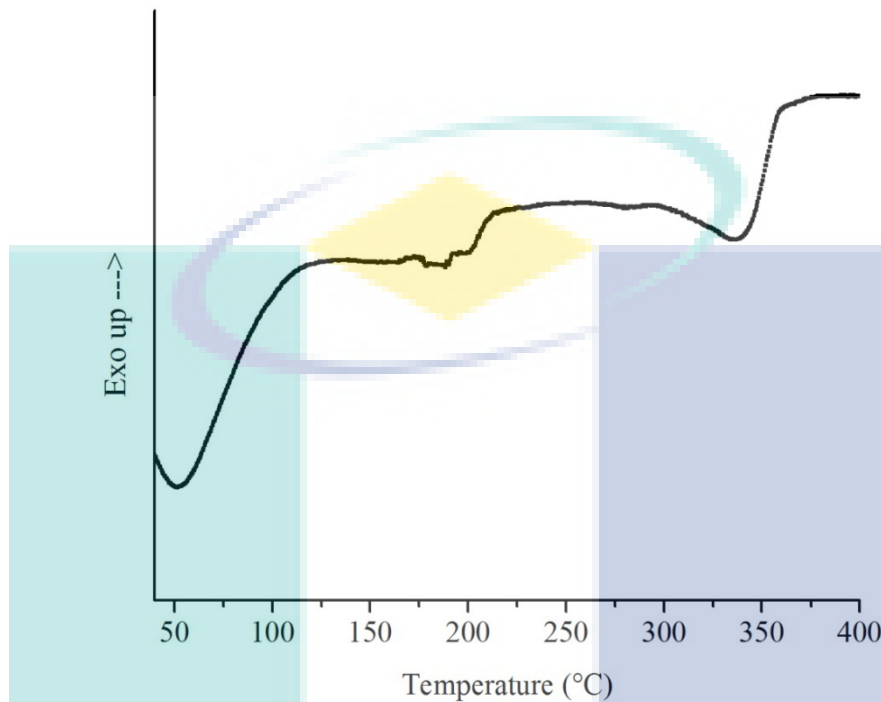


Figure 4.3 DSC thermograms of CNC nanoparticle

4.2 Characterization of HEC/PVA and HEC/PVA/CNCs scaffolds

In producing a favorable and compatible porous scaffold for bone tissue engineering application, several characterizations are necessary to be studied. In this present work, the morphology including the porosity, chemical and thermal properties of all scaffolds will be observed by SEM, ATR-FTIR, TGA and DSC.

Figure 4.4 shows the polymeric solution of HEC/PVA and HEC/PVA incorporated with varied concentration of CNC (1, 3, 5, and 7 wt%). All solutions were milky in color and as the concentration of CNCs increased, the solution become cloudier. These polymeric solutions were freeze at $-80\text{ }^{\circ}\text{C}$ and undergo freeze-drying process for 72 h. After that, the samples were cross linked via heat treatment using microwave oven to increase the degradation time of produced scaffolds. From Figure 4.5, it can be observed that all scaffolds were brittle but in a hard spongy-like structure.

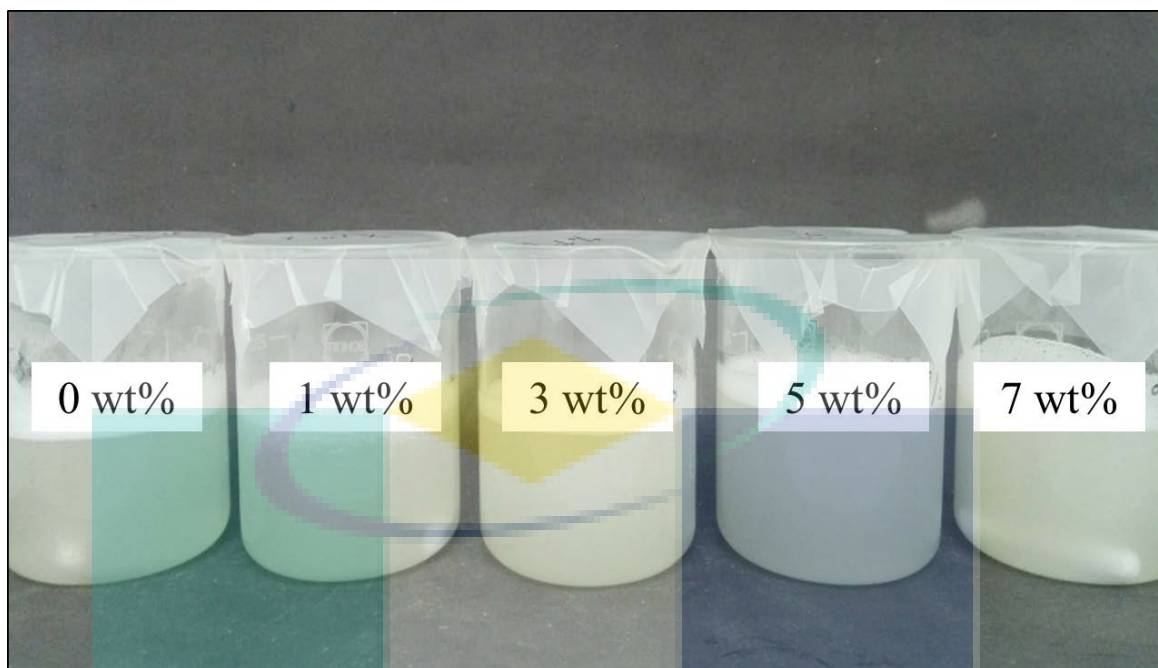


Figure 4.4 HEC/PVA and HEC/PVA/CNC (1, 3, 5, and 7 wt%) polymeric solutions



Figure 4.5 HEC/PVA and HEC/PVA/CNC (1, 3, 5 and 7 wt%) scaffolds

4.2.1 Morphology of scaffolds

The main criteria to produce a functional tissue start from designing a scaffold. In bone tissue engineering, scaffolds need to be designed to have appropriate characteristics such as porosity and interconnected geometry to guide the tissue regeneration. Hence, the morphology of scaffolds material should be taken consideration. The microstructures of HEC/PVA and HEC/PVA/CNC (1, 3, 5, and 7 wt%) are illustrated as in Figure 4.6 until Figure 4.10.

From the SEM images, the produced scaffolds were most likely showed high interconnectivities between pores. The HEC/PVA scaffolds have larger porous structure compared to HEC/PVA/CNC scaffolds. Meanwhile, the scaffolds containing CNCs showed an open microstructure with interspacing pore. By varying the concentration of CNC, a controllable pore size with particular wall structure could be produced. There were more porous structure presented with a three-dimensionally interconnection all over the scaffolds compared to HEC/PVA scaffolds.

The average pore size for interconnected HEC/PVA porous material is $\sim 54 \mu\text{m}$ where the scaffolds incorporated with different concentration of CNC have average pore size ranging from $\sim 48 \mu\text{m}$ to $28 \mu\text{m}$, respectively. As the concentration of CNC content increasing, the average pore size shows a decreasing trend. There are few micropores less than $10 \mu\text{m}$ were observed at higher magnification for all scaffolds. This could be attributed from rapid sublimation where surrounding pressure is reduced during freeze-drying process. Anyhow, the existence of micropores can be beneficent is as it might increase the interconnectivity and interface area of the porous scaffolds. Nano and micro structured porous scaffolds should be considered in giving support and guiding cells, also in mimicking the physical structure of the extracellular matrix. Overall, it can be seen that all scaffolds have shrink-like structure due to the effect of heat treatment, which disturbed to round pores appeared as the distortion in the pore formation occurs. Other than that, CNCs that acts as reinforcing fillers could improve the mechanical properties of biocomposites. It has been reported that using reinforcing

materials in a starch matrix become an effective method to obtain high performance starch-based biocomposites (Nasution, Harahap, Afandy, & Fath, 2017)

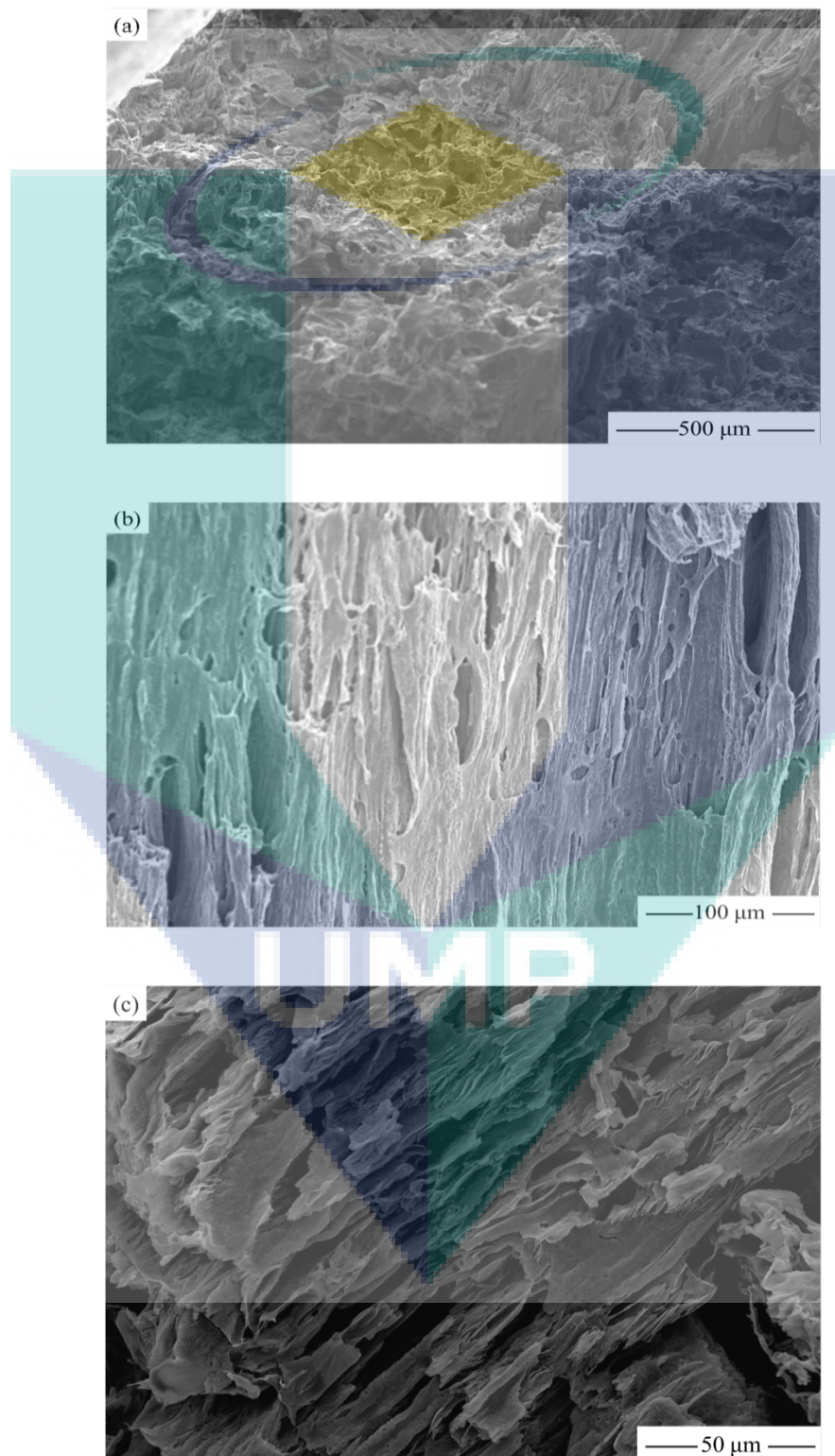


Figure 4.6 SEM micrographs of HEC/PVA at (a) 230 \times , (b) 1000 \times and (c) 2000 \times

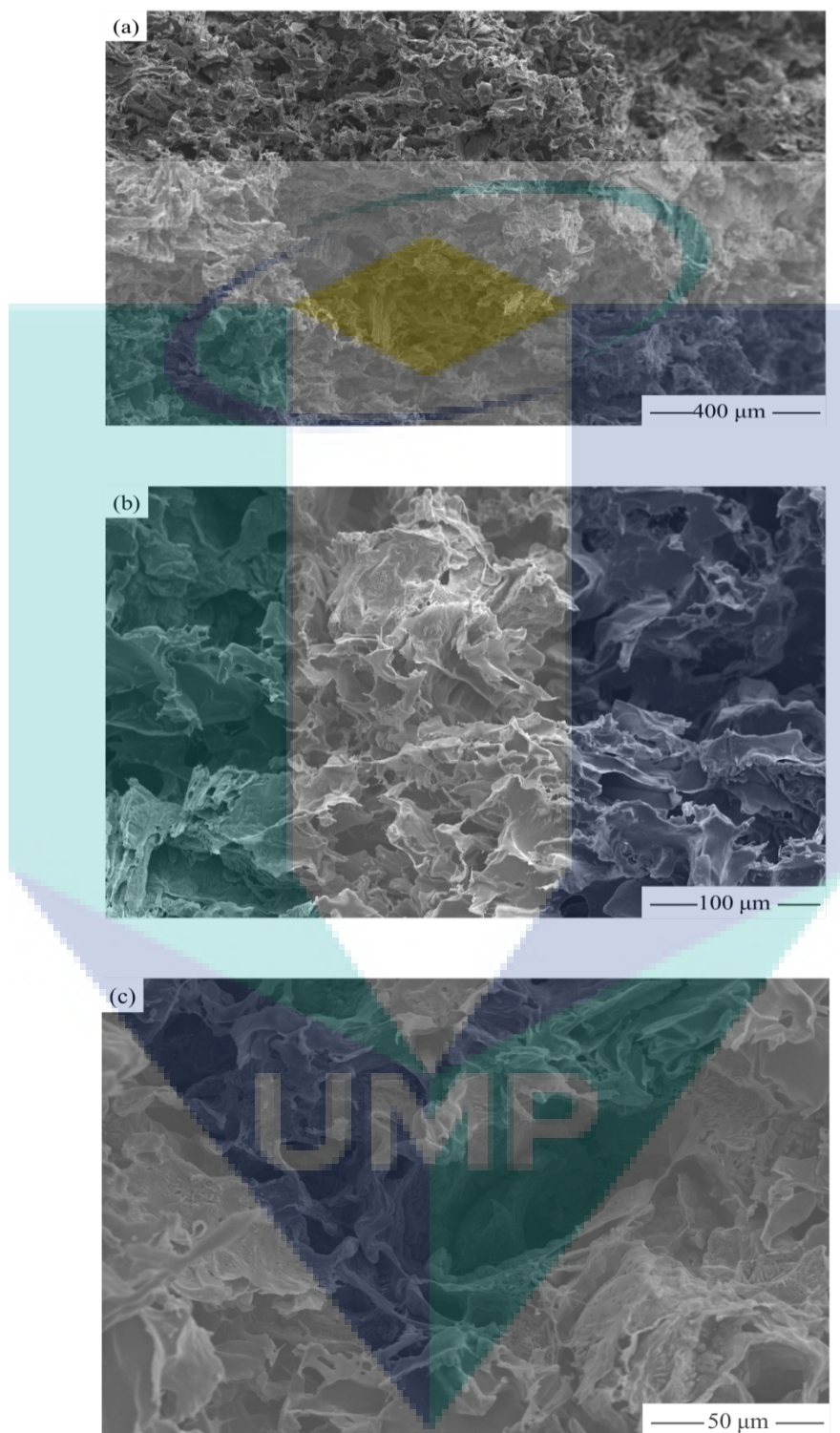


Figure 4.7 SEM micrographs of HEC/PVA/CNC (1 wt%) at (a) 250 \times , (b) 1000 \times and (c) 2000 \times

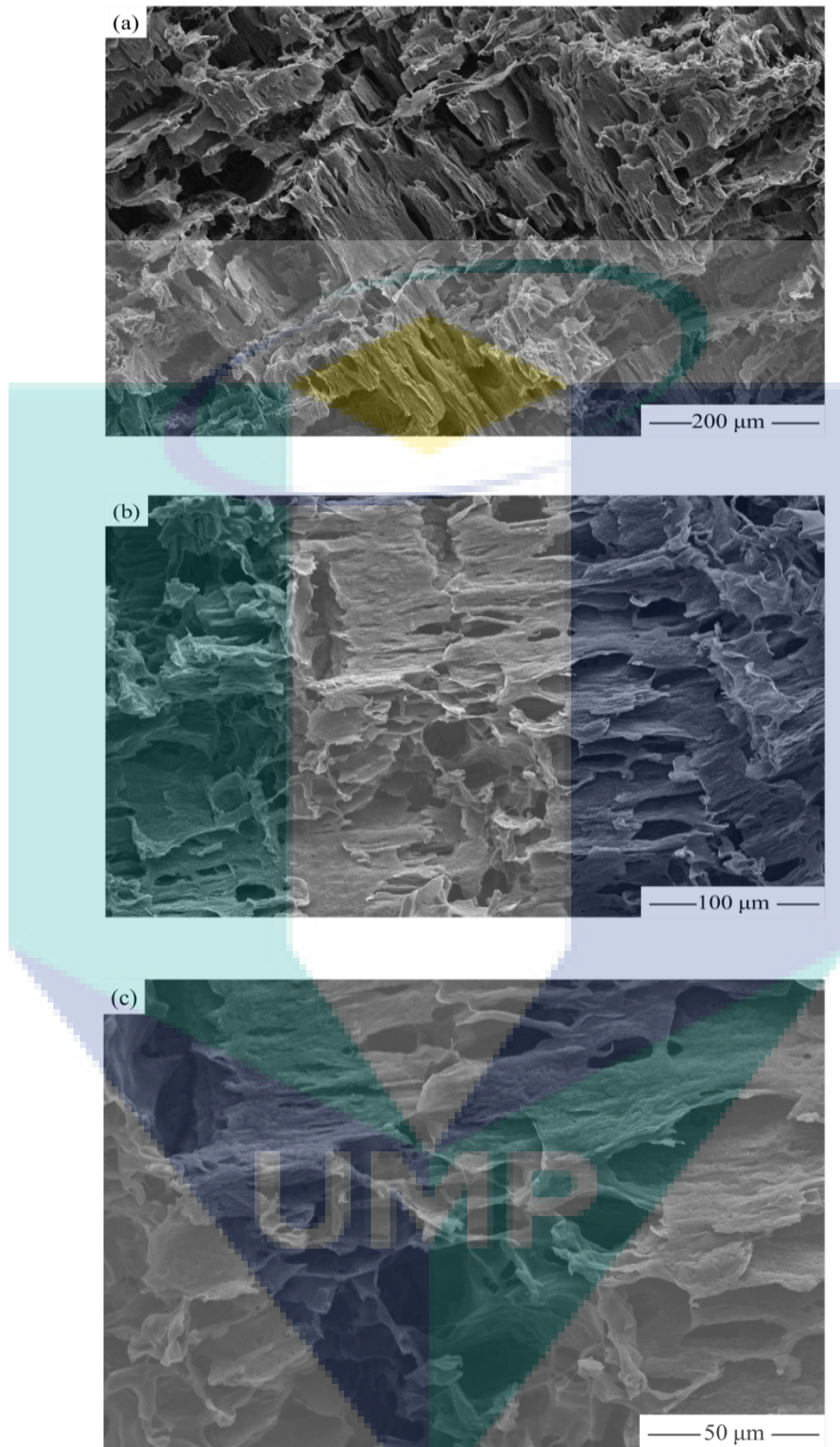


Figure 4.8 SEM micrographs of HEC/PVA/CNC (3 wt%) at (a) 500 ×, (b) 1000 × and (c) 2000 ×

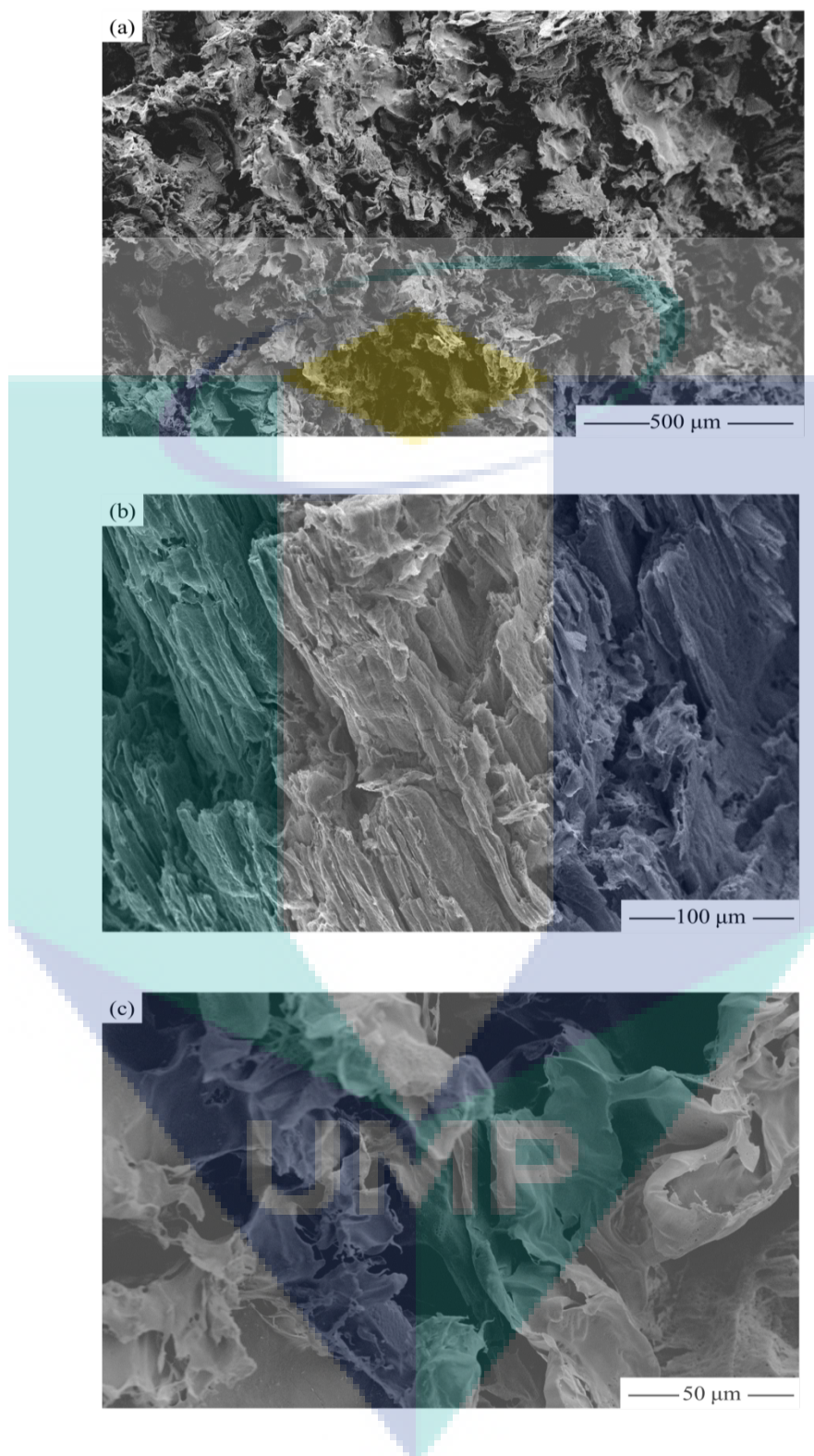


Figure 4.9 SEM micrographs of HEC/PVA/CNC (5 wt%) at (a) 250 \times , (b) 1000 \times and (c) 2000 \times

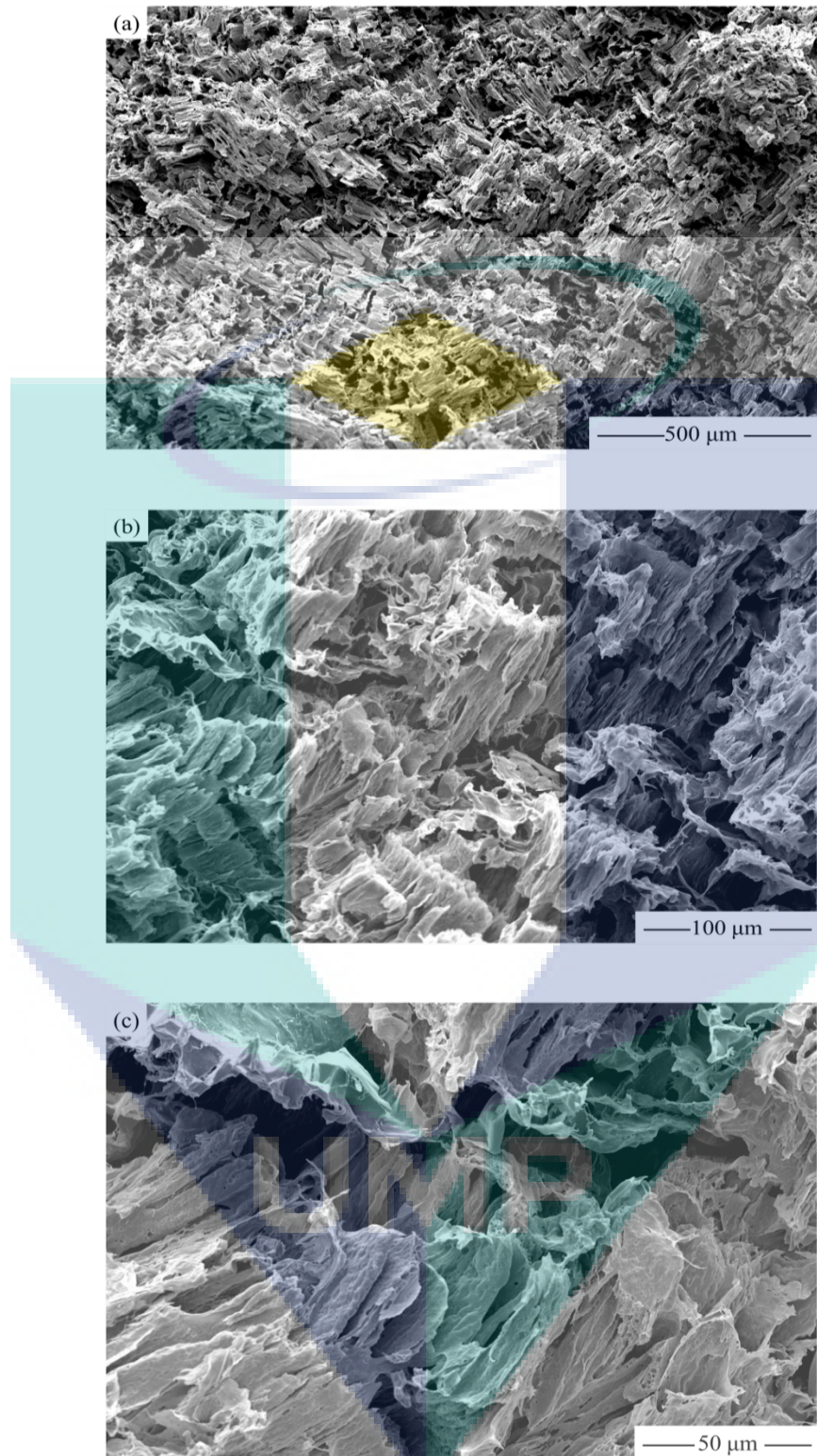


Figure 4.10 SEM micrographs of HEC/PVA/CNC (7 wt%) at (a) 250 \times , (b) 1000 \times and (c) 2000 \times

4.2.2 Porosity

Porosity is an important feature in evaluating the scaffolds properties for bone tissue engineering. Note that, polymers used in this research which is HEC and PVA are water-soluble biopolymers. Due to that, they are not likely suitable for cell culture studies. Hence, it can be solved by cross link these materials in order to decrease solubility and give mechanical strength. Porosity measurement of scaffolds is carried out by liquid displacement method with the use of deionized water as the displacement liquid.

As illustrated in Figure 4.11, all porous scaffolds show high porosity with percentage value above 77.49% at a maximum of 99.59 % for pure HEC freeze-dried scaffolds. The results pointed that porosity of scaffold containing CNC decreases with the addition of CNC content due to the greater influence of the cross-linking mechanism among –OH groups of HEC, PVA, and CNC. The morphology of three-dimensional scaffold structure should possess high porosity. Even though the porosity of HEC/PVA scaffolds is higher than other scaffolds, the variation of porosity was basically having more or less the same. This is probably due to internal pores may be formed due to uneven slurry and the accuracy of measurement and calculation of porosity could not be ensured one hundred percent. Other than that, the decomposition of CNC at high temperature may cause some difference in actual density.

Overall, all scaffolds showed a high porosity and it must be suitable for cell proliferation and transplantation especially in bone tissue engineering application. In general, the scaffolds with higher porosity are likely to support greater cellular proliferation and infiltration in tissue engineering.

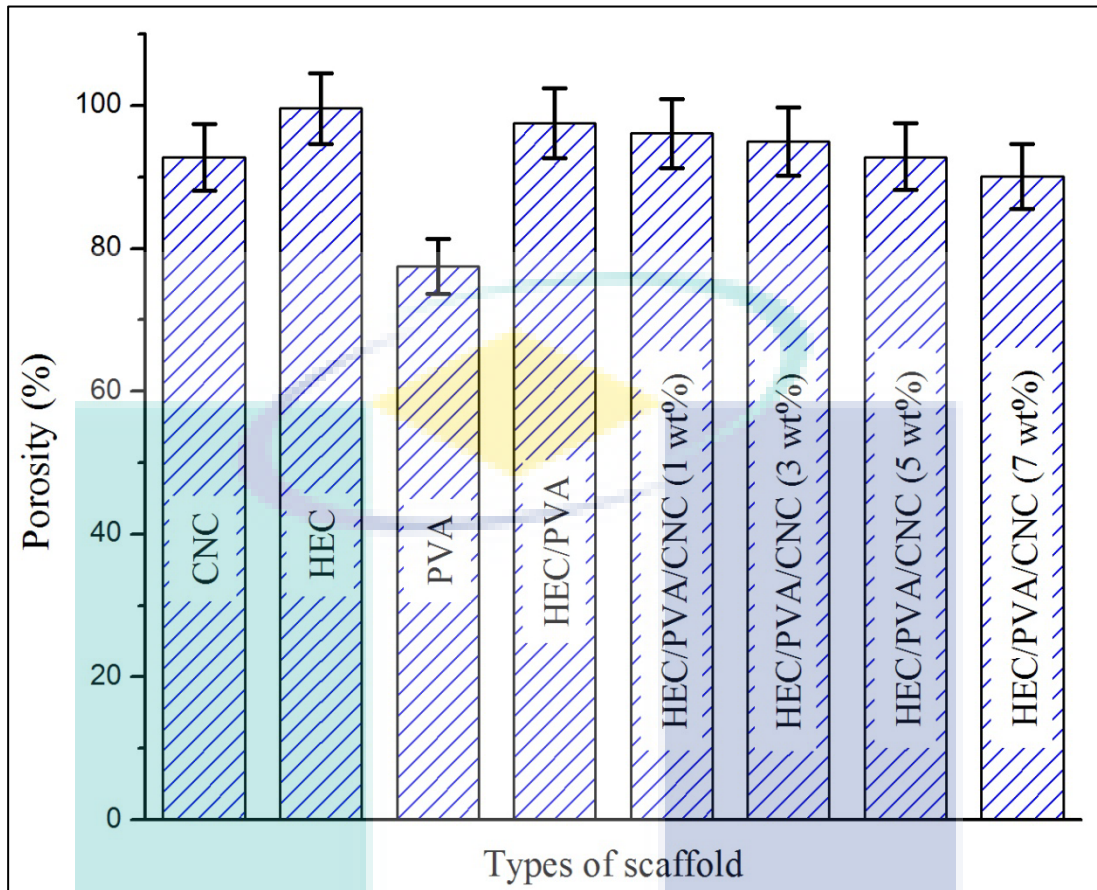


Figure 4.11 Porosity of CNC, HEC and PVA alone and HEC/PVA scaffolds with different CNC concentration at (1, 3, 5 and 7 wt%)

Table 4.2 Porosity of all samples

Types of scaffold	Porosity (%)
CNC	92.8
HEC	99.59
PVA	77.49
HEC/PVA	97.58
HEC/PVA/CNC (1 wt%)	96.09
HEC/PVA/CNC (3 wt%)	94.98
HEC/PVA/CNC (5 wt%)	92.84
HEC/PVA/CNC (7 wt%)	90.11

4.2.3 ATR-FTIR study

The basic principle of ATR-FTIR is basically helps the researchers to identify chemical bonds in a molecule by producing an infrared absorption spectrum. For this study, FTIR spectra analysis was carried out to enlighten the presence of HEC, PVA, and CNC inside the porous materials and to figure out the interaction occurs among them and to analyze the interaction (hydrogen bonding) between them. ATR-FTIR spectra of pure HEC and PVA, HEC/PVA and HEC/PVA/CNC (1, 3, 5 and 7 wt%) cross-linked porous scaffolds is illustrated as in Figure 4.12.

From past researches, it is reported that the absorption spectra of pure HEC appeared in specific bands which are at 1463, 1354, 1310 and 932 cm^{-1} vibrations at which it is corresponding to a characteristic of amorphous region and possible heterogeneity on the distribution of the replaced groups in the polymer chains. A broad peak at 3376 cm^{-1} were assigned to O-H stretching vibrations and 2929 cm^{-1} assigned to C-H aliphatic stretching. For pure PVA, a large band appeared at 3303 cm^{-1} , representing the O-H stretching from the intermolecular and intramolecular hydrogen bonds while the vibrational bond at 2944 cm^{-1} contributed to the stretching of C-H from alkyl groups of PVA. Strong peaks emerged at 1709 cm^{-1} and 1655 cm^{-1} referring to the stretching of C-O from acetate groups remaining in PVA, while peaks for 1429 cm^{-1} were related to the bending vibrations of CH_2 .

By referring to Figure 4.12(ii), it is clearly can be seen that the FTIR spectra for HEC/PVA/CNC scaffolds showed the combination of major peaks of HEC, PVA and CNC. The ratio of absorption intensities of O-H stretching increased as well as shifted to left with the addition of CNC. The broad pattern observed at 3274 – 3335 cm^{-1} indicates stretching vibrations of the hydroxyl groups due to the intramolecular and intermolecular hydrogen bands of the OH groups of PVA, HEC and CNC. The peaks at 2886 to 2922 cm^{-1} are due to CH_2 stretching vibrations. The presence of peaks at 1659 to 1695 cm^{-1} indicates presence of C=C chains. At FTIR spectra of 1053 to 1077 cm^{-1} , C-O stretching were assigned.

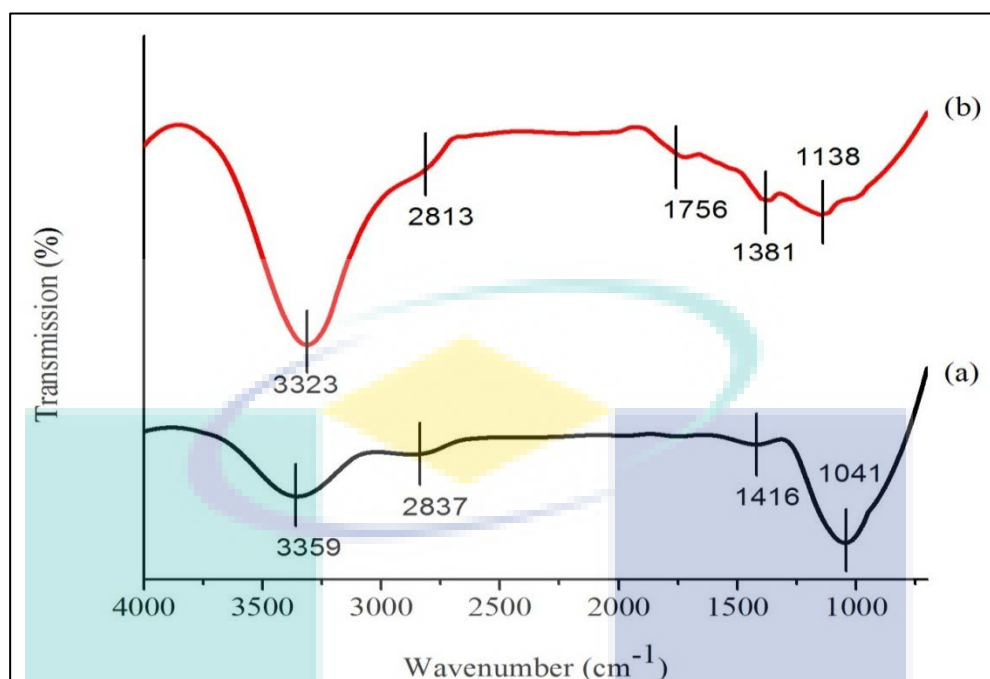


Figure 4.12 (i) ATR-FTIR spectra of (a) HEC and (b) PVA alone

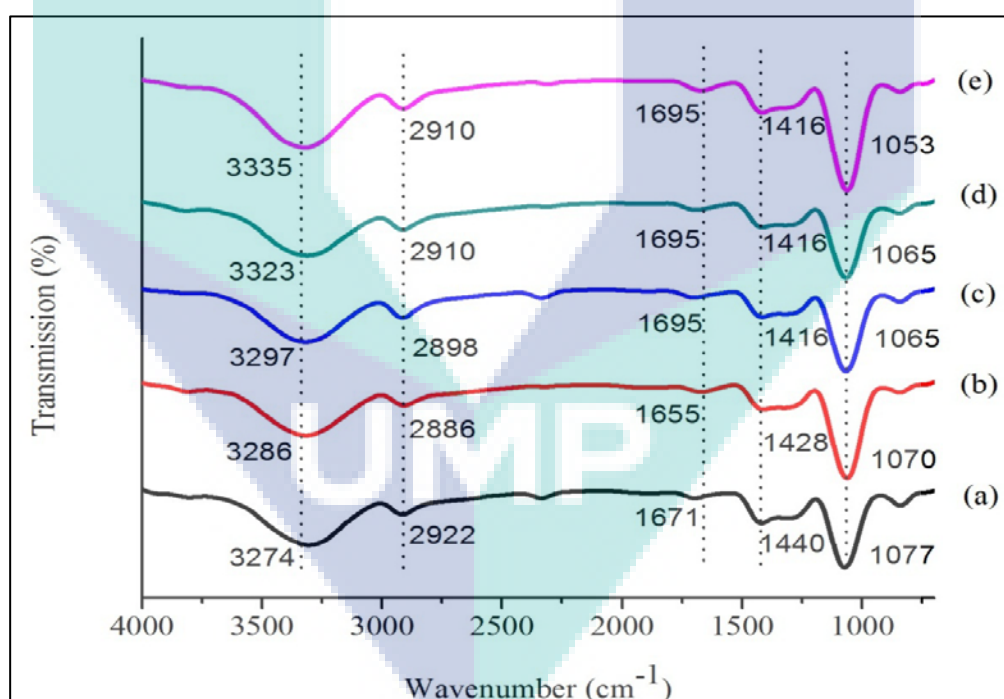


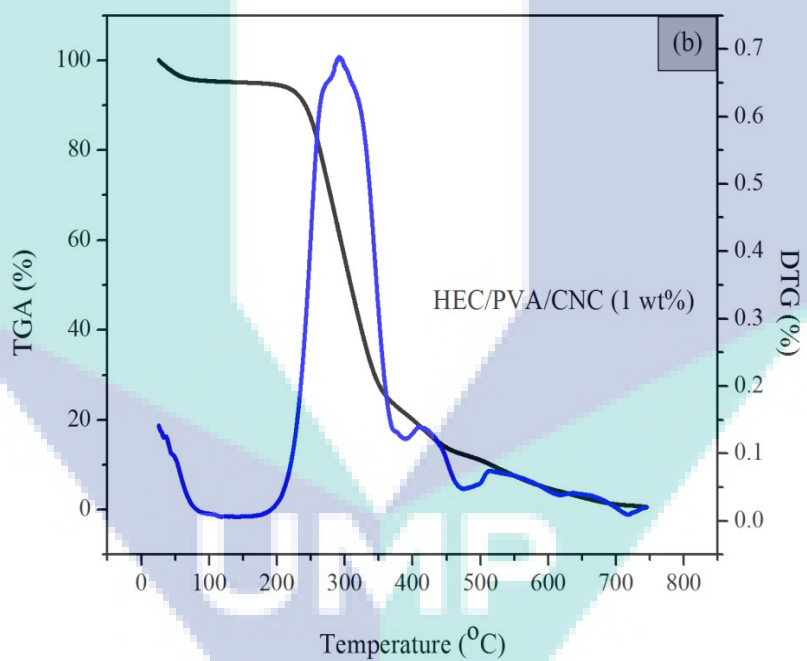
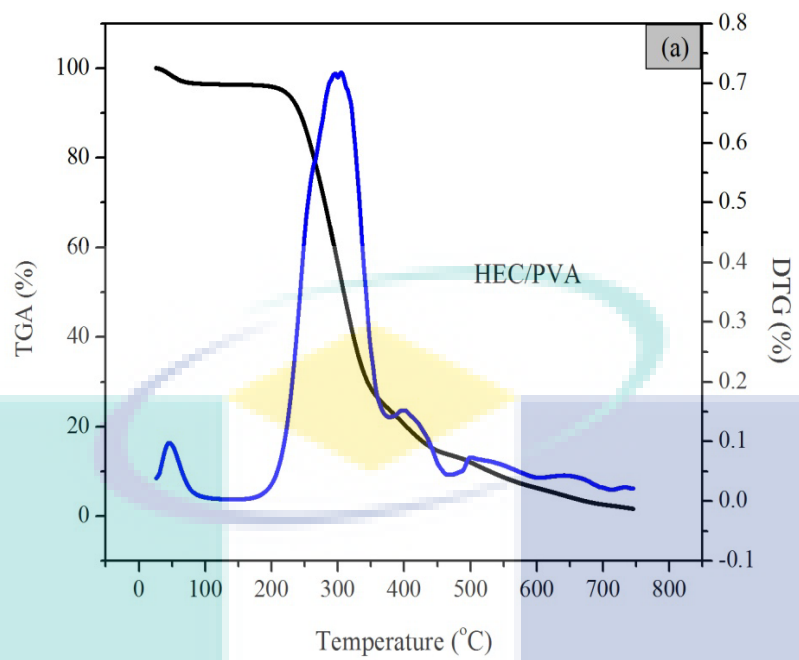
Figure 4.12 (ii) ATR-FTIR spectra of (a) HEC/PVA and HEC/PVA/CNC (b) 1 wt%, (c) 3 wt%, (d) 5 wt% and (e) 7 wt% scaffolds

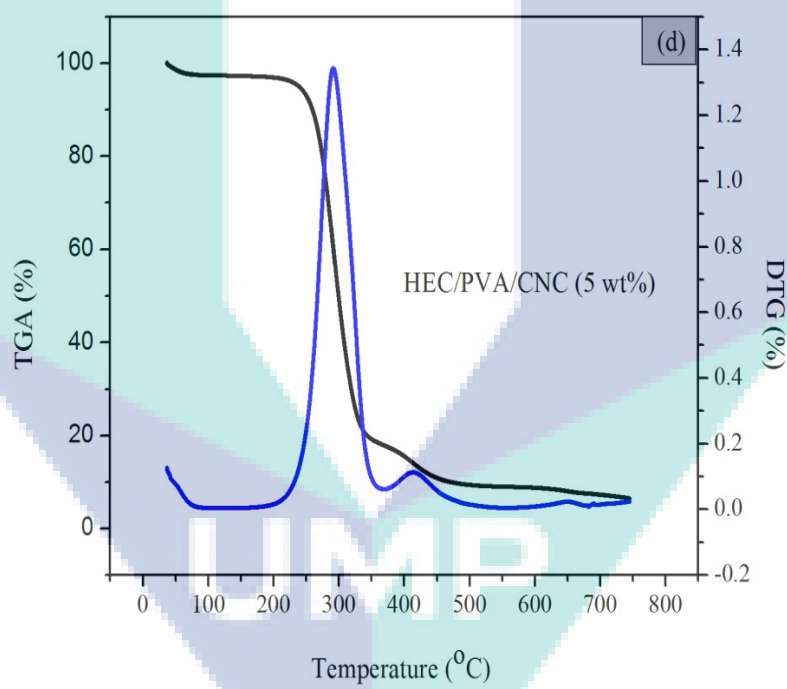
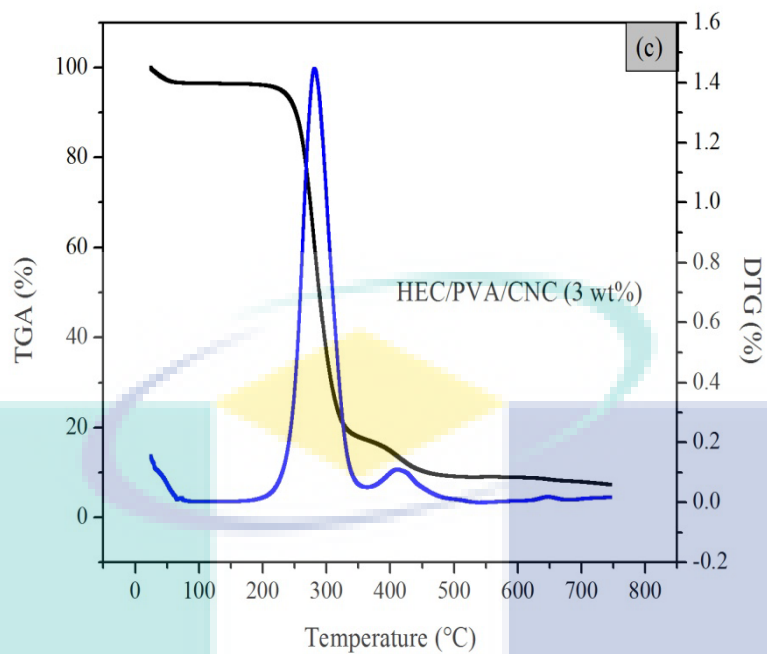
4.2.4 TGA measurements

Thermal stability of HEC/PVA and HEC/PVA/CNC scaffolds was studied using TGA. The thermograms and its derivatives (DTG) of all scaffolds are illustrated in Figure 4.13. All curves exhibited three major weight losses. These steps were distinguishable in the diagram of mass loss (TGA %) during heating as well as more clearly in the diagram of derivative mass loss (DTG %). The details of the decomposition step and percentage mass loss for HEC/PVA and HEC/PVA/CNC scaffolds are summarized in detail as shown in Table 4.3. The difference in thermal decomposition behavior of HEC/PVA and HEC/PVA/CNC blend samples can be seen more clearly from DTG curves.

From the results, all curves exhibited three major weight losses where at the first stage, water evaporated from CNC indicates that the decomposition of O-H. The lower values of weight loss percentage, varied from 3.04 to 5.44 % starting from 25 °C to 275 °C, affirmed the presence of a thermal process due to moisture evaporation or weak physisorption of water. At the second stage, starting from 124 °C to 387 °C, there were more side chains like C-O, C-H and O-H were degraded. Hence, the major weight loss which ranging from 71.26 % up until 79.09 % was detected at this stage. Next, the third stage where the backbone of cellulose started to degrade at 358 °C until 534 °C, where the weight loss percentage is in the range of 10.62 % to 22.33%.

It is clear that all the scaffolds exhibited almost similar trends in their thermal properties. It is interesting to note that the shape of the TGA/DTG curves for the HEC/PVA/CNC combines the main characteristics of HEC, PVA and CNC. These TGA results provide further evidence to the successful fabrication of scaffolds via freeze-drying technique. It can conclude that the thermal stability of HEC/PVA scaffold was increased by mixing it with CNC. The maximum mass loss rate of HEC/PVA/CNC scaffolds shifted to a lower temperature compared with HEC/PVA scaffold, which indicate that CNC degraded at low temperature than HEC/PVA scaffold.





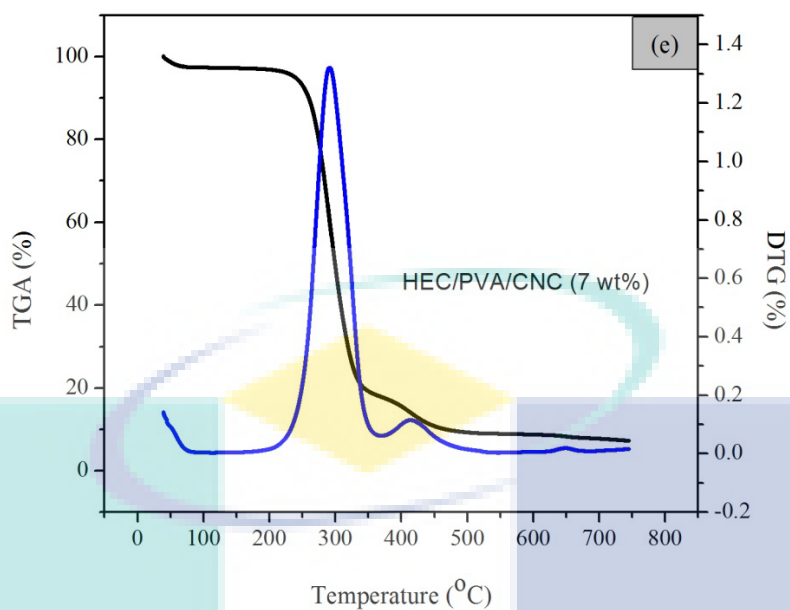


Figure 4.13 TGA and DTG curves for (a) HEC/PVA, HEC/PVA/CNC (b) 1 wt%, (c) 3 wt%, (d) 5 wt% and (e) 7 wt% scaffolds

Table 4.3 TGA and DTG for all scaffolds

Sample	Region of decomposition	Temperature (°C)			Weight loss (%)	
		T _{start}	T _{end}	T _{peak}	Partial	Total
HEC/PVA	1 st	26	175	46	4.100	98.43
	2 nd	175	378	304	72.00	
	3 rd	378	465	400	22.33	
HEC/PVA/CNC (1wt%)	1 st	25	190	140	5.438	97.548
	2 nd	190	387	290	71.26	
	3 rd	387	511	422	20.85	
HEC/PVA/CNC (3wt%)	1 st	25	197	75	3.860	94.77
	2 nd	197	360	280	78.90	
	3 rd	360	494	412	12.01	
HEC/PVA/CNC (5wt%)	1 st	36	196	149	3.044	93.574
	2 nd	196	358	291	79.05	
	3 rd	358	534	415	11.48	
HEC/PVA/CNC (7wt%)	1 st	39	192	124	3.119	92.829
	2 nd	124	359	291	79.09	
	3 rd	359	509	418	10.62	

4.2.5 DSC study

DSC is an analytical instrument that measure the glass transition and melting temperature of materials. This is very important in understanding how well any polymer will behave and what it can be used for. The development of new materials based on polymeric blends is miscibility between the polymers in the mixture, because the degree of miscibility is directly related to final properties of polymeric blend. The molecular structures of polymer are strongly affects crystallinity. At high temperature, the polymer chains can move around easily so that the molecules have no trouble moving into new positions to relieve the stress that have placed on them. But, when the sample of polymer is bending below T_g , the polymer chains were unable to move into new positions to relieve the stress. Thus, the glass transition temperature value of a polymer can be modified with a blending small amount of additive.

Thermograms for pure components and all porous scaffolds are shown in Figure 4.14. From Table 4.4, it is found that the T_g of all scaffold is varied at 42.4 °C to 60.9 °C while the T_m started at 293.4 °C to 312.4 °C. The crystallinity, χ_c of HEC/PVA incorporated with and without CNC were calculated based on the melting enthalpy, ΔH_m from DSC thermograms. As the concentration of CNC increased, the χ_c also increased from 1.12 % to 4.16 %. Thermal stability in high concentration CNC was better than in low concentration of CNC. This is due to the introduced of sulphate groups into CNC by acid hydrolysis of sulphuric acid. The sulphate groups at the outer layer of cellulose during acid hydrolysis caused dehydration of cellulose to reduce the thermal stability.

Past research from Vestena et al reported that the presence of CNC in poly(lactic acid) (PLA) or poly(hydroxyalkanoates) increased the thermal stability and resistance toward heat (Vestena, Gross, Müller, & Pires, 2015). This could be due to the properties of CNC which they have a very high heat resistance. Hence, they could hinder the heat flow to the materials. Moreover, the addition of CNC is also beneficial for the reduction of thermal expansion and rapid heat dissipation of polymer.

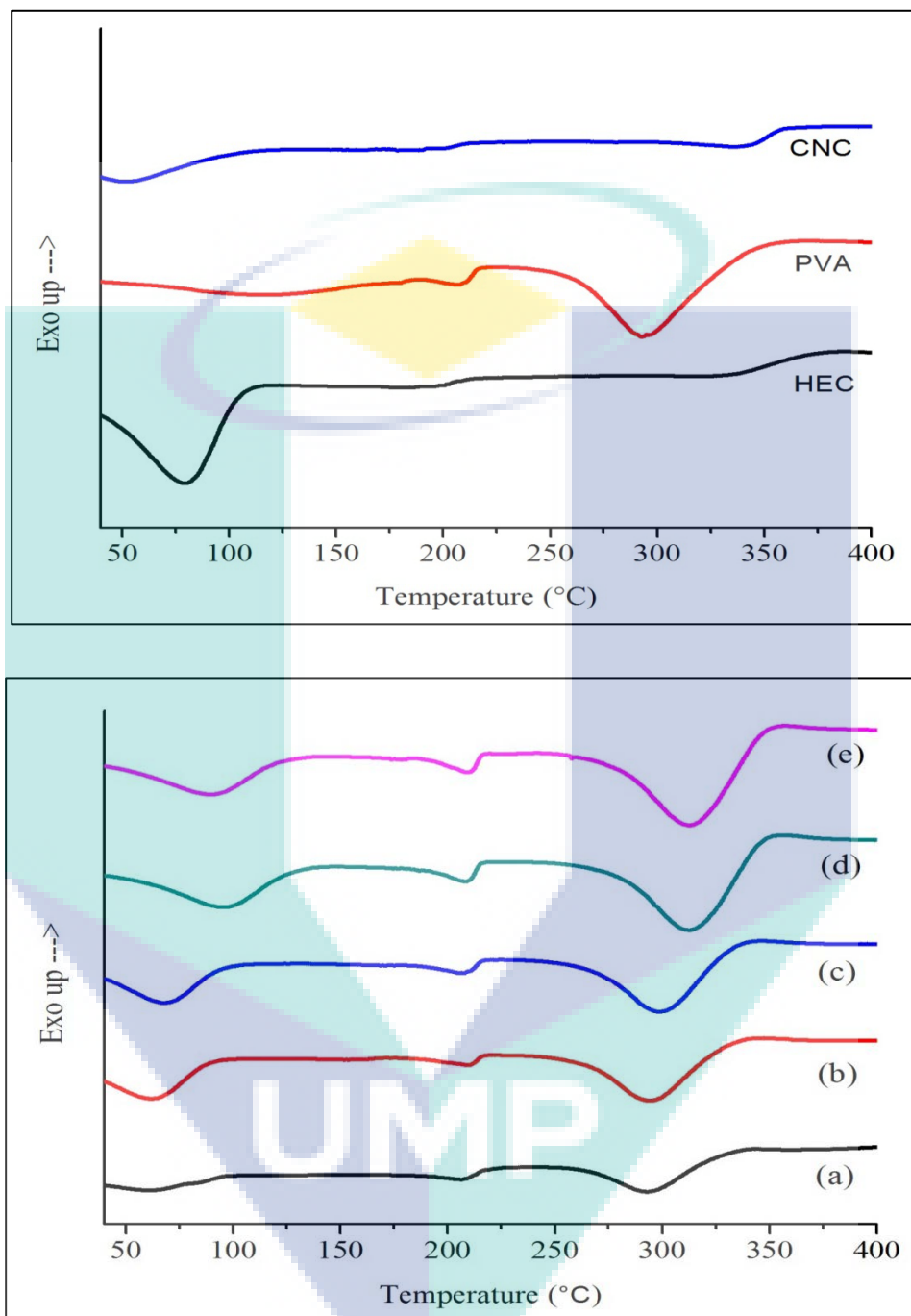


Figure 4.14 DSC thermograms of CNC, HEC and PVA alone and HEC/PVA scaffolds with different CNC concentration at (1,3,5 and 7 wt%)

Table 4.4 DSC data for all scaffolds

Types of scaffold	T _g (°C)	T _m (°C)	ΔH _m (J/g)	χ _c (%)
HEC	51.4	79.2	400.6	-
PVA	60.1	292.3	526.6	3.79
CNC	43.5	336.4	26.42	-
HEC/PVA	45.6	293.4	154.9	1.12
HEC/PVA/CNC (1 wt%)	42.4	293.9	341.6	2.46
HEC/PVA/CNC (3 wt%)	45.2	298.6	404.8	2.92
HEC/PVA/CNC (5 wt%)	60.9	312.3	576.1	4.16
HEC/PVA/CNC (7 wt%)	55.1	312.4	605.7	4.37

4.2.6 Mechanical properties

In developing scaffolds, the role of mechanical properties should also be considered, especially in the applications that require load bearing function. Scaffolds with excellent mechanical properties are most likely being favored in products for hard tissues, such as bone and teeth.

Figure 4.15 shows the compressive strength for all porous scaffolds and Table 4.5 displays the compressive strength and Young's modulus value. All cross linked porous materials of HEC/PVA/CNC show slightly higher ultimate tensile stress and ultimate tensile strain compared to HEC/PVA scaffolds which ranging from 0.5 MPa to 0.92 MPa and 5.83 % to 11.03 %, respectively. It can be seen that the Young's modulus of the crosslinking HEC/PVA incorporated with CNC increased with increasing of CNC content. These results suggest that CNC offers an improvement in the mechanical performance of the material. The combination of CNC in HEC/PVA provides strength and stiffness to the final HEC/PVA/CNCs scaffolds. In summary, mechanical strength

must be considered in well-designed 3D porous scaffolds to enable load-bearing function in bone tissues.

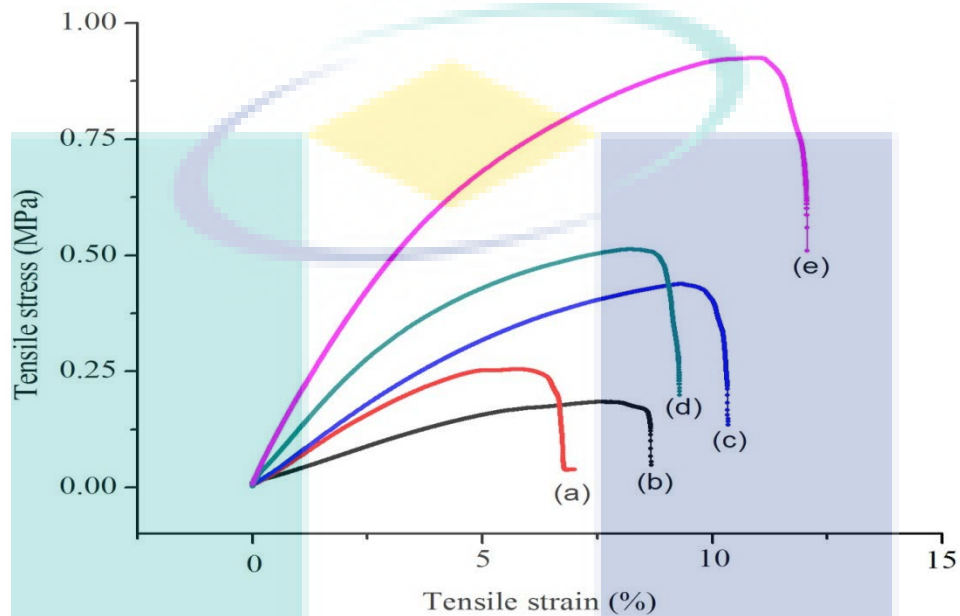


Figure 4.15 Stress-strain curves for (a) HEC/PVA and HEC/PVA/CNC (b) 1 wt%, (c) 3 wt%, (d) 5 w% and (e) 7 wt% scaffolds

Table 4.5 Mechanical data observed for all scaffolds

Type of scaffolds	Ultimate tensile stress (MPa)	Ultimate tensile strain (%)	Young's modulus (MPa)
HEC/PVA	0.25	5.83	12.67
HEC/PVA/CNC (1 wt%)	0.18	7.76	18.04
HEC/PVA/CNC (3 wt%)	0.44	9.33	30.25
HEC/PVA/CNC (5 wt%)	0.51	9.43	31.63
HEC/PVA/CNC (7 wt%)	0.92	11.03	52.85

4.3 In vitro degradation study of HEC/PVA and HEC/PVA/CNCs scaffolds

For bone tissue engineering application, the degradation behavior of porous scaffold is important criteria that need to be stressed. From the literature review, it is found that the total time required to complete a remodeling cycle for a typical bone-remodeling unit for a young adult is estimated to be about 200 days where one bone-remodeling unit takes approximately 3 weeks to complete the bone resorption. Then finally takes 3 months to form bone. Due to this concern, the scaffolds should be biodegradable in order to works well in human body system. Hence, weight loss, swelling ratio and pH value analysis were carried out in this research.

4.3.1 Weight loss, swelling ratio and pH value analysis

In tissue engineering, porous biodegradable scaffolds are said to facilitate and provide sufficient spaces for cell growths and tissue formation. In this study, the degradation behavior of all scaffolds in PBS at 37 °C for 7 days incubation period was observed. Generally, all porous scaffolds will exhibits increment in weight loss percentage of degradation with time. Figure 4.16 shows the percentage of weight loss for all prepared scaffolds. After 7 days of degradation, HEC/PVA scaffolds had a high percentage weight loss at 80 % compared to HEC/PVA/CNC scaffolds which ranging from 43 % to 68 %, respectively. From the analysis, it can be conclude that the higher concentration of CNC content will have the lower percentage value of weight loss. This is because basically nanocelluloses are hydrophilic in nature which hampers interfacial compatibility with most hydrophobic polymer matrices. By providing hydrophobicity surfaces to the nanocelluloses, interfacial wetting and interactions with commodity polymer matrices were improved.

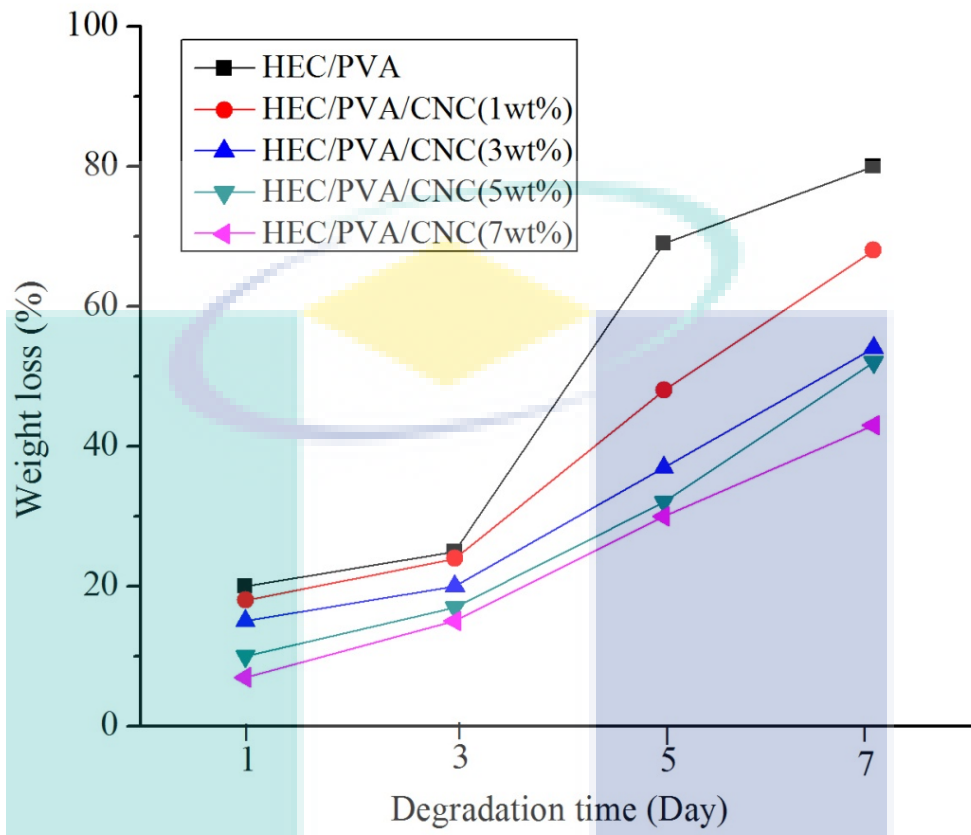


Figure 4.16 Weight loss of HEC/PVA scaffolds with different CNC concentration at (1, 3, 5 and 7 wt%)

Next, the swelling ratios of all porous scaffolds are illustrated in Figure 4.17, as a function of polymer composition. After day 1 of conducting this experiment, all scaffolds have a very high degree of swelling ratio that reflecting the hydrophilic properties of the scaffolds. It is basically occurs when a materials with highly porous network enables the absorption of an amount of bulky water. The values of swelling ratio of all scaffolds increased parallel throughout the 7 days of experiment. It is worth to note that after 7 days, at some time point, the swelling capability of the scaffolds will achieve maximum swelling capacity and will ultimately start to degrade due to the breaking of polymer chains.

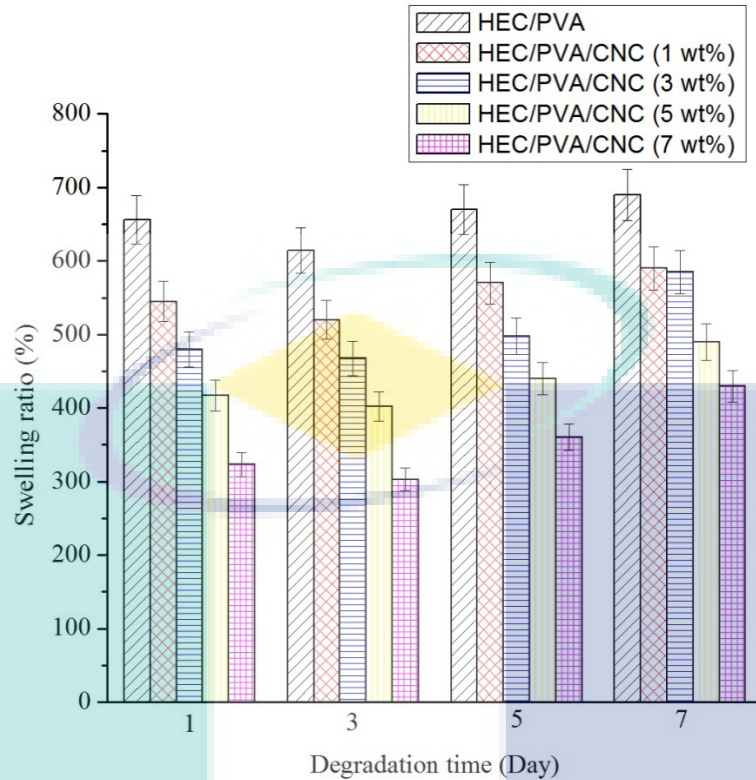


Figure 4.17 Swelling ratio of HEC/PVA scaffolds with different CNC concentration at (1, 3, 5 and 7 wt%)

pH is a scale used to specify how acidic or basic a water-based solution is. Hence, pH measurement is one of the important tests to perform in order to check the compatibility of the scaffold materials prepared especially when the materials were need to react with living tissue in human body. Researchers need to make sure that the scaffolds do not bring any harmful to the living cell as well as do not give any bad effect to the internal organ. pH changes of PBS solution is illustrated in Figure 4.18. During 4 weeks of degradation in PBS solution, it shows that pH value was decreased to ~6.8 from its original pH which is 7.4 for all porous scaffolds. However, the decreasing trend did not bring any significant effect to the entire cell culture as it still consider safe to be used in human body.

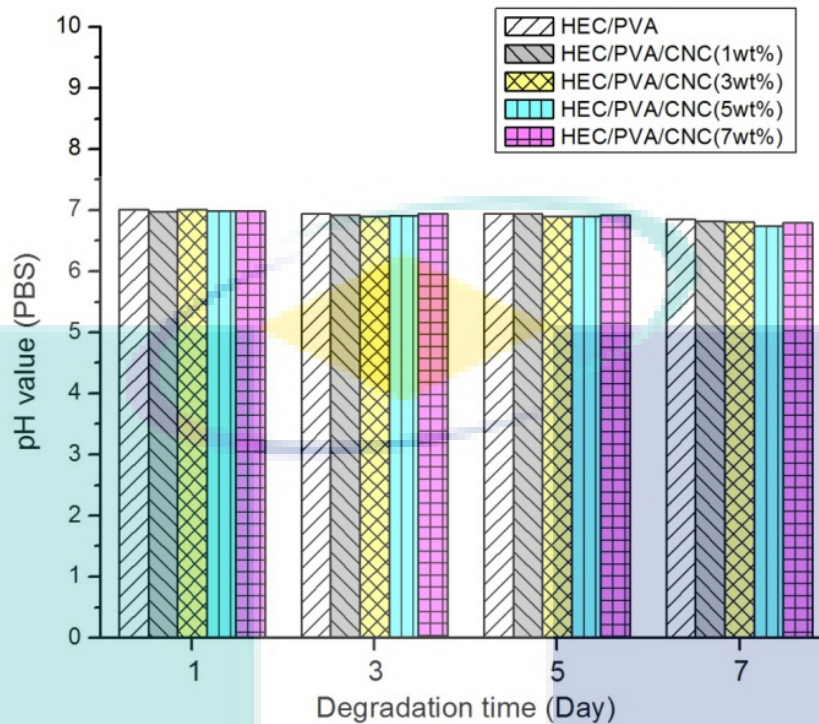


Figure 4.18 pH value analysis of HEC/PVA and HEC/PVA/CNC (1, 3, 5, 7 wt%) porous scaffolds

4.4 Cell culture studies on HEC/PVA and HEC/PVA/CNCs scaffolds for bone tissue engineering application

Cell culture experiment is conducted to test the toxicity and biocompatibility of the materials towards the living cells. Generally, good biocompatibility requires the cells to attach and grow well internally and externally of the scaffolds. Hydroxyapatite is the major inorganic component present in human bone that is often integrated in a scaffold for bone regeneration because of its biocompatibility and osteoconductive properties and as a neutralizing additive due to its alkaline property. Attentions were focused on the morphology, viability and proliferation of human fetal osteoblast cells (hFOB) on scaffold. Mature and active osteoblasts synthesize most of the proteins in bone extracellular matrix. Some osteoblasts are buried in bone matrix and become osteocytes, while some osteoblasts become flattened cell on bone surface bone lining cells (inactive osteoblasts) (Sommerfeldt & Rubin, 2001).

4.4.1 hFOB cells proliferation on scaffolds

The viability of hFOB cells cultured on scaffolds was measured by an MTT cell proliferation assay, and the number of viable cells was assayed by cell counting under an inverted fluorescence microscope. The intrinsic mechanism of the MTT assay is that active cells react with a tetrazolium salt in the MTT reagent to produce a soluble formazan dye, which can be absorbed at a wavelength of 490 nm. The results obtained by MTT assay were compared with hFOB cells in a complete media without the presence of scaffolds as a positive control.

According to the results, there were no significant difference in biocompatibility between control and all scaffolds after 7 days. Though there was no significant difference in the proliferation of osteoblast cells in all porous scaffolds, HEC/PVA/CNC scaffolds shows more osteoblast cell proliferation compare to HEC/PVA scaffold.

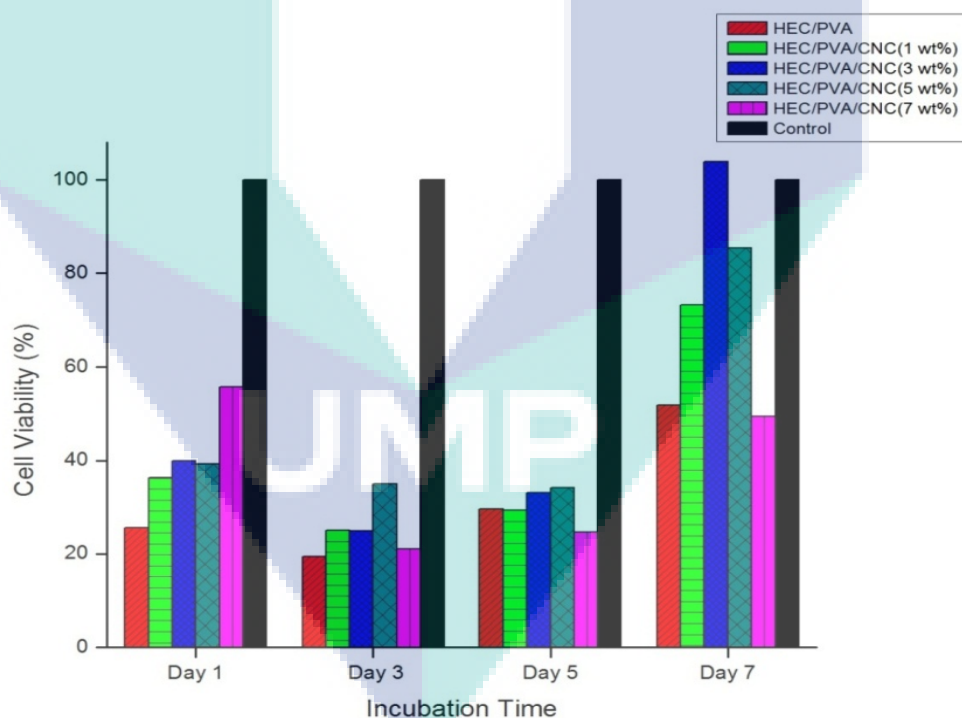
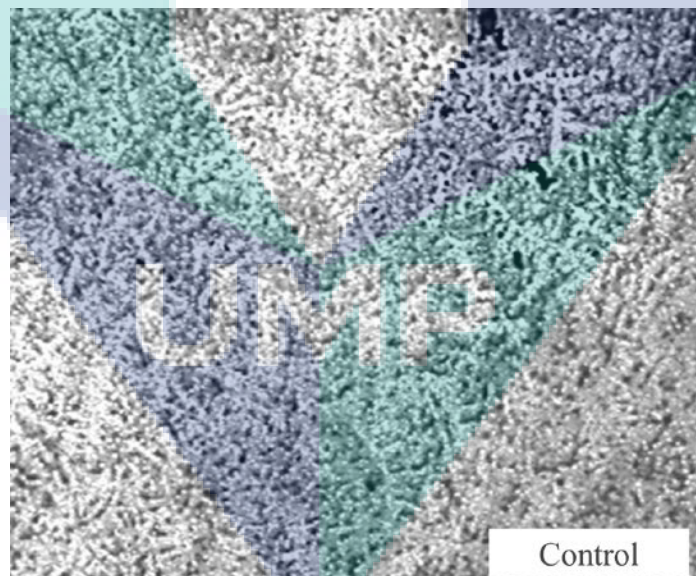


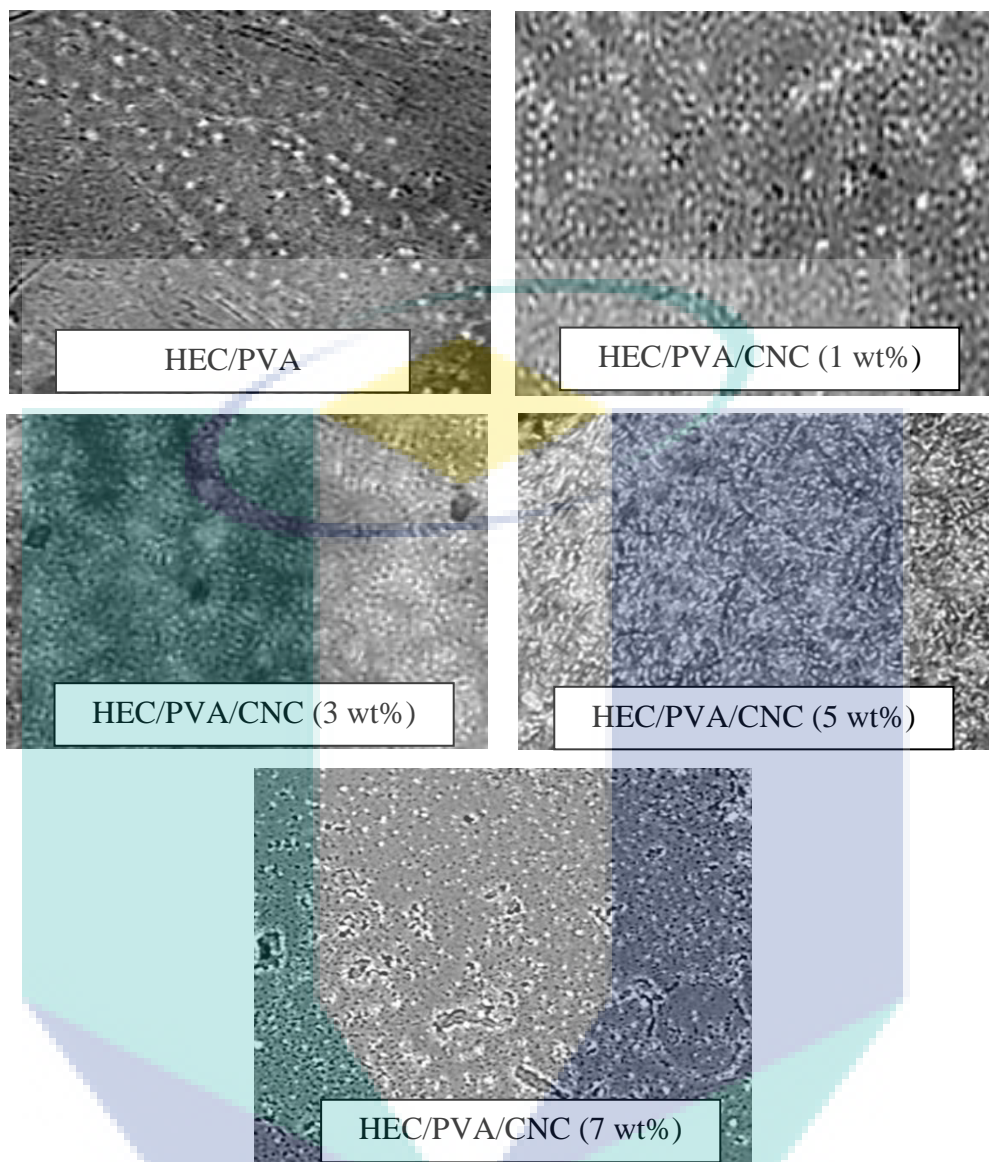
Figure 4.19 Graph showing hFOB cell viability after 1, 3, 5 and 7 days of incubation (1×10^5 cells/well in complete DMEM) at different weight ratios of scaffolds.

Figure 4.19 above presents the proliferation of hFOB cells cultured on all scaffolds as determined by MTT assay. The cell numbers on all scaffolds increased significantly from 1 to 7 days but there is some reduction in cell numbers at day 3. In addition, the cell numbers on HEC/PVA scaffolds incorporated with various amount of CNC increased obviously starting from day 3 to day 7 but no significant difference existed between them. However, the cell numbers on HEC/PVA scaffolds exhibited only smaller significant increase from day 3 to day 7, respectively.

The quantitative analysis of Trypan blue of hFOB cells cultured on all scaffolds is shown in Figure 4.20. The results obtained from fluorescent microscope that detect nucleus cells indicate that more cells grew on the HEC/PVA/CNC scaffolds than on HEC/PVA scaffolds at each time point. Results exhibited that the incorporation of CNC up to 7 wt% into HEC/PVA scaffolds did not present any inhibitory influence on the cytocompatibility characteristic of the HEC/PVA scaffolds, however further addition of CNC up to 5 wt% reduced the cell viability. This result also shows how the CNC sheets provide a noncytotoxic environment for cells to remain viable, as cell metabolism was constant between 3 and 7 days for S-CNC aerogels (Daniel A. Osorio, 2019).



(i)



(ii)

UMP

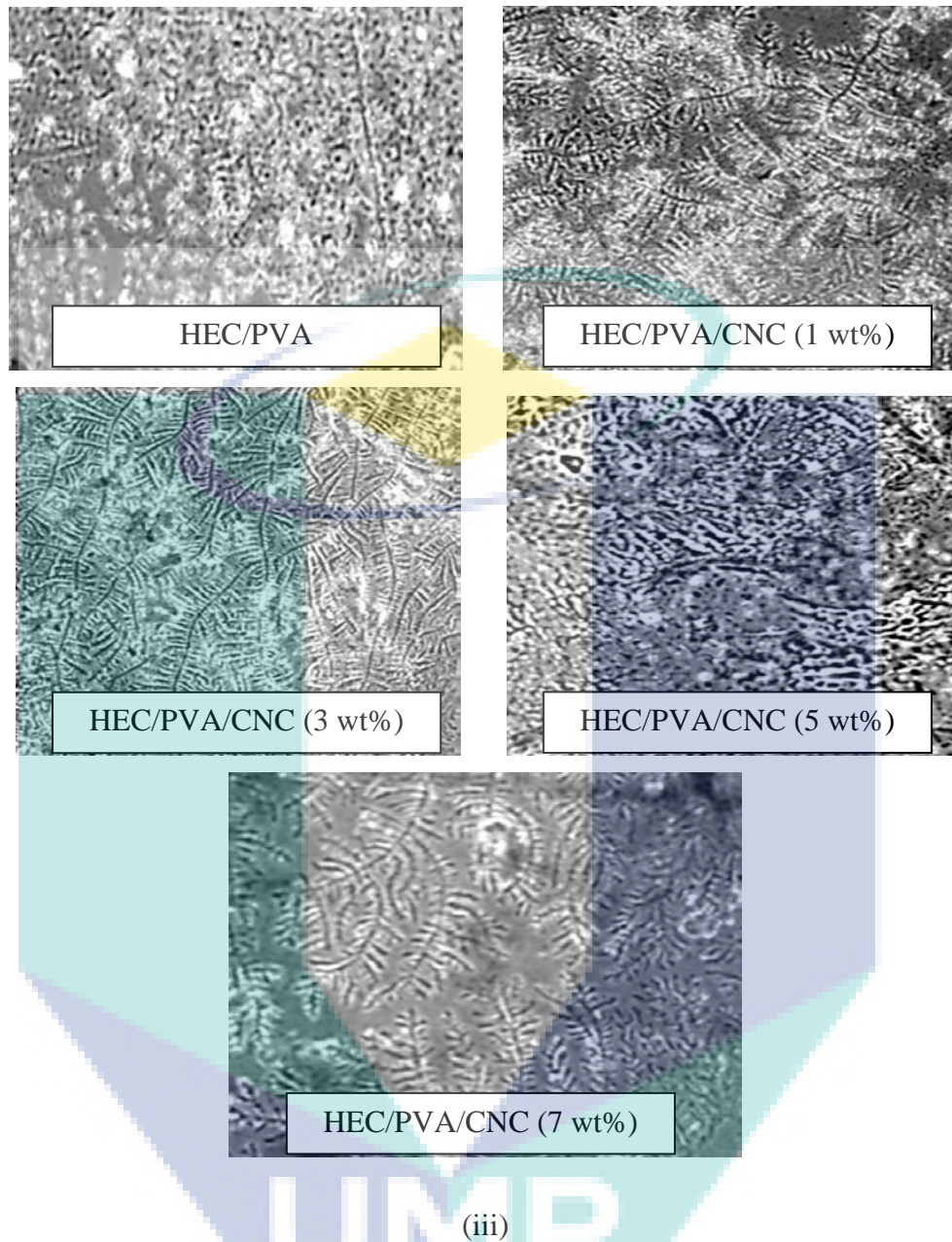


Figure 4.20 Light micrograph images of hFOB cells (i) control and hFOB cells attached on scaffolds after (ii) day 3 and (iii) day 7 cell culture.

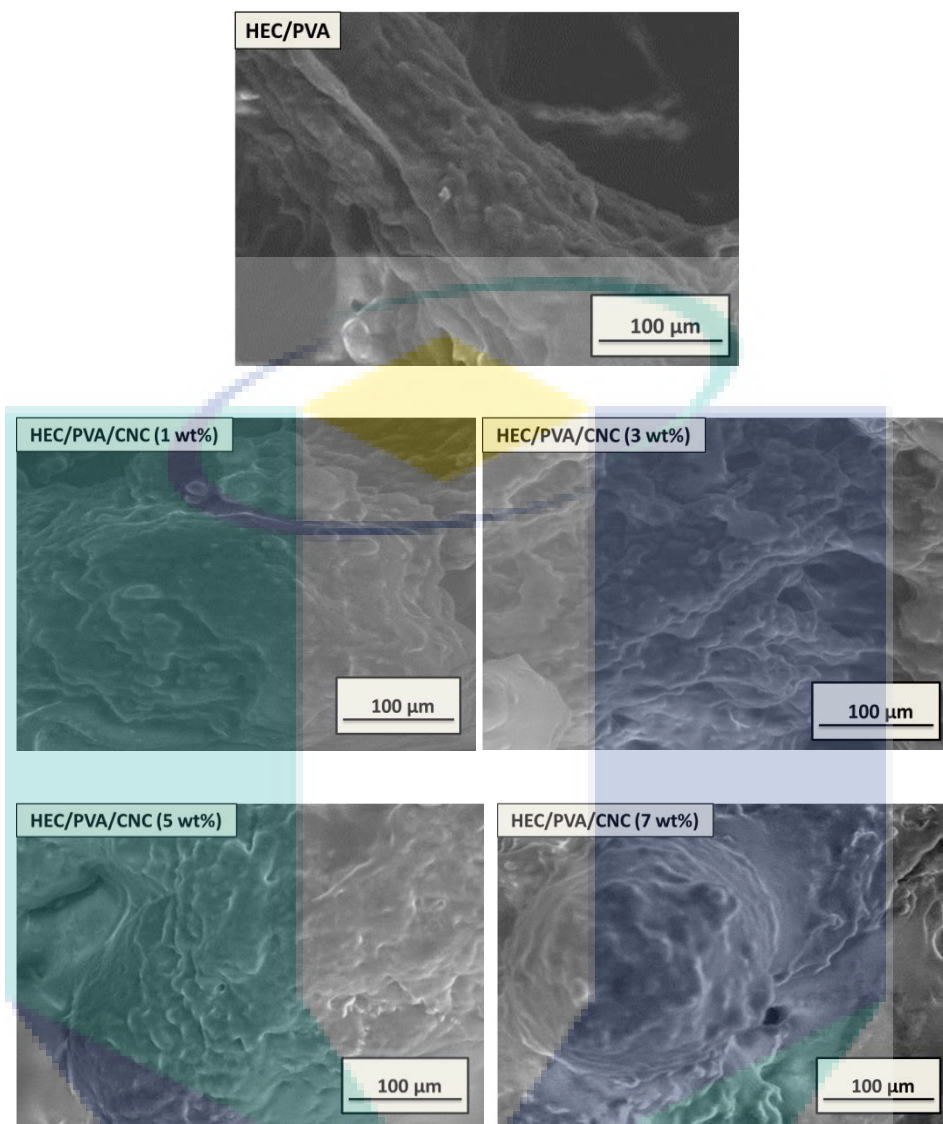
Based on cell proliferation results, it suggests that hFOB cells are quite sensitive to subtle changes in temperature. When hFOB cells are cultured at 37°C, the restrictive temperature at which the large T antigen is not expressed, the cells proliferate rapidly. However, when the cells are switched to the permissive temperature of 39.5°C, cell proliferation slows and cell number does not increase further (Henry J. Donahue, 2000). This reported was similar to the research carried out by Henry et al.

4.4.2 hFOB cells morphology studies on scaffolds

hFOB cells cultured for 3 and 7 days on the samples were also observed by SEM. Figure 4.21 presents the SEM images of cells cultured on the samples at 3 and 7 days. Round shape morphology of osteoblast cells adhered on the surface of the all scaffolds. It is clearly observed that the cells exhibited slightly rough surface for all blended scaffolds. Incorporated scaffolds with CNC make the surface even rougher. After 3 days of cell culture, it was observed that cells get adhered to the scaffold and have polygonal morphology with the cell membrane being somewhat flattened onto the rough surface of the scaffold, created by HEC/PVA/CNC particles.



UMP



(i)

UMP

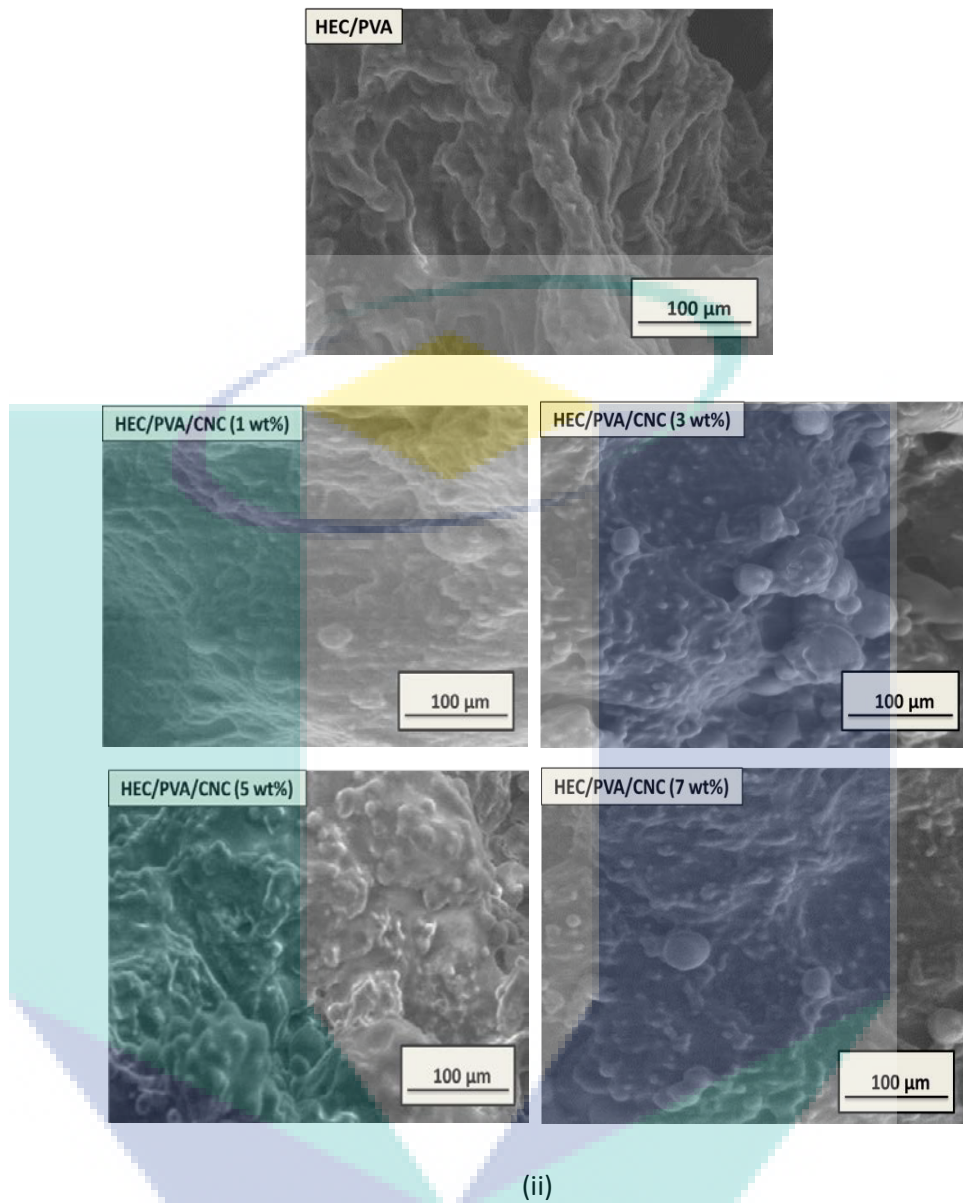


Figure 4.21 SEM micrograph images of hFOB cells attached on after (i) day 3 and (ii) day 7 cell culture

At 7 days of cell culture, more flat osteoblast cells were produced indicating that the osteoblast cell proliferation had begun. SEM image of osteoblast cell-scaffolds depicts that osteoblast cells have spread all around the porous structure of the scaffold and covered almost the entire scaffold's surface at 7 days. The cells on the HEC/PVA/CNC scaffolds spread better than on HEC/PVA scaffolds as the incubation time increased. This result was also supported with MTT assay, which confirmed the potential of HEC/PVA/CNC scaffold towards bone tissue regeneration.

All scaffolds showed low toxicity and supported the growth of hFOB cells. This observation will be further proven by the following statistics analysis of cellular proliferation and viability of cell growth. Great cell attachment, adherence and proliferation are suitable remarks for in vivo culture.



UMP

CHAPTER 5

CONCLUSION

5.1 Summary

To conclude, HEC/PVA/CNCs demonstrate greater response towards hFOB cells with highest number of viable cells. All freeze-dried scaffolds show excellent cell attachment, adherence and proliferation, with more prominent results in HEC/PVA/CNC (3 wt%). In this study, incorporated CNC indicating the great influence with HEC/PVA blended for tissue engineering. Overall, all scaffolds endorse good biocompatibility, non-toxicity and could be potential substrates for skin tissue engineering.

The results demonstrated that the HEC/PVA/CNC scaffold should be a promising candidate for proliferation, differentiation and mineralization of osteoblasts, and potentially can be used for bone tissue regeneration. These scaffolds can promote cells migration and stimulate cell proliferation and mineralization. Osteoblasts play an important role in the formation, growth, and repair of the bone, as they can form organic, non-mineralized bone matrix. Osteoblasts were found to be viable within all scaffolds suggesting that the environment could sustain osteoblast growth and proliferation.

5.2 Recommendation for further research

1. There are several characterization testing could be conducted such as antimicrobial, XRD analysis, contact angle of samples to ensure its effectiveness.
2. The polymer solution and prepared freeze-dried porous scaffolds should be kept in dry cabinet to avoid any contamination occur such as fungal growth.
3. Hydrolysis by using deionized water to reduce the ions on the surface of material. Deionized water is more pure than distilled water.

The logo for UMP (Universitas Muhammadiyah Purwokerto) is a large, downward-pointing arrow shape. It is composed of several overlapping geometric shapes in shades of teal, light blue, and yellow. The letters 'UMMP' are written in a bold, white, sans-serif font across the bottom of the arrow.

UMMP

REFERENCES

- Abd-Khorsand, S., Saber-Samandari, S., & Saber-Samandari, S. (2017). Development of nanocomposite scaffolds based on TiO₂ doped in grafted chitosan/hydroxyapatite by freeze drying method and evaluation of biocompatibility. *Int J Biol Macromol*, 101, 51-58.
- Ali, M. E., & Lamprecht, A. (2017). Spray freeze drying as an alternative technique for lyophilization of polymeric and lipid-based nanoparticles. *Int J Pharm*, 516(1-2), 170-177.
- Alizadeh, M., Abbasi, F., Khoshfetrat, A. B., & Ghaleh, H. (2013). Microstructure and characteristic properties of gelatin/chitosan scaffold prepared by a combined freeze-drying/leaching method. *Mater Sci Eng C Mater Biol Appl*, 33(7), 3958-3967.
- Anandan, D., Madhumathi, G., Nambiraj, N. A., & Jaiswal, A. K. (2019). Gum based 3D composite scaffolds for bone tissue engineering applications. *Carbohydr Polym*, 214, 62-70.
- Bhardwaj, N., Chakraborty, S., & Kundu, S. C. (2011). Freeze-gelled silk fibroin protein scaffolds for potential applications in soft tissue engineering. *Int J Biol Macromol*, 49(3), 260-267.
- Bhat, S., & Kumar, A. (2013). Biomaterials and bioengineering tomorrow's healthcare. *Biomatter*, 3(3).
- Borkotoky, S. S., Dhar, P., & Katiyar, V. (2018). Biodegradable poly (lactic acid)/Cellulose nanocrystals (CNCs) composite microcellular foam: Effect of nanofillers on foam cellular morphology, thermal and wettability behavior. *Int J Biol Macromol*, 106, 433-446.
- Butylina, S., Geng, S., & Oksman, K. (2016). Properties of as-prepared and freeze-dried hydrogels made from poly(vinyl alcohol) and cellulose nanocrystals using freeze-thaw technique. *European Polymer Journal*, 81, 386-396.
- Caló, E., & Khutoryanskiy, V. V. (2015). Biomedical applications of hydrogels: A review of patents and commercial products. *European Polymer Journal*, 65, 252-267.
- Chocholata, P., Kulda, V., & Babuska, V. (2019). Fabrication of Scaffolds for Bone-Tissue Regeneration. *Materials (Basel)*, 12(4).

- Clarke, B. (2008). Normal bone anatomy and physiology. *Clin J Am Soc Nephrol*, 3 Suppl 3, S131-139.
- Daniel A. Osorio, B. E. J. L., Jacek M. Kwiecien, Xiaoyue Wang, Iflah Shahid, Ariana L. Hurley, Emily D. Cranston, Kathryn Grandfield. (2019). Cross-linked Cellulose Nanocrystal Aerogels as Viable Bone Tissue Scaffolds.
- Edwards, J. V., Prevost, N., Sethumadhavan, K., Ullah, A., & Condon, B. (2013). Peptide conjugated cellulose nanocrystals with sensitive human neutrophil elastase sensor activity. *Cellulose*, 20(3), 1223-1235.
- Fereshteh, Z., Fathi, M., Bagri, A., & Boccaccini, A. R. (2016). Preparation and characterization of aligned porous PCL/zein scaffolds as drug delivery systems via improved unidirectional freeze-drying method. *Mater Sci Eng C Mater Biol Appl*, 68, 613-622.
- Fonte, P., Reis, S., & Sarmiento, B. (2016). Facts and evidences on the lyophilization of polymeric nanoparticles for drug delivery. *J Control Release*, 225, 75-86.
- Gavasane, A. J. (2014). Synthetic Biodegradable Polymers Used in Controlled Drug Delivery System: An Overview. *Clinical Pharmacology & Biopharmaceutics*, 3(2).
- Geetha, B., Premkumar, J., Pradeep, J. P., & Krishnakumar, S. (2019). Synthesis and characterization of bioscaffolds using freeze drying technique for bone regeneration. *Biocatalysis and Agricultural Biotechnology*, 20.
- Ghafari, R., Jonoobi, M., Amirabad, L. M., Oksman, K., & Taheri, A. R. (2019). Fabrication and characterization of novel bilayer scaffold from nanocellulose based aerogel for skin tissue engineering applications. *Int J Biol Macromol*, 136, 796-803.
- Ghorbani, F., Nojehdehian, H., & Zamanian, A. (2016). Physicochemical and mechanical properties of freeze cast hydroxyapatite-gelatin scaffolds with dexamethasone loaded PLGA microspheres for hard tissue engineering applications. *Mater Sci Eng C Mater Biol Appl*, 69, 208-220.
- Ghorbani, F., Zamanian, A., & Nojehdehian, H. (2017). Effects of pore orientation on in-vitro properties of retinoic acid-loaded PLGA/gelatin scaffolds for artificial peripheral nerve application. *Mater Sci Eng C Mater Biol Appl*, 77, 159-172.
- Gokmen, F. O., Rzayev, Z. M., Salimi, K., Bunyatova, U., Acar, S., Salamov, B., & Turk, M. (2015). Novel multifunctional colloidal carbohydrate nanofiber electrolytes with excellent conductivity and responses to bone cancer cells. *Carbohydr Polym*, 133, 624-636.
- Henry J. Donahue, Z. L., Zhiyi Zhou, and Clare E. Yellowley. (2000). Differentiation of human fetal osteoblastic cells and gap junctional intercellular communication. *American Physiological Society*, 278, C315-C322.

- Hirano, Y., & Mooney, D. J. (2004). Peptide and Protein Presenting Materials for Tissue Engineering. *Advanced Materials*, 16(1), 17-25.
- Hoggatt, J., & Pelus, L. M. (2013). Hematopoiesis. In *Brenner's Encyclopedia of Genetics* (pp. 418-421).
- Huang, C., Bhagia, S., Hao, N., Meng, X., Liang, L., Yong, Q., & Ragauskas, A. J. (2019). Biomimetic composite scaffold from an in situ hydroxyapatite coating on cellulose nanocrystals. *RSC Advances*, 9(10), 5786-5793.
- Jia An, C. K. C., Ting Yu, Huaqiong Li & Lay Poh Tan. (2013). Advanced nanobiomaterial strategies for the development of organized tissue engineering constructs. *Nanomedicine*, 8(4), 591-602.
- Kai, D., Prabhakaran, M. P., Stahl, B., Eblenkamp, M., Wintermantel, E., & Ramakrishna, S. (2012). Mechanical properties and in vitro behavior of nanofiber-hydrogel composites for tissue engineering applications. *Nanotechnology*, 23(9), 095705.
- Kanimozhi, K., Khaleel Basha, S., & Sugantha Kumari, V. (2016). Processing and characterization of chitosan/PVA and methylcellulose porous scaffolds for tissue engineering. *Mater Sci Eng C Mater Biol Appl*, 61, 484-491.
- Kasper, J. C., Winter, G., & Friess, W. (2013). Recent advances and further challenges in lyophilization. *Eur J Pharm Biopharm*, 85(2), 162-169.
- Kavitha Sankar, P. C., Rajmohan, G., & Rosemary, M. J. (2017). Physico-chemical characterisation and biological evaluation of freeze dried chitosan sponge for wound care. *Materials Letters*, 208, 130-132.
- Khoshkava, V., & Kamal, M. R. (2014). Effect of drying conditions on cellulose nanocrystal (CNC) agglomerate porosity and dispersibility in polymer nanocomposites. *Powder Technology*, 261, 288-298.
- Koc Demir, A., Elcin, A. E., & Elcin, Y. M. (2018). Strontium-modified chitosan/montmorillonite composites as bone tissue engineering scaffold. *Mater Sci Eng C Mater Biol Appl*, 89, 8-14.
- Kordjamshidi, A., Saber-Samandari, S., Ghadiri Nejad, M., & Khandan, A. (2019). Preparation of novel porous calcium silicate scaffold loaded by celecoxib drug using freeze drying technique: Fabrication, characterization and simulation. *Ceramics International*, 45(11), 14126-14135.
- Kousaku Ohkawa, D. C., Hakyong Kim, Ayako Nishida, Hiroyuki Yamamoto¹. (2004). Electrospinning of Chitosan. *Macromolecular Rapid Communications*, 1600-16005.
- Kumar, A., Mandal, S., Barui, S., Vasireddi, R., Gbureck, U., Gelinsky, M., & Basu, B. (2016). Low temperature additive manufacturing of three dimensional scaffolds for bone-tissue engineering applications: Processing related challenges and property assessment. *Materials Science and Engineering: R: Reports*, 103, 1-39.

- Lamaming, J., Hashim, R., Leh, C. P., Sulaiman, O., Sugimoto, T., & Nasir, M. (2015). Isolation and characterization of cellulose nanocrystals from parenchyma and vascular bundle of oil palm trunk (*Elaeis guineensis*). *Carbohydr Polym*, 134, 534-540.
- Li, J., Wang, Y., Wei, X., Wang, F., Han, D., Wang, Q., & Kong, L. (2014). Homogeneous isolation of nanocelluloses by controlling the shearing force and pressure in microenvironment. *Carbohydr Polym*, 113, 388-393.
- MacNeil, S. (2007). Progress and opportunities for tissue-engineered skin. *Nature*, 445(7130), 874-880.
- Maji, S., Agarwal, T., Das, J., & Maiti, T. K. (2018). Development of gelatin/carboxymethyl chitosan/nano-hydroxyapatite composite 3D macroporous scaffold for bone tissue engineering applications. *Carbohydr Polym*, 189, 115-125.
- Merrill, N. A. P. a. E. W. (1976). Differential Scanning Calorimetry of Crystallized PVA Hydrogels. *Journal of applied polymer science*, 20, 1457-1465.
- Mohammadi, Z., Mesgar, A. S., & Rasouli-Disfani, F. (2016). Reinforcement of freeze-dried chitosan scaffolds with multiphasic calcium phosphate short fibers. *J Mech Behav Biomed Mater*, 61, 590-599.
- N. J. Cao, Q. X., and L. F. Chen. (1995). Acid Hydrolysis of Cellulose in Zinc Chloride Solution. *Applied Biochemistry and Biotechnology*, 51/52.
- Nasution, H., Harahap, H., Afandy, Y., & Fath, M. T. A. (2017). The effect of cellulose nanocrystal (CNC) from rattan biomass as filler and citric acid as co-plasticizer on tensile properties of sago starch biocomposite.
- Ng, H. M., Saidi, N. M., Omar, F. S., Ramesh, K., Ramesh, S., & Bashir, S. (2018). Thermogravimetric Analysis of Polymers. In *Encyclopedia of Polymer Science and Technology* (pp. 1-29).
- Preethi Soundarya, S., Sanjay, V., Haritha Menon, A., Dhivya, S., & Selvamurugan, N. (2018). Effects of flavonoids incorporated biological macromolecules based scaffolds in bone tissue engineering. *Int J Biol Macromol*, 110, 74-87.
- Qasim, S. B., Husain, S., Huang, Y., Pogorielov, M., Deineka, V., Lyndin, M., . . . Rehman, I. U. (2017). In- vitro and in -vivo degradation studies of freeze gelated porous chitosan composite scaffolds for tissue engineering applications. *Polymer Degradation and Stability*, 136, 31-38.
- Reys, L. L., Silva, S. S., Pirraco, R. P., Marques, A. P., Mano, J. F., Silva, T. H., & Reis, R. L. (2017). Influence of freezing temperature and deacetylation degree on the performance of freeze-dried chitosan scaffolds towards cartilage tissue engineering. *European Polymer Journal*, 95, 232-240.

- Saber-Samandari, S., Saber-Samandari, S., Kiyazar, S., Aghazadeh, J., & Sadeghi, A. (2016). In vitro evaluation for apatite-forming ability of cellulose-based nanocomposite scaffolds for bone tissue engineering. *Int J Biol Macromol*, 86, 434-442.
- Salehpour, S., Rafieian, F., Jonoobi, M., & Oksman, K. (2018). Effects of molding temperature, pressure and time on polyvinyl alcohol nanocomposites properties produced by freeze drying technique. *Industrial Crops and Products*, 121, 1-9.
- Sayed, M., Mahmoud, E. M., Bondioli, F., & Naga, S. M. (2019). Developing porous diopside/hydroxyapatite bio-composite scaffolds via a combination of freeze-drying and coating process. *Ceramics International*, 45(7), 9025-9031.
- Schardosim, M., Soulie, J., Poquillon, D., Cazalbou, S., Duployer, B., Tenailleau, C., . . . Combes, C. (2017). Freeze-casting for PLGA/carbonated apatite composite scaffolds: Structure and properties. *Mater Sci Eng C Mater Biol Appl*, 77, 731-738.
- Schieker, M., Seitz, H., Drosse, I., Seitz, S., & Mutschler, W. (2006). Biomaterials as Scaffold for Bone Tissue Engineering. *European Journal of Trauma*, 32(2), 114-124.
- Shahbazarab, Z., Teimouri, A., Chermahini, A. N., & Azadi, M. (2018). Fabrication and characterization of nanobiocomposite scaffold of zein/chitosan/nanohydroxyapatite prepared by freeze-drying method for bone tissue engineering. *Int J Biol Macromol*, 108, 1017-1027.
- Shazni, Z. A., Mariatti, M., Nurazreena, A., & Razak, K. A. (2016). Properties of Calcium Phosphate Scaffolds Produced by Freeze-Casting. *Procedia Chemistry*, 19, 174-180.
- Sofla, M. R. K., Brown, R. J., Tsuzuki, T., & Rainey, T. J. (2016). A comparison of cellulose nanocrystals and cellulose nanofibres extracted from bagasse using acid and ball milling methods. *Advances in Natural Sciences: Nanoscience and Nanotechnology*, 7(3).
- Sommerfeldt, D. W., & Rubin, C. T. (2001). Biology of bone and how it orchestrates the form and function of the skeleton. *Eur Spine J*, 10 Suppl 2, S86-95.
- Sultan, S., & Mathew, A. P. (2018). 3D printed scaffolds with gradient porosity based on a cellulose nanocrystal hydrogel. *Nanoscale*, 10(9), 4421-4431.
- Tabuchi, R., Azuma, K., Izumi, R., Tanou, T., Okamoto, Y., Nagae, T., . . . Anraku, M. (2016). Biomaterials based on freeze dried surface-deacetylated chitin nanofibers reinforced with sulfobutyl ether beta-cyclodextrin gel in wound dressing applications. *Int J Pharm*, 511(2), 1080-1087.
- Vestena, M., Gross, I. P., Müller, C. M. O., & Pires, A. T. N. (2015). Nanocomposite of Poly(Lactic Acid)/Cellulose Nanocrystals: Effect of CNC Content on the Polymer Crystallization Kinetics. *Journal of the Brazilian Chemical Society*.

- Yan, L., Wu, J., Zhang, L., Liu, X., Zhou, K., & Su, B. (2017). Pore structures and mechanical properties of porous titanium scaffolds by bidirectional freeze casting. *Mater Sci Eng C Mater Biol Appl*, 75, 335-340.
- Yang, W., Xu, H., Lan, Y., Zhu, Q., Liu, Y., Huang, S., . . . Guo, R. (2019). Preparation and characterisation of a novel silk fibroin/hyaluronic acid/sodium alginate scaffold for skin repair. *Int J Biol Macromol*, 130, 58-67. doi:10.1016/j.ijbiomac.2019.02.120
- Ye, M., Mohanty, P., & Ghosh, G. (2014). Morphology and properties of poly vinyl alcohol (PVA) scaffolds: impact of process variables. *Mater Sci Eng C Mater Biol Appl*, 42, 289-294.
- Yılmaz, P., öztürk Er, E., Bakırdere, S., ülgen, K., & özbek, B. (2019). Application of supercritical gel drying method on fabrication of mechanically improved and biologically safe three-component scaffold composed of graphene oxide/chitosan/hydroxyapatite and characterization studies. *Journal of Materials Research and Technology*.
- Youssef Habibi, L. A. L., and Orlando J. Rojas. (2009). Cellulose Nanocrystals: Chemistry, Self-Assembly, and Applications. *Chem. Rev*, 110, 3479–3500.
- Zhang, C., Salick, M. R., Cordie, T. M., Ellingham, T., Dan, Y., & Turng, L. S. (2015). Incorporation of poly(ethylene glycol) grafted cellulose nanocrystals in poly(lactic acid) electrospun nanocomposite fibers as potential scaffolds for bone tissue engineering. *Mater Sci Eng C Mater Biol Appl*, 49, 463-471.
- Zhang, H., Nie, H., Li, S., White, C. J. B., & Zhu, L. (2009). Crosslinking of electrospun polyacrylonitrile/hydroxyethyl cellulose composite nanofibers. *Materials Letters*, 63(13-14), 1199-1202.
- Zhang, J., Zhou, A., Deng, A., Yang, Y., Gao, L., Zhong, Z., & Yang, S. (2015). Pore architecture and cell viability on freeze dried 3D recombinant human collagen-peptide (RHC)-chitosan scaffolds. *Mater Sci Eng C Mater Biol Appl*, 49, 174-182.
- Zhou, X. H., Wei, D. X., Ye, H. M., Zhang, X., Meng, X., & Zhou, Q. (2016). Development of poly(vinyl alcohol) porous scaffold with high strength and well ciprofloxacin release efficiency. *Mater Sci Eng C Mater Biol Appl*, 67, 326-335.
- Zulkifli, F. H., Hussain, F. S., Rasad, M. S., & Mohd Yusoff, M. (2014). Nanostructured materials from hydroxyethyl cellulose for skin tissue engineering. *Carbohydr Polym*, 114, 238-245.
- Zulkifli, F. H., Hussain, F. S. J., Harun, W. S. W., & Yusoff, M. M. (2019). Highly porous of hydroxyethyl cellulose biocomposite scaffolds for tissue engineering. *Int J Biol Macromol*, 122, 562-571.